SYNTHESIS OF DISULFIDE, THIOETHER, AND HYDROCARBON CYCLOPHANES USING SELF-ASSEMBLY, COVALENT CAPTURE, AND PHOTOCHEMICAL SULFUR EXTRUSION

by

NGOC MINH PHAN

A DISSERTATION

Presented to the Department of Chemistry and Biochemistry
and the Graduate School of the University of Oregon
in partial fulfillment of the requirements
for the degree of
Doctor of Philosophy

September 2020

DISSERTATION APPROVAL PAGE

Student: Ngoc Minh Phan

Title: Synthesis of Disulfide, Thioether, and Hydrocarbon Cyclophanes Using Self-Assembly, Covalent Capture, and Photochemical Sulfur Extrusion

This dissertation has been accepted and approved in partial fulfillment of the requirements for the Doctor of Philosophy degree in the Department of Chemistry and Biochemistry by:

Ramesh Jasti	Chairperson
Darren Johnson	Advisor
Michael Haley	Core Member
Benjamín Alemán	Institutional Representative

and

Kate Mondloch	Interim Vice Provost and Dean of the Graduate School

Original approval signatures are on file with the University of Oregon Graduate School.

Degree awarded September 2020

DISSERTATION ABSTRACT

Ngoc Minh Phan

Doctor of Philosophy

Department of Chemistry and Biochemistry

September 2020

Title: Synthesis of Disulfide, Thioether, and Hydrocarbon Cyclophanes Using Self-Assembly, Covalent Capture, and Photochemical Sulfur Extrusion

Self-assembly involves the self-driven incorporation of smaller components into large molecules, a process analogous to a puzzle programmed to put itself together. Nature has made use of self-assembly in biological processes such as the formation of double helical DNA. In chemical synthesis, the importance of disulfide bridges in proteins has spurred the development of processes that can direct thiols to self-assemble into disulfides. The DWJ laboratory has introduced the use of metalloids as an additive that enables the rapid and selective self-assembly of thiols into complex disulfide structures. We are able to trap these disulfides as the more stable thioethers in high yield, with the process taking under two days as compared to lengthy syntheses (several weeks) with traditional methods.

This Dissertation describes an effort to improve our previously published method. The study on the role of the Group 15 elements (or pnictogens) in the self-assembly process has led to the discovery of copper(II) as an alternative directing group. While both the pnictogens and copper(II) are important reagents in the self-assembly reaction, the latter additive is a more environmentally benign option, and its directing ability has been demonstrated by the synthesis of 13 new disulfides and thioethers in two steps.

Expanding the scope of our method, new unsymmetrical disulfides and thioethers

have been made by mixing two different thiols. Instead of a statistical distribution of products, different-sized disulfides (dimers, trimers, tetramers) have been amplified through various reaction conditions. For instance, the yield of the unsymmetrical trimers could be amplified to 65% from the statistical yield of 20%. The ability to selectively prepare unsymmetrical disulfide and thioether species can have a significant impact on the current synthetic field, which is dominated by symmetrical, dimeric species constructed from traditional methods.

Finally, photochemical sulfur extrusion has been applied on the thioether cyclophanes to give hydrocarbon cyclophanes. The four new hydrocarbon cyclophanes synthesized using our new method are very challenging to obtain with traditional methods. These new hydrocarbon structures will be great targets for fundamental studies and may lead to potential new monomers for insulating plastics in the $1B US polymerization market.

CURRICULUM VITAE

NAME OF AUTHOR: Ngoc Minh Phan

GRADUATE AND UNDERGRADUATE SCHOOLS ATTENDED:

University of Oregon, Eugene
University of Dallas, Irving

DEGREES AWARDED:

Doctor of Philosophy, Chemistry, 2020, University of Oregon
Master of Science, Chemistry, 2018, University of Oregon
Bachelor of Science, Biochemistry, 2016, University of Dallas

AREAS OF SPECIAL INTEREST:

Organic Chemistry

PROFESSIONAL EXPERIENCE:

Graduate Teaching Assistant, University of Oregon, Sept 2016 – present

Teaching Assistant, University of Dallas, Sept 2015 – May 2016

Undergraduate Researcher, Southern Methodist University, Sept 2015 – Jan 2016

Undergraduate Researcher, UT Southwestern Medical Center, Feb – Aug 2015

GRANTS, AWARDS, AND HONORS:

Dean's First Year Merit Award, University of Oregon, 2016

Robert A. Welch Undergraduate Chemistry Award, University of Dallas, 2015

PUBLICATIONS:

Phan, N-. M.; Zakharov, L. N.; Johnson, D. W. An Efficient Route to Symmetrical and Unsymmetrical Disulfide, Thioether, and Hydrocarbon Cyclophanes. *Manuscript submitted*.

Phan, N-. M.; Guzmán-Percástegui, E.; Johnson, D. W. Dynamic Covalent Chemistry as a Facile Route to Unusual Main Group Thiolate Assemblies and Disulfide Hoops and Cages. *ChemPlusChem*. **2020**, *85*, 1270–1282.

Phan, N-. M.; Choy, E. P. K. L; Zakharov, L. N.; Johnson, D. W. Self-Sorting in Dynamic Disulfide Assembly: New Biphenyl-Bridged "Nanohoops" and Unsymmetrical Cyclophanes. *Chem. Commun.* **2019**, *55*, 11840–11843.

Phan, N-. M.; Zakharov, L. N.; Johnson, D. W. Copper(II) Serves as an Efficient Additive for Metal-Directed Self-Assembly of over 20 Thiacyclophanes. *Chem. Commun*. **2018**, *54*, 13419–13422.

Collins, M. S.; Phan, N-. M.; Zakharov, L. N.; Johnson, D. W. Coupling Metaloid-Directed Self-Assembly and Dynamic Covalent Systems as a Route to Large Organic Cages and Cyclophanes. *Inorg. Chem*. **2018**, *57*, 3486–3496.

ACKNOWLEDGMENTS

Thank you, Darren, for believing in me. You constantly provided me with opportunities to challenge myself and became the scientist I am today. You are an excellent teacher and have guided my projects closely and encouraged me during difficult times. You taught me so many sophisticated words for scientific writing.

I must also thank the other professors at UO. Professors Ramesh Jasti and Michael Haley, thank you for agreeing to be on my dissertation committee and for all your feedback during my time here. Professor Benjamín Alemán, thank you for being the last member of my committee and sitting through all my chemistry presentations.

I thank the expert facility managers at UO for all their help with various characterization methods: Drs. Michael Strain and Nanette Jarenwattananon with NMR help and Dr. Lev Zakharov for his golden hands while handling my “not-good crystals”.

I want to thank past and current members of the “cyclophane team”. I am indebted to Dr. Mary Collins for training me when I first joined the lab. My graduate school career overlapped with Trevor Shear’s and it was great working with such a knowledgeable person. I want to thank all my mentees: Turner Newton, Emma Choy, Julia Fehr, Hunter Edelen, Henry Trubenstein, Jacob Mayhugh, and Tara Clayton. You are very good students and I wish you the best of luck with your future adventures.

I would not be the scientist I am today without the support of my lab mates in the Johnson group. Everyone in the Johnson group has been a tremendous resource to me. Dr. Jessica Lorhman is one of the most fun and weird people. I was fortunate to join the group with 3 fantastic scientists and friends, Hazel Fargher, Jeremy Bard, and Jordan Levine. Thank you for soldiering with me through all the major milestones at UO, be it

classes, advancement, or graduation. I must also thank my seniors and postdocs for their friendship and wisdom, including Dr. Meredith Sharps, Dr. Brandon Crocket, Dr. Sean Fontenot, Dr. Susan Cooper, Dr. Brantly Fulton, Dr. Tobias Sherbow, and Dr. Chun-Lin Deng. I am also thankful for my juniors, including Thaís de Faria, Hannah Bates and Grace Kuhl. You are great friends and graduate school would be different without you.

I have been blessed to have found a supportive community outside of my lab: Dr. Matthew Cerda, Kiana Kawamura, Terri Lovell, Dr. Curtis Colwell, Ruth Maust, and Marisa Choffel. I also want to thank Gabrielle Warren, Joshua Barker and Grace Lindquist as great leaders of UO GCF. I also have tremendous friends outside of the department: Dr. Micah & Tai Donor, Steve & Kathy Ellisen, Robert & Nancy Roseburg, Dan & Stacey Lauterbach. Thank you helping me grow a lot as a Christian. My undergraduate friends Jenny Feng, Sarah Klatt and Elizabeth Herrera, thank you for all your love and support, especially with my first few years of graduate school.

Finally, I must thank my beloved family. Heavenly Father, thank you for getting me into graduate school and for always being there with me. I deeply love my grandparents Diet and Tai and my parents Minh and Binh. Thank you for guiding me prudently and loving me unconditionally. I thank my brother Duy for all his support. I am also grateful for the rest of the Phan, Dao and Lau clans, whose love and collaboration taught me how to live well in community. And finally, Nathan Lau, dearly loved husband, I could not have completed this work without standing on your shoulders. You have taught me so much about graphic design and have showered me with utmost love and care. Life with you is a trillion times better than without you. I cannot wait to begin my life with you and participate in all exciting Team N adventures.

TABLE OF CONTENTS

Chapter Page

Chapter Page

LIST OF FIGURES

Figure Page

Figure Page

LIST OF TABLES

Table Page

LIST OF SCHEMES

Scheme Page

Scheme Page

CHAPTER I

INTRODUCTION

Recent Dynamic Motifs and Insights into Factors Modulating their Reversibility

Thiol-disulfide exchange is a chemical reaction in which a thiolate group (R−S⁻) attacks a sulfur atom in a disulfide bond (R−S−S−R').[1] The original disulfide bond is broken, and a new disulfide bond forms between the attacking thiolate and the original sulfur atom. Meanwhile, the other sulfur atom in the original disulfide bond is released as a new thiolate, now carrying the negative charge (Figure 1.1a). Thiol–disulfide exchange is observed in many proteins, in which the rearrangement of disulfide bonds occurs when a thiolate group of a cysteine residue attacks a disulfide bond in a protein.[2] This process of disulfide rearrangement does not change the number of disulfide bonds within a protein, merely their location, as is observed in the process of hair curling (Figure 1.1b).[3] Chemical reduction of the disulfide bonds in the keratin proteins of hair is followed by shuffling the thiol groups to "curl" the hair, which is then made "permanent" by re-oxidizing the thiols to form new disulfide bonds.

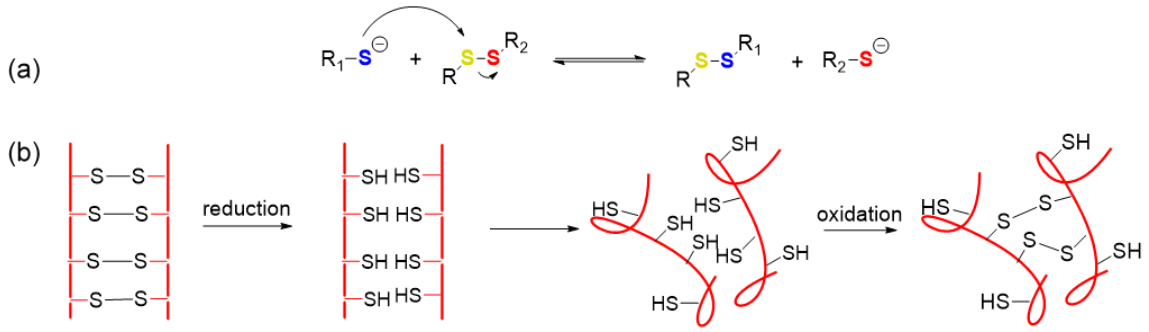

Figure 1.1. (a) Figurative representation of a thiol-disulfide exchange reaction, with attacking thiolate S-atom depicted in blue. The sulfur atom depicted in yellow remains in the new disulfide bond. (b) The process of hair curling involves multiple thiol-disulfide exchanges taken place on the keratin fiber of the hair.

Since disulfide bonds possess the ability to form and break reversibly under thermodynamic control, they are of significant interest in the field of dynamic covalent chemistry (DCC), which takes advantage of the rapidly equilibrating coexistence of multiple species to access highly complex assemblies.[4] For instance, thiol–disulfide exchange was utilized to make a dynamic combinatorial library (DCL) of macrocyclic disulfides in water, which features 45 different species formed spontaneously upon stirring a mixture of dithiols in basic solution with O_2 from the air.[5] This DCL is shown to respond to external stimuli to amplify specific components of equilibrating mixtures, also known as the templating effect. Upon adding a template, the equilibrium will shift in the direction of the receptor that binds this template with high affinity. Manifestation of templating effect has been observed in the optimization of multiple receptors from complex DCLs, such as a 400x amplification of a diastereomer that binds cations, or a selection of a neutral receptor that binds inorganic anions in water, among many other examples.[6]

Since the 1980s, DCC has proved to be a powerful way to synthesize mechanically interlocked compounds.[7] Specifically, the reversible nature of disulfide linkages was first utilized to synthesize a disulfide-based rotaxane in 2000.[8] A symmetrical dumbbell-shaped compound with two ammonium centers and a central disulfide bond was prepared as a dynamic covalent component for rotaxane synthesis (Figure 1.2a). This dumbbell and a crown ether react to afford [2] and [3]rotaxanes in good yields. This transformation does not occur in the absence of benzenethiol, which initiates the thiol-disulfide exchange process to break the dumbbell into two halves, forming two open sites for threading the crown ether. The dynamic nature of the disulfide

bond allows for the two pieces to reform and give rise to the rotaxanes. Different thermodynamic conditions, such as temperature, solvent, initial ratios of substrates, and concentrations are all shown to play a role in affecting the yields of the two rotaxanes species, highlighting the reversible nature of disulfide linkages.

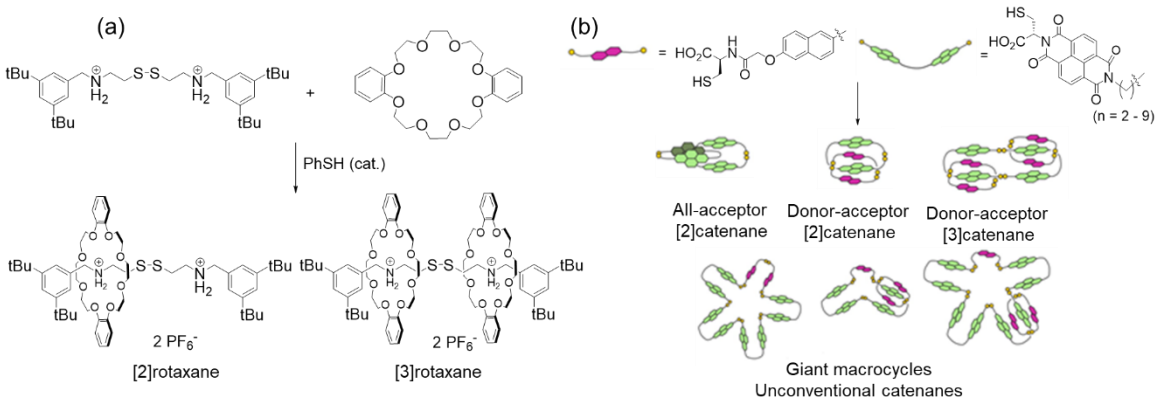

Figure 1.2. Recent selected studies utilizing dynamic covalent disulfide bonds. Synthesis of disulfide-based (a) rotaxanes and (b) catenanes. Adapted with permission from *J. Am. Chem. Soc*. **2012**, *134*, 19129–19135. Copyright 2012 American Chemical Society

Thiol-disulfide exchange has also been used to synthesize catenanes, another important mechanically interlocked molecular structure. The first dynamic combinatorial synthesis in water of an all-acceptor [2]catenane and multiple donor–acceptor [2] and [3]catenanes was reported (Figure 1.2b).[9] The authors synthesized a DCL using a series of dithiols containing two electron-poor naphthalenediimide (NDI) groups held apart by alkyl spacers (Figure 1.2b, green blocks, acceptors). In the DCLs in which the number of alkyl linkers (defined as n) is ≥ 8, an all-acceptor [2]catenane is formed. This formation is driven by hydrophobic effect in which the hydrophobic side of each NDI is buried inside the catenane pocket, and the more hydrophilic side is exposed to water. Addition of dithiols containing electron-rich groups (Figure 1.2b, purple blocks, donors) gives rise to

donor–acceptor [2]catenanes when $6 < n < 9$. When $n \leq 6$, an odd−even effect with respect to n is observed: an even n will result in [3]catenanes while an odd n will give giant macrocycles (Figure 1.2b). The odd–even effect arises from differences in the stability of intermediates along the kinetic pathway to the [3]catenanes, which is strongly expressed with smaller n. The authors conclude, "when disulfide DCC is conducted in water, supramolecular interactions affecting equilibrium positions may arise along with kinetic limitations, leading to complex behavior, not unlike biological systems." This study has also inspired additional research on complex disulfide DCC chemistry in water.[10]

Disulfide bonds are certainly not the only moieties that are used in DCC. Undoubtedly, DCC is a judicious choice to facilitate the construction of complex assemblies both in modular fashion and high yields, since it combines the robustness of covalent bonding with the self-correcting attributes of supramolecular chemistry. The "proof reading and editing" property *via* repeated bond dissociation–recombination processes ensures that side products are recyclable, allowing theoretically complete conversion into the desired product. The amplification of a desired component *via* internal/external stimuli also simplifies the process of forming otherwise unfavored structures. Therefore, multiple novel dynamic motifs have been identified and greater insights into the factors modulating their reversibility are under investigation. Some key DCC motifs include formals,[11] quinoidal radicals,[12] cyclobenzoins,[13] alkynes,[14] orthoesters,[15] and imines,[16] among other functional groups.

Self-assembly as a Tool for Supramolecular Architectures

A contemporary tool to access complex supramolecular architectures is self-assembly, a process in which building blocks, facilitated and bound by one or more secondary interactions, link together to form larger aggregates of repeating units.[17] Beautiful examples of self-assembled systems can be found in nature (Figure 1.3a). For example, the double helix of DNA is constructed *via* the self-assembly of two single-stranded DNA chains held together primarily by hydrogen bonding between the base pairs.[18] Another example of self-assembly occurs in the formation of phospholipid bilayers, in which the hydrophobic effect drives the self-assembly of two-layered structures that point hydrophobic tails internally and hydrophilic heads externally to generate the bilayer structure.[19] Viral self-assembly is a more complicated process in which replicated viral proteins, RNA, and lipids self-assemble into a new virus.[20] Because these biomacromolecular building blocks are combined in the most efficient way to assist the virus with its spread and cellular invasion, obliterating some viruses has been a challenging task, as observed with the current COVID-19 pandemic.[21]

Viruses often make mistakes in self-assembly, for instance they may fail to include all the necessary components into the enclosed volume.[22] Learning from biological specimens, when translating to making biological mimics, chemists typically utilize metals in their synthetic schemes since metal-ligand bonds are labile and can thus

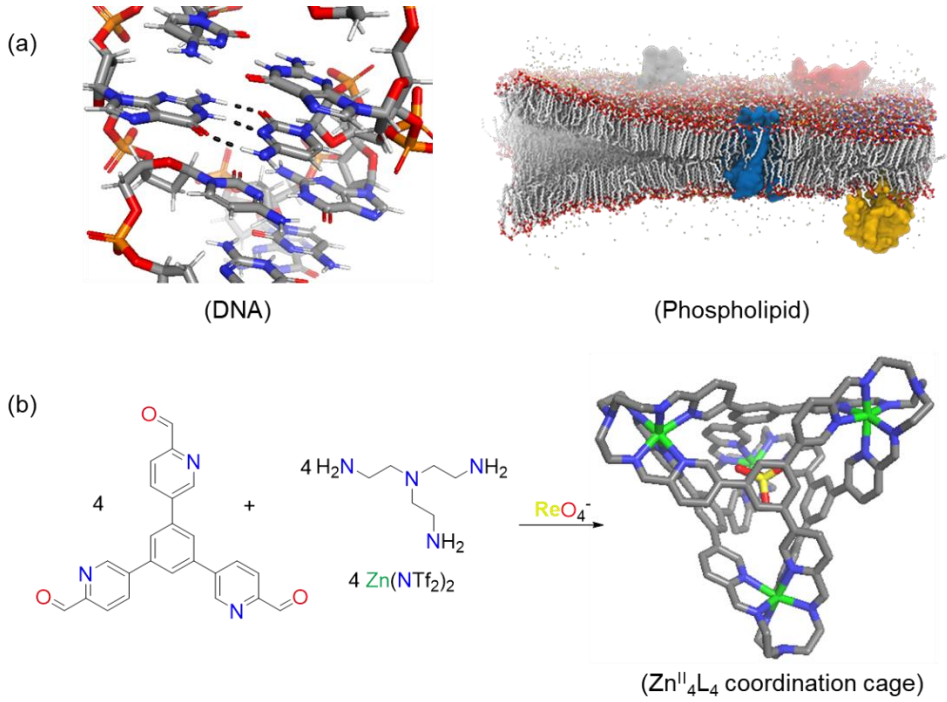

Figure 1.3. Selected self-assembly systems: (a) in nature – DNA double helix held together by hydrogen bonds and phospholipid bilayers held together by hydrophobic effect; (b) in current synthetic chemistry – a $Zn^{II}_4L_4$ coordination cage. Adapted from NDB ZD0012 and lipidbuilder.epfl.ch/home.

allow for the correction of "kinetic mistakes."[23] Metal-directed self-assembly has allowed chemists to access a variety of elegant thermodynamic products over kinetic side products.[24] As such, with careful ligand design, binding elements that enable directional self-assembly can be incorporated in the system, imposing the stereochemical preference and symmetry of metal coordination onto the self-assembling system of interest.[25] Many research laboratories have used the well-defined coordination geometry of transition metals as a directional tool for their self-assembled systems. For example, a $Zn^{II}_4L_4$ coordination cage was assembled from 12 components (Figure 1.3b). This cage binds tightly to ReO_4^-, an anion of great physicochemical similarity to pertechnetate, both of which have uses in nuclear medicine.[26] In a follow-up report, a similar $Fe^{II}_4L_4$

coordination cage is shown to transport 1-fluoroadamantane from water into an ionic liquid with a simple counter-anion exchange.[27] Other recent spectacular supramolecular architectures constructed from metal-directed self-assembly include an *O*-symmetric coordination cage with eight chiral vertices self-assembled from 62 components;[28] two 46-membered [2+2] macrocyclic dinuclear Zn(II) complexes,[29] and monometallic cryptates self-assembled from orthoester bridgeheads,[15] among many other examples.

Research Conducted in the DWJ Laboratory: Combining Dynamic Covalent Chemistry and Metal-Directed Self-Assembly

Rigid linear, square-planar, tetrahedral, or octahedral coordination geometries of transition metal ions can allow for predictable and unequivocal programming of the shape and size of assembly products.[30] On the other hand, metals with more unpredictable and flexible coordination geometries have been typically avoided due to the challenges of controlling the molecular composition and structure of products. This difficulty first motivated Darren W. Johnson's (DWJ) laboratory to investigate and design strategies for facile preparation of pnictogen (Pn)-containing assemblies. Early work in the laboratory featured metal/metalloid-containing organic compounds formed *via* coordination-directed self-assembly routes, which is a simple synthesis and guarantees access to novel structures in exceptional yields. Despite its known toxicity and carcinogenicity in humans, our laboratory first selected arsenic(III) as a design component because of its unusual coordination geometry and well-known affinity to thiolates. $AsCl_3$ was allowed to react with dithiol H_2L (**1**) (α,α'-dimercapto-para-xylene) in KOH, yielding the cryptand As_2L_3 (**2**) in 52% yield (Scheme 1.1).[31] The simplicity of the ^{1}H and ^{13}C NMR

spectra evidenced a highly symmetrical product and the presence of a $[H\{As_2L_3\}]^+$ species in the mass spectrum supported an As_2L_3 molecular composition. Short As–C_{aryl} distances were observed from the crystal structure of As_2L_3 product (3.18–3.33 Å), suggesting the existence of attractive and stabilizing interactions between the phenyl rings of the ligands and the As^{III} ions (Scheme 1.1).

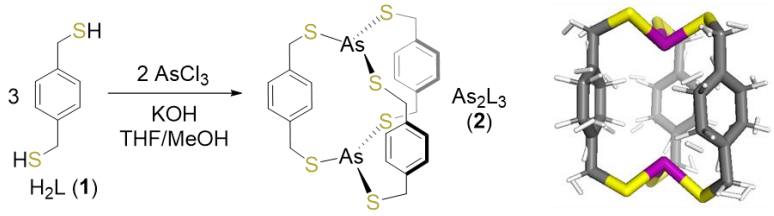

Scheme 1.1. Synthesis of arsenic(III)-thiolate assemblies. The reaction of $AsCl_3$ and dithiol (**1**) in the presence of base affords the As_2L_3 cryptand (**2**) as the main product. Crystal structure of (**2**) shown at right.

Having a general framework in hand to synthesize self-assembled arsenic-thiol complexes, many other thiol ligands (dithiol, trithiol, tetrathiol)[32] and Pn ions (Sb^{III}, Bi^{III}, P^{III})[33] were investigated. During these studies, 1,5-dimercaptomethylnaphthalene was found to crystallize as a disulfide trimer under slow atmospheric oxidation, seemingly only when a Pn ion is present.[34] An intentional oxidation of ligand (**1**) with iodine (I_2) and a small amount of Pn salts was found to form a library of dynamic disulfide assemblies (Figure 1.4). In this case, the directing behavior of the Pn salts enabled selective syntheses of discrete disulfide assemblies of macrocycles/cages over competing oligomers/polymers. The usually low yielding cyclization step was replaced by a self-assembly performed under thermodynamic control in the presence of $SbCl_3$. This self-assembly approach has many advantages over traditional stepwise syntheses, which often suffer from very long reaction times, extensive purifications, and poor yields.

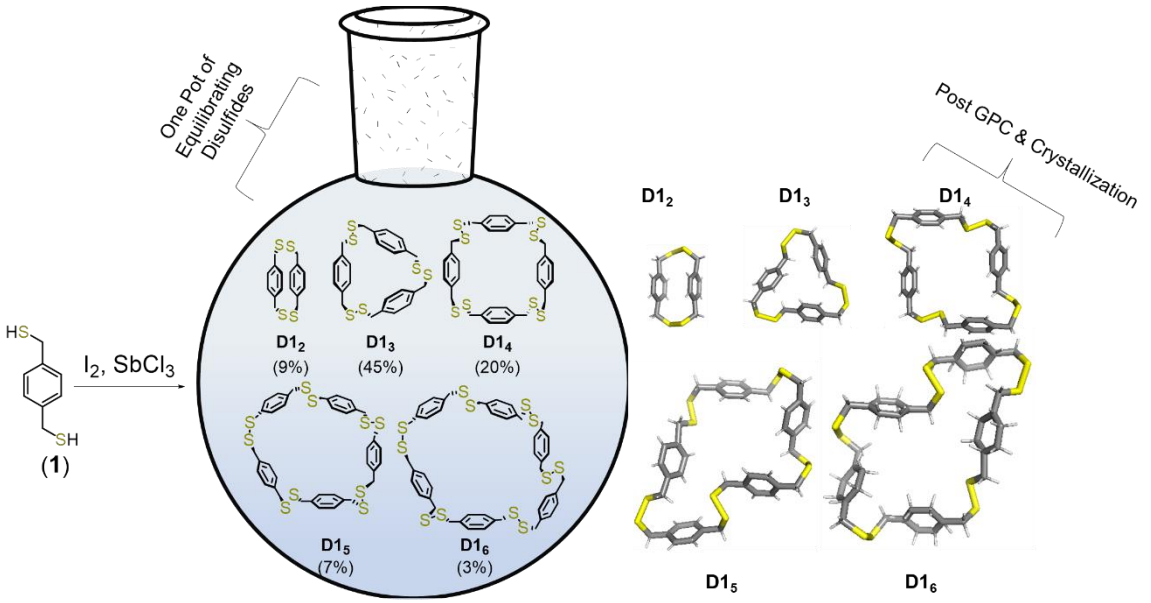

Figure 1.4. Pn-activated iodine oxidation of thiol ligand (**1**) to form disulfides of different sizes, including dimer **D1$_2$**, trimer **D1$_3$**, tetramer **D1$_4$**, pentamer **D1$_5$**, and hexamer **D1$_6$**. GPC and/or selective crystallization isolates each species, allowing for solution and solid-state characterization.

Since this initial discovery, we have established a "DWJ cocktail" to form traditionally elusive disulfide cyclophanes. This protocol combines the motif of metal-directed self-assembly and dynamic disulfide covalent chemistry in a single system. The mercaptomethyl substituents is used as a preorganizing binding motif to accommodate the trigonal pyramidal geometry and thiophilicity of the templating Pn ion. This system works really well because the formed thiol-Pn complex is supported by electron density from the aromatic ring of the ligand, which acts as a non-covalent stabilizing force through Pn-π interactions.[35] Using this method, a variety of disulfide structures are accessible, such as those shown in Figure 1.4. Traditionally elusive structures like trimer **D1$_3$** and unknown larger macrocycles like hexamer **D1$_6$** can be formed in the same reaction flask from a single 2-fold symmetric building block (**1**). Gel permeation chromatography (GPC) cleanly separates each disulfide by size, followed by ^{1}H NMR

spectroscopy and single crystal X-ray diffraction to confirm the identity of this family of compounds. We were able to grow crystals for all disulfides **D1$_2$ – D1$_6$** and their structures are shown in Figure 1.4. To minimize the unfavorable void space formed by the extended pores, the larger macrocycles **D1$_4$**, **D1$_5$** and **D1$_6$** all co-crystallize with solvent chloroform molecules.

We also found that 3D cages are accessible through 3-fold symmetric ligands. One example of such a cage is **D3$_4$**, constructed from the self-assembly of four molecules of (**3**) (Scheme 1.2). This disulfide cage can be contracted through sulfur extrusion with hexamethylphosphoroustriamide (HMPT) resulting in thioether **T3$_4$** (Scheme 1.2).[36] This process requires the extrusion of six sulfur atoms from the tetrahedron, representing a total of 24 bonds broken and formed in a single step. The reaction proceeds smoothly at ambient temperature in 94% yield. **T3$_4$** co-crystallizes with a chloroform solvent although its small cavity remains empty; instead, **T3$_4$** collapses in on itself, avoiding unfavorable void space. The C–S–C angles within the cyclophane are in the expected range for cyclic thioethers (~ 100 – 105°).[37]

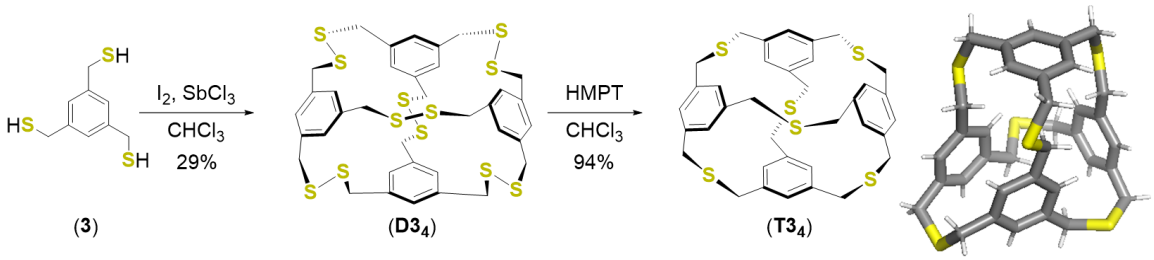

Scheme 1.2. Pn-activated iodine oxidation of thiol ligand (**3**) to form disulfide tetrahedral cage **D3$_4$**. Sulfur extrusion on **D3$_4$** gives thioether cage **T3$_4$**. The crystal structure of **T3$_4$** is shown on the right.

Translating the basic science developed by the DWJ group into application-based research has been an ongoing broader impact goal in our laboratory. One way we

envision accomplishing this goal is to extrude the final sulfur atoms of thioethers to yield hydrocarbon cyclophanes. These hydrocarbon derivatives can have unusual properties and serve as precursors for sensing molecules, organic materials, insulating plastics, and as new precursors for conjugated polymers.[38] Most recently, Mastalerz has published a method to generate large cages constructed of only C – C bonds from imine precursors (Scheme 1.3).[39] This is one of the rare examples that incorporate DCC bond formation in the first step to generate large hydrocarbon cages, including derivatives of $C_{72}H_{72}$, an unknown cage suggested by Vögtle 50 years ago.[40] With the goal of making new C – C based macrocycles and cages, we proposed to use disulfide and thioether cyclophanes as the precursors, especially since we have now established an efficient protocol to synthesize these structures. Access into unsymmetrical cyclophanes has also been a highly desired goal of the field; to this end, we realized that a facile route to unsymmetrical disulfide, thioether and hydrocarbon cyclophanes is an important next step for our research. We proposed to utilize self-sorting behavior to achieve this goal.

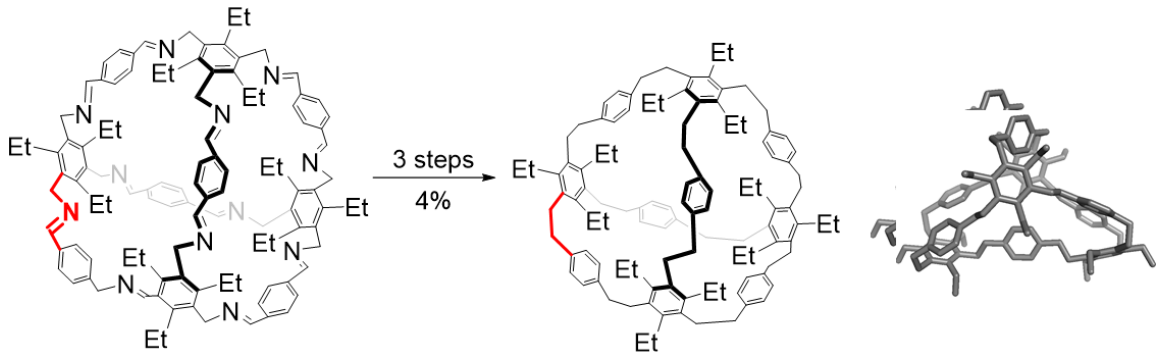

Scheme 1.3. Masterlez's method to synthesize hydrocarbon cages from imine cages. Transformation of imine functionalities into amine, followed by nitrosoamine, allows for the ultimate formation of hydrocarbon functionalities. Crystal structure of the derivative of $C_{84}H_{84}$ shown at right.

Self-sorting as a Route to Access Unsymmetrical Cyclophanes

The tobacco mosaic virus, which is composed of 2130 identical protein building blocks, requires each building block to be programmed similarly to ensure that the next building block is attached correctly.[41] Contrast this behavior to the enzyme ATP synthase, which is constructed from many different subunits that all need to find their correct positions for a functional assembly. Therefore, these building blocks need many different binding sites to ensure that only the correct building block attaches. The difference in binding sites thus leads to a selection process known as self-sorting.[41] Different types of self-sorting can be distinguished: narcissistic self-sorting,[42] which provides homomeric assemblies, or social self-sorting,[43] which leads to heteromeric assemblies. The field of bionanotechnology has drawn inspiration from self-sorting in nature. For example, by engineering teal fluorescent protein (red fragments in Figure 1.5a) to have a sequence compatible with a bacterial encapsulin (purple fragments in Figure 1.5a), the fluorescent protein will be selectively packaged inside the encapsulin upon bacterial self-assembly into stable icosahedral structure.[44] Similar self-assembling systems equipped with self-sorting capabilities would open up exciting opportunities for molecular storage and/or detoxification.

Supramolecular chemists have also utilized self-sorting to induce reconstitutions within a DCL. A DCL mixture of seven cages (with blue and red components in Figure

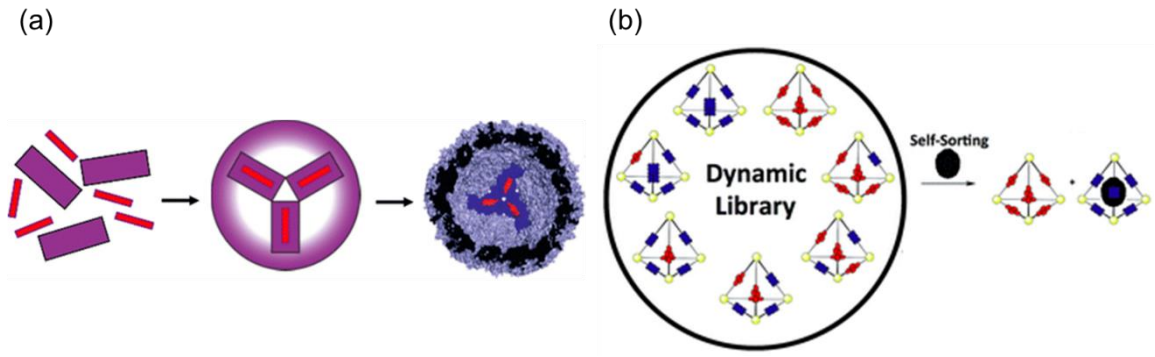

Figure 1.5. (a) Self-sorting of foreign proteins (red fragment) in a bacterial nanocompartment (purple fragment), an example of a self-assembling systems equipped with self-sorting capabilities with high fidelity and exceptional loading capacity. Reprinted (adapted) with permission from *J. Am. Chem. Soc*. **2014**, *136*, 3828–3832. Copyright 2014 American Chemical Society. (b) Encapsulation of the guest C_{70} (black ball) induces reconstitutions within a DCL mixed-ligand Zn_4L_6 cages, resulting in the formation of only two homoleptic cages (all-red and all-blue). Reproduced with permission from *Chem. Sci.* **2016**, *7*, 2614–2620 - Published by The Royal Society of Chemistry.

1.5b) can self-sort into two homoleptic cages (all-red and all-blue) when C_{70} (black ball) is introduced as a guest to the DCL. In this case, the all-blue cage encapsulates C_{70} to form a thermodynamically stable host-guest complex, removing all the blue fragments from DCL while leaving only the all-red cage as the residual product.[45] Self-sorting behavior has also been widely exploited and has demonstrated its utility to undertake other challenging experiments such as construction of multi-component cage complexes,[46] maintaining high homo- or hetero- selectivity behavior in chiral environment,[47] and separating libraries of discrete products.[48]

After working on multiple self-assembly systems from different thiol ligands, we were curious if we could observe self-sorting behavior in our “mixed” ligand system. The lack of traditional methods[49] to synthesize unsymmetrical structures might explain why these species remain unknown despite active cyclophane R&D in academic and industrial

laboratories.[50] In this Dissertation, we summarize the recent observation of self-sorting in our systems, in which combination of two different thiol ligands – with carefully chosen reaction conditions – gives rise to traditionally elusive lower-symmetry cyclophanes as the dominant products (Chapter IV). We were also able to access unsymmetrical thioether and hydrocarbon cyclophanes through unsymmetrical disulfide precursors (Chapter V). These unsymmetrical structures are extremely challenging to synthesize using traditional methods and have now been successfully constructed using our 3-step strategy.

Overview of the Next Chapters

This Dissertation summarizes an effort to understand the fundamental role of the Sb^{III} additive in the self-assembly of thiols into disulfide cyclophanes and discovering other metals that can substitute for the Sb^{III} additive (Figure 1.6). A better understanding of how the metal additives work as directing elements in the self-assembly step allows for a thorough investigation of how other DCC conditions can affect disulfide product distribution from multiple ligand systems. Adding self-sorting behavior to the self-assembly system increases the complexity of the study. Nonetheless, the information we acquired during the studies of a single thiol system has given us great insight into the studies of "mixed" systems, giving us access to traditionally elusive unsymmetrical structures. The pinnacle of this study is the complete extrusion of all sulfur atoms to give unsymmetrical hydrocarbon cyclophanes, a highly desirable target for classical cyclophane synthesis with promising materials application (Figure 1.6).

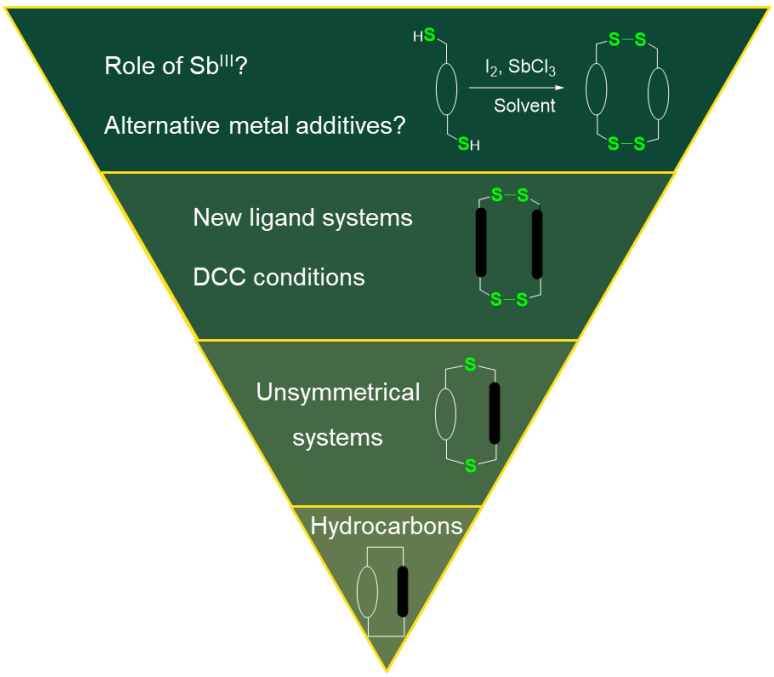

Figure 1.6. Overview of the structure of this Dissertation: the knowledge we acquired from fundamental studies of the metal additives and simple thiol systems allows us a deeper understanding of more complex unsymmetrical structures (disulfides, thioethers, hydrocarbons), which possess promising optoelectronic and host/guest properties.

CHAPTER II

STUDYING THE EFFECT OF THE Sb^{III} ADDITIVE AND THE SEARCH FOR AN ALTERNATIVE METAL CENTER FOR THE SELF-ASSEMBLY OF THIOLS INTO DISCRETE DISULFIDE CYCLOPHANES

Introduction

Metal-directed self-assembly has shown its use in the construction of many complex supramolecular structures.[1] One way metal ions assist in the process of self-assembly is through complexing with the ligand(s) present in the supramolecular scaffold. For instance, Cu^{I} is known to form a strong complex with phenanthroline, a useful ligand for building catenanes, rotaxanes, and knots.[2] The main function of Cu^{I} is to hold the two phenanthroline ligands together in the perpendicular arrangement required for the preparation of interlocked molecules such as the [2]catenane in Scheme 2.1a. Once the desired framework is established, the Cu^{I} ion template is removed, either by demetalating with KCN[3] or the more recently discovered method of using NH_4OH solution (Scheme 2.1a).[4]

Another class of well-known metal ions used as templates for the formation of complex supramolecular structures is alkali metals, which are capable of forming complexes with oxygen-containing ligands such as crown ethers.[5] While complexes formed *via* alkali metals typically demonstrate weaker binding affinity than those with transition metals, it has been shown that counter anions (such as tetrakis[3,5-bis(trifluoromethyl)phenyl]borate or TFPB) can strengthen the interactions between alkali metal ions and the ligands.[6] The lower toxicity of alkali metals is another desirable

trait for their use as templates in the synthesis of interlocked molecules. One example of such structures is shown in Scheme 2.1b. The rotaxane synthesis involves dynamic imine bond formation between a diamine and a dialdehyde. In the presence of 0.5 equiv of NaTFPB, a [2]catenane **.** [Na] complex forms as the dominant product. The imine bonds are reduced to amine bonds with benzeneselenol (PhSeH), and no extra reaction is needed to remove the Na^+ ion from the [2]catenanes – it is lost during the workup and purification process.

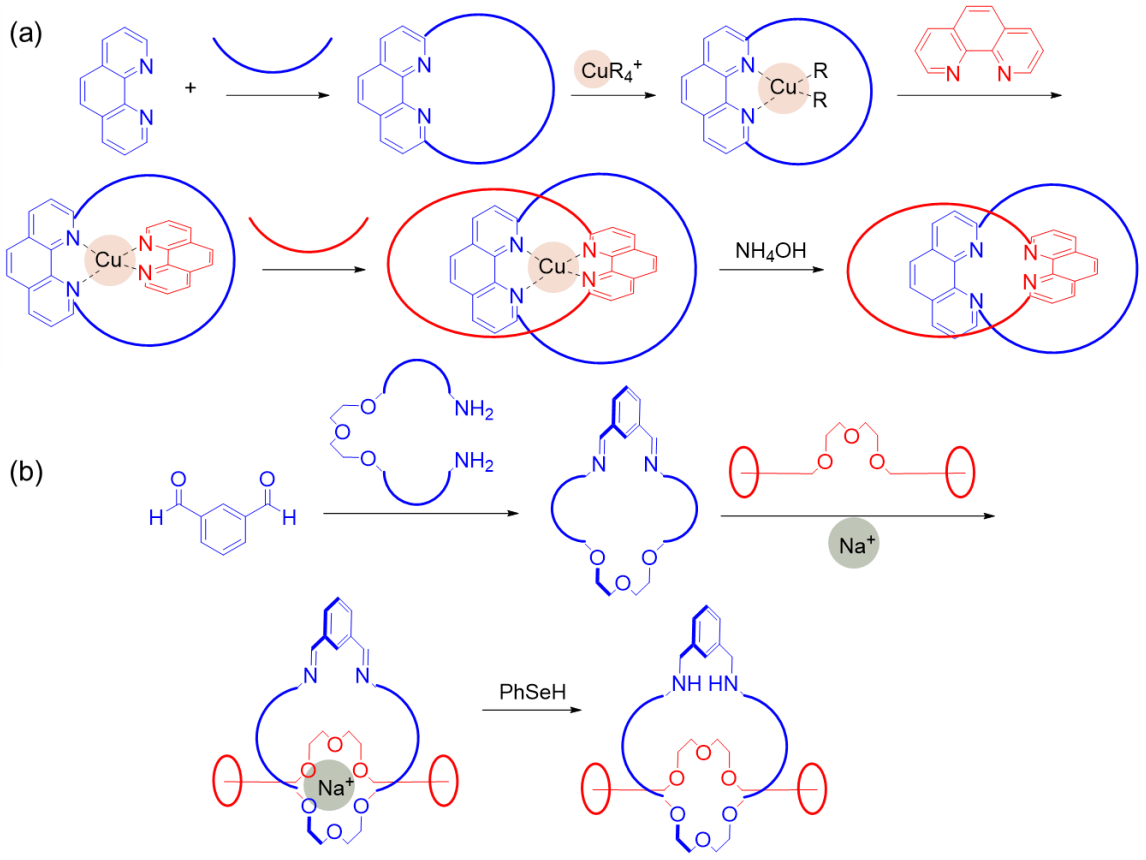

Scheme 2.1. Figurative representation of using metal ions to template the synthesis of interlocked molecular structures. (a) After templating the synthesis of a [2]catenane, Cu^I was removed from solution with NH_4OH. (b) After templating the synthesis of a [2]rotaxane, Na^+ was lost during work up conditions, giving a metal-free [2]rotaxane.

As mentioned in the Introduction chapter, metal-directed self-assembly is utilized in our laboratory to synthesize strained cyclophanes and high-ordered species. While investigating the reactivity of a 1,5-naphthalene-based arsenic-thiolate self-assembled complexes constructed from ligand (**4**), we discovered that in the presence of oxygen in the air, the arsenic-thiolate complex was oxidized into a discrete trimeric disulfide-bridged macrocycle **D4$_3$** (Scheme 2.2).[7] A subsequent study showed that the arsenic-thiolate cryptand is not a prerequisite for the formation of the disulfide cyclophanes; since this report, we have routinely oxidized thiol ligands with I_2 in the presence of Sb^{III} as the directing element. Our method facilely forms libraries of discrete disulfide-bridged cyclophanes, ranging from small and strained macrocycles to large and multifaceted 3D cages, as opposed to unspecific polymerization typically observed in dithiol oxidation without a directing group (Scheme 2.3). The Sb^{III} additive is also easily lost when the reaction is quenched with Na_2SO_3, giving the metalloid-free disulfide complexes. The disulfide structures are isolable by size through gel permeation chromatography (GPC) and are confirmed structurally *via* ^{1}H NMR spectroscopy, MS, and single crystal X-ray diffraction crystallography. The disulfides can be kinetically trapped into the more stable thioethers using hexamethylphosphorous triamide (HMPT).[8]

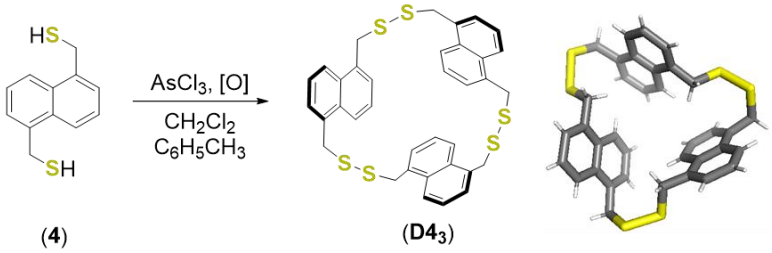

Scheme 2.2. Serendipitous oxidation of (**4**) forms macrocyclic disulfide trimer **D4$_3$**. Crystal structure of **D4$_3$** shown at right.

Since the exact role of the Sb^{III} additive was unknown, we investigated its role in the self-assembly reaction. A quantitative study of Sb-assisted iodine oxidation of ligand (**1**) (Scheme 2.3) revealed that Sb^{III} is most likely a stoichiometric reagent. Since the use of toxic pnictogen (Pn) metalloids would be undesirable in potential large-scale production of the desired disulfide cyclophanes, we investigated if less toxic additives, specifically Ag^{I}, Zn^{II}, Ca^{II}, Bi^{III} and Cu^{II}, could replace As^{III} and Sb^{III}. The most promising additive was Cu^{II}, as it was used as the directing element in our method to successfully prepare 7 known cyclophanes and 11 new naphthalene-bridged compounds, including 9 disulfides and 2 thioethers.

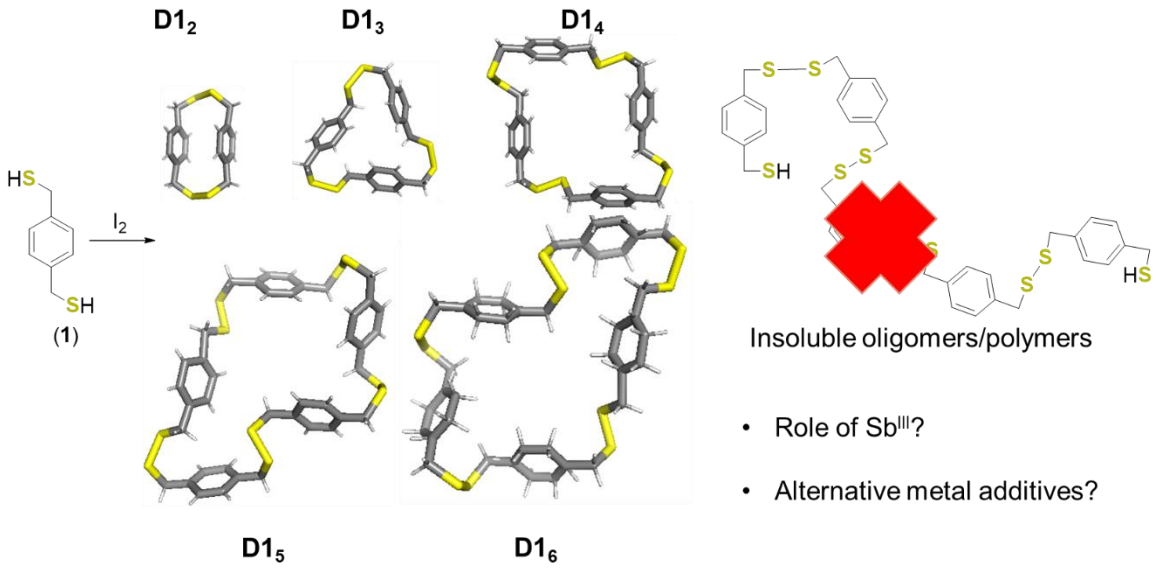

Scheme 2.3. This chapter discusses the study of the role of the Sb^{III} additive on the self-assembly of thiol (**1**) into disulfide dimer – hexamer cyclophanes **D1**$_{2-6}$. The search for other metal ions that can replicate the behavior of the Sb^{III} additive is also discussed.

Results and Discussion

Studying the effect of Sb^{III} in the self-assembly of thiol ligands into disulfide macrocycles

Since the exact role of the Sb^{III} additive was unknown, a quantitative study of Sb-assisted iodine oxidation was conducted with 1 equiv. of thiol (**1)** and 2 equiv. I_2. Experiments elucidated that the rate of consumption of dithiol increased as the concentration of Sb^{III} increased (Figure 2.1). At 0.0 equiv. $SbCl_3$, we observed almost no consumption of starting material even after 2 days of reaction. At 0.3 equiv. $SbCl_3$, the disulfide products started appearing as the reaction progressed even though unreacted starting material was still present after 2 days. We observed only a small amount of starting materials remained with higher equiv. of $SbCl_3$ (0.4 – 0.6 equiv.), indicating that we were slowly approaching the required amount of $SbCl_3$. Finally, at 0.7 equiv. $SbCl_3$, complete conversion into macrocycles was observed after only 5 minutes of reaction. The 0.7 equiv. value aligns with the stoichiometric formation of SbI_3 as a side product, supporting the hypothesis that Sb^{III} serves as a stoichiometric reagent for our self-assembling reaction.[9]

We postulate that Sb^{III} likely participates in Pn bonding, an attractive interaction between the electron accepting Pn and an electron donor (i.e., thiolate, iodide, or arene π system).[10] Early work in our laboratory has shown that Pn···π interactions can assist in

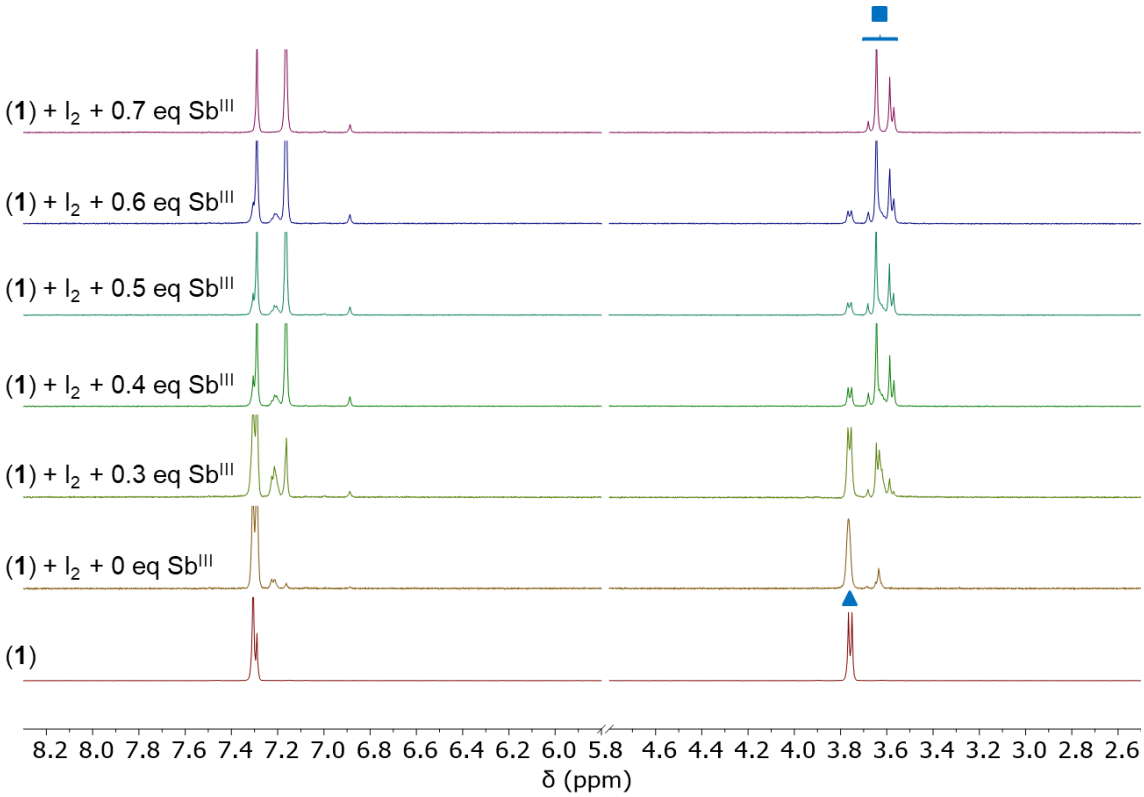

Figure 2.1. Quantitative study on the role of $SbCl_3$. The blue triangle symbolizes starting material (**1**) and the blue square symbolizes the products **D1**$_2$ – **D1**$_5$ observable with NMR spectroscopy ($CDCl_3$ – 7.26 ppm).

the self-assembly of Pn coordination complexes, and this interaction structurally supported in crystallographic examples where the arsenic lone pair is oriented at a preferred angle relative to the aromatic ring (Figure 2.2) to participate in what appears to be a form of "pnictogen bonding".[11] Control reactions on ligand (**1**) using solely I_2 yielded very broad disulfide peaks, suggesting slow, nonselective conversion, in comparison to the sharp, defined resonances that corresponded to the mixtures of discrete disulfide products in experiments containing $SbCl_3$ (Figure 2.1). This data shows that Sb^{III} is required for the selectivity and rapid reaction rate and to avoid unwanted polymerization side products from overactive iodine species. We concluded that in

forming discrete self-assembled disulfide structures, the Sb^{III} additive, as a stoichiometric reagent, could be assisting in organizing and converging the ligands to form a cyclic product.

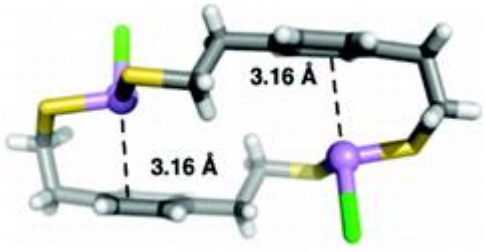

Figure 2.2. Pn···π interaction as a component in the supramolecular assembly design. Carbon atoms are colored in grey; arsenic atoms are colored in purple; sulfur atoms are colored in yellow; chlorine atoms are colored in green and hydrogen atoms are colored in white. Reprinted (adapted) with permission from *Crystal Growth & Design* **2010**, *10*, 3531–3536. Copyright 2010 American Chemical Society.

Finding alternative metals to substitute for As^{III} and Sb^{III} additives

Although the Pn-based protocol has been highlighted as a powerful method in supramolecular chemistry, the known toxicity of As^{III} and Sb^{III} hinder the scalability and scope of this self-assembly process. This led to an investigation of alternative additives, divided into four groups of candidates: (a) Ag^{I} and Zn^{II} due to their well-known thiophilicity,[12] which could assist in the formation of the metal-thiolate complex intermediate; (b) Ca^{II} due to its encapsulation in many macrocyclic systems;[13] (c) Bi^{III} since it is also a member of the Pn family;[14] and (d) Cu^{II} since metal complexes of this ion with thiols have substantial literature precedent.[15] Table 2.1 reports the relative yield of each member of the assembled disulfide library **D1**$_2$ – **D1**$_6$ and the yield of the undesired intermediate metal-thiol complex. While all of the metal ions tested are capable of yielding the desired macrocycles, they have very different activities, as evident in their

reaction times. Upon the addition of 1 equiv. (**1**), 2 equiv. I_2 and 2 equiv. of M (M = metal ion), the NMR spectra of group (a) and (b) metal ions (Ag^{I}, Zn^{II} and Ca^{II}) showed the slowest conversion to disulfide macrocycles, along with the formation of many undesirable oligomeric/polymeric species and the thiol-metal complex intermediates. Even after 2 days, complete conversion to disulfide products was not observed in these systems. On the other hand, group (c) and (d) metal ions (Bi^{III} and Cu^{II}) showed complete conversion into macrocycles after 5 minutes.[16] The fact that Bi^{III} could be a substitute for As^{III} and Sb^{III} was not surprising since Bi^{III} is a member of the Pn family. We were more interested in understanding how Cu^{II} can assist in the formation of discrete disulfide structures since its preferred coordination geometry and coordination number are very different from those of the Pn ions.

Salt	Dimer (D1$_2$)	Trimer (D1$_3$)	Tetramer (D1$_4$)	Pentamer (D1$_5$)	Hexamer (D1$_6$)	Intermediate Complex
No salt	33	8	9	3	3	44
AgOAC	30	19	12	8	5	26
$Zn(acac)_2$	19	32	8	4	6	31
$ZnCl_2$	25	25	8	7	5	30
$Ca(NO_3)_2$	14	16	5	11	10	44
$Ca(ClO_4)_2$	22	13	8	2	2	53
$BiCl_3$	27	55	11	3	4	0
$CuCl_2$	32	30	21	6	7	0

Table 2.1. Product distribution of the library of disulfides **D1$_2$** – **D1$_6$** from the oxidation of (**1**) using different metal salts additives. The number in each cell shows the relative yield of each species.

We attempted to demonstrate the directing behavior of Cu^{II} in the self-assembly reaction by oxidizing a different ligand in the presence of this additive. We chose ligand (**3**) since disulfide derivatives from this system have been previously reported with $SbCl_3$ as the additive.[8] Upon the addition of I_2 and $CuCl_2$ to (**3**), both dimer **D3₂** and tetrahedron **D3₄** formed as the main products, similar to the previously published results (Figure 2.3). However, we observed that the product distribution was different, depending on the additive that was used. For instance, keeping the equivalents of the reagents constant (1 equiv. ligand to 3 equiv. I_2 to 1.5 equiv. salt), the ratio of **D3₂** and **D3₄** was quantified as 3:1 in the system with Sb^{III} and 1.8:1 in the system with Cu^{II}. This data demonstrated that the identity of the additive could be another way to control product distribution during macrocyclic disulfide synthesis, in addition to the well-known and commonly used factors, such as solvent and concentration.[17] **D3₄** has traditionally been a harder target to synthesize than **D3₂** due to entropic effects; therefore, our ability to increase the yield of **D3₄** by 1.5-fold just by substituting the additives highlights the role of Cu^{II} in "templating" the formation of this large 3D cage.

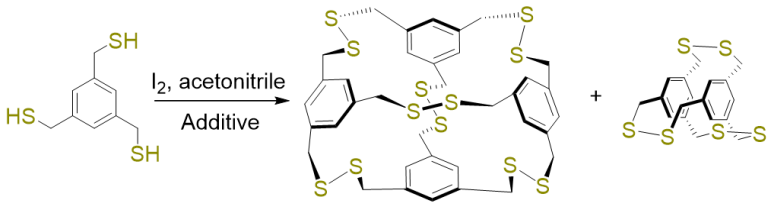

(3) (D3₄) (D3₂)

Additive	Yield of D3₄	Yield of D3₂	Total yield
Sb^{III}	22%	66%	88%
Cu^{II}	29%	53%	82%

Figure 2.3. Synthesis of **D3₄** and **D3₂** along with respective yields from the oxidation of (**3**) with two different metal ion additives. While the total yield does not change significantly with the choice of additive, Cu^{II} favors the more elusive tetrahedron **D3₄**.

Knowing that Cu^{II} can replicate the behavior of the Pn additives in our protocol, we turned to the self-assembly of naphthalene-based thiols due to the absence of cyclophanes formed from these building blocks. Previously, the crystal structure of trimer **D4$_3$** was reported from the serendipitous oxidizing reaction shown in Scheme 2.2, but a directed synthesis was not yet reported. We thus oxidized (**4**) with I_2 in the presence of $CuCl_2$ in acetonitrile. The Cu^{II} additive was lost during reaction work-up with Na_2SO_3, giving **D4$_3$** as a dominant product in ~80% yield (Scheme 2.4).

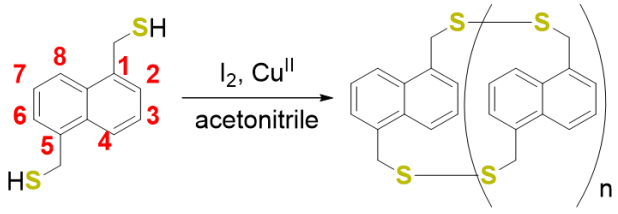

Ligand	Substitution	Products observed
(4)	1,5-naphthalene	Dominantly trimer
(5)	1,4-naphthalene	Dimer to pentamer
(6)	2,6-naphthalene	Dimer to hexamer

Scheme 2.4. Oxidation of thiols (**4**), (**5**) and (**6**) to give a library of different-sized naphthalene-based disulfide macrocycles. Same reaction condition for all three thiols result in different types of macrocycle: (**4**) gives mostly trimer disulfide while (**5**) gives dimer to pentamer disulfides, and (**6**) gives dimer to hexamer disulfides.

The straight-forward synthesis of **D4$_3$** with Cu^{II} encouraged us to try oxidizing other thiols that are isomers of (**4**). We experimented on the self-assembly of thiols (**5**) and (**6**) using our newly discovered Cu^{II} additives while keeping the same reaction condition as that for the oxidation of (**4**) (Scheme 2.4). We observed different product distributions when (**5**) and (**6**) were the starting materials. While in all three cases trimer disulfide cyclophanes still formed in the highest yield, the secondary products had very

different distributions. Instead of the highly selective formation of **D4$_3$** as observed with the system with (**4**), trimer **D5$_3$** formed in 43% yield along with a product distribution from dimer to pentamer **D5$_2$** – **D5$_5$** and trimer **D6$_3$** formed in 45% yield along with the remainder of products ranging from dimer to hexamer **D6$_2$** – **D6$_6$**.

Single crystals suitable for X-ray diffraction for **D5$_2$** and **D6$_2$** were obtained, confirming the success of our method (Figure 2.4). There are significant differences between the single crystals of these two isomers. While **D5$_2$** crystallizes in the $P2_1/n$ space group, **D6$_2$** crystallizes in the Aba2 space group. **D5$_2$** experiences less strain than **D6$_2$**, as the naphthalene groups in **D5$_2$** only bend 2.25^o from planarity compared to the 7.82^o bend angle observed in **D6$_2$**. Both structures possess C–S–S–C torsion angles deviating substantially from ideality (90°): 69.44^o for **D5$_2$** and 79.78^o and 68.70^o for **D6$_2$**. We observe π···π stacking in **D5$_2$**, where one aromatic ring of one naphthalene unit is in close contact with another aromatic ring of a naphthalene unit adjacent to it, resulting in multiple parallel π···π patterns in the crystal. The π···π stacking distance is 3.65 Å between aromatic rings. On the other hand, we do not observe any similar interactions in the stacking pattern of **D6$_2$**, perhaps because the aromatic rings cannot be perfectly angled in such a strained structure.

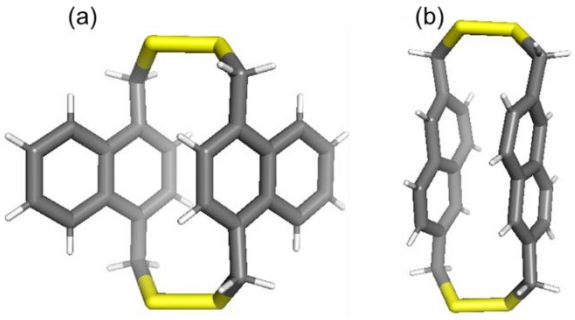

Figure 2.4. Single crystal structure of naphthalene-based dimer disulfide structures (a) **D5$_2$** (1,4-substitution) and (b) **D2$_6$** (2,6-substitution).

Due to the dominance of dimeric and tetrameric species resulting from traditional stepwise approaches, we conducted sulfur extrusion on the trimeric disulfides **D5$_3$** and **D6$_3$** to give trimeric thioethers **T5$_3$** and **T6$_3$**. These are the first examples of symmetrical naphthalene-bridged thioether cyclophanes, and one of the rare non-dimeric cyclophane structures in the literature. Each thioether shows only one singlet in the methylene region (~ 3 – 4 ppm) of the NMR spectra, indicating complete sulfur extrusion on all three sulfurs of each trimer cyclophane. The aromatic region of **T5$_3$**, featuring two multiplets and one singlet, supports the 1,4-isomer naphthalene core, whereas the spectrum of **T6$_3$** features two doublets and one singlet, confirming the 2,6-isomer naphthalene core (Figure 2.5).

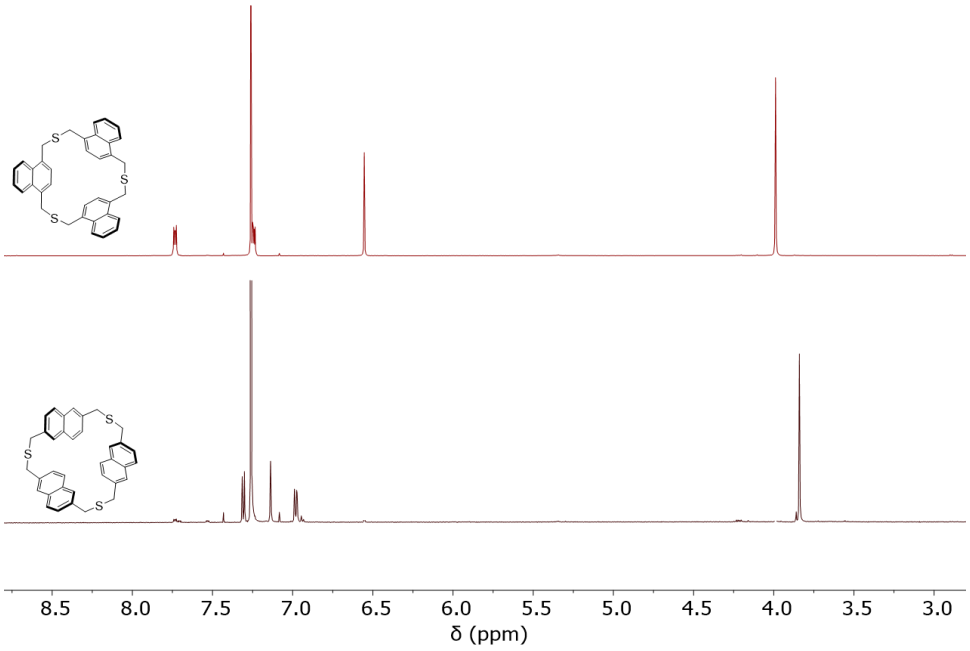

Figure 2.5. ^{1}H NMR spectra of two new naphthalene-based trimer thioether cyclophanes: (top) **T5$_3$** and (bottom) **T6$_3$** ($CDCl_3$ – 7.26 ppm).

Conclusions

This chapter reported NMR spectroscopic evidence that the Sb^{III} additive serves as a stoichiometric reagent in the self-assembly reaction of thiol ligands into discrete disulfide macrocycles. NMR spectroscopy was successfully utilized for the screening of metal additives that could replicate the behavior of Sb^{III}, in which Bi^{III} and Cu^{II} arose as good candidates to substitute for the mildly toxic Sb^{III} additive. Further studies with Cu^{II} revealed that this metal ion is an excellent choice to assist in the formation of both known and new cyclophanes from simple thiol building blocks. Single crystal structures confirmed the formation of new families of naphthalene-based disulfide and thioether cyclophanes synthesized from this new metal additive. The ease of removing Cu^{II} from the reaction and its solubility in polar solvents like acetonitrile suggest future possibility for scale-up self-assembly reactions in such solvent systems.

Experiment section

^{1}H NMR spectra were measured using Varian INOVA and Bruker 500 and 600 MHz spectrometers and ^{13}C Bruker-600 spectrometer in $CDCl_3$ and C_6D_6. Spectra were referenced using the residual solvent resonances as internal standards and reported in ppm. Single crystal X-ray diffraction studies were performed on a Bruker SMART APEX diffractometer. Commercially available reagents were used as received. The reported yields are for isolated samples.

Quantitative Study of the Role of $SbCl_3$

A quantitative study of Pn-assisted iodine oxidation was performed. First, stock solutions of (**1**) and I_2 were made. In a 20 mL scintillation vial, (**1**) (11.6 mg, 0.068 mmol) was dissolved in 2.5 mL of $CDCl_3$. In a separate 20 mL scintillation vial, I_2 (35 mg, 0.136 mmol) was dissolved in 2.5 mL of $CDCl_3$. Each NMR experiment contained 0.5 mL from the (**1**) stock and 0.5 mL from the I_2 stock. A stock solution of $SbCl_3$ was then made with 7.7 mg in 2.5 mL of $CDCl_3$. The amount of $SbCl_3$ was varied from 0.3 to 0.7 equiv. For each reaction, NMR spectra was recorded as a function of time: 1 min after all of the reagents were added, 5 min, 15 min, 30 min, 1 h, 3 h, 5 h, overnight, and over 2 days.

Quantitative Study for Alternative Thiophilic Metals.

In separate NMR tubes, 0.85 mg of (**1**) (0.005 mmol) and 2.54 mg of I_2 (0.010 mmol) along with 0.010 mmol of each salt were added to acetone-d_6. The salts tested were $AgOA_C$, $Zn(acac)_2$, $ZnCl_2$, $Ca(NO_3)_2$, $Ca(ClO_4)_2$, $BiCl_3$ and $CuCl_2$. Each reaction was monitored *via* NMR spectroscopy. The methylene protons corresponding to the discrete disulfide macrocycles were integrated in comparison to unreacted starting material and intermediate metal-thiol complex.

General Conditions for Cu^{II} additive in the oxidation of dithiol ligand to produce disulfides

In a 100 mL round bottom flask, (**1**) (25.5 mg, 0.30 mmol) and I_2 (51.2 mg, 0.30 mmol) were added in 50 mL acetonitrile. $CuCl_2{\cdot}2H_2O$ (51.2 mg, 0.30 mmol) was added in the flask and the solution was stirred for two hours. The reaction was quenched with

saturated sodium sulfite and extracted with ethyl acetate. The organic layer was washed with deionized water (2X). The solution was dried with $MgSO_4$, filtered and concentrated. The powder was then redissolved in 3 mL of chloroform and purified by GPC (96% combined yield: 32% dimer; 30% trimer, 21% tetramer; 6% pentamer; 7% hexamer).

Synthesis $D3_4$ and $D3_2$ using Cu^{II} and Sb^{III}

In two separate NMR tubes, (**3**) (0.54 mg, 0.0025 mmol) and I_2 (1.90 mg, 0.0075 mmol) were added in 1.6 mL acetonitrile-d_3. $CuCl_2{\cdot}2H_2O$ (0.638 mg, 0.0038 mmol) was added to the first tube and $SbCl_3$ (0.85 mg, 0.0038 mmol) was added to the second tube. NMR spectra were taken immediately after all the reagents were added in.

Synthesis of naphthyl thiacyclophane $D4_3$

In two separate NMR tubes, (**4**) (0.55 mg, 0.0025 mmol) and I_2 (1.27 mg, 0.0050 mmol) were added in 1.6 mL acetonitrile-d_3. $CuCl_2{\cdot}2H_2O$ (0.341 mg, 0.0020 mmol) was added to the first tube and $SbCl_3$ (0.454 mg, 0.0020 mmol) was added to the second tube. NMR spectra were taken immediately after all the reagents were added in.

Synthesis of 1,4-naphthalene disulfide structures ($D5_2$ – $D5_6$)

In a 50 mL round bottom flask, 1,4-naphthalene dithiol (**5**) (11 mg, 0.050 mmol) and I_2 (38 mg, 0.15 mmol) were added in 15 mL acetonitrile. $CuCl_2{\cdot}2H_2O$ (6.8 mg, 0.040 mmol) was added to the flask. The solution was stirred for 30 minutes. Reaction was quenched with saturated sodium sulfite and diluted with toluene. The organic layer was washed

with deionized water (2X). The solution was dried with $MgSO_4$, filtered and concentrated. The powder was then redissolved in 3 mL of chloroform and purified by GPC (96% combined yield: 26% dimer; 43% trimer, 16% tetramer; 8% pentamer; 3% hexamer). ^{1}H NMR (500 MHz, C_6D_6, 70^{o}C): dimer: δ 7.76-7.78 (m, 4H, $C_{10}H_2$), 7.29-7.31 (m, 4H, $C_{10}H_2$), 6.10 (s, 4H, $C_{10}H_2$), 3.65 (s, 8H, CH_2); $^{13}C\{^1H\}$ NMR (125 MHz, $CDCl_3$): δ 134.63, 131.65, 126.62, 125.79, 124.59, 43.16 ppm; trimer: δ 8.03-8.05 (m, 6H, $C_{10}H_2$), 7.52-7.54 (m, 6H, $C_{10}H_2$), 6.89 (s, 6H, $C_{10}H_2$), 4.02 (s, 12H, CH_2); $^{13}C\{^1H\}$ NMR (125 MHz, $CDCl_3$): δ 133.06, 131.75, 128.00, 126.27, 124.89, 41.72 ppm; tetramer: δ 7.96-7.98 (m, 8H, $C_{10}H_2$), 7.51-7.53 (m, 8H, $C_{10}H_2$), 6.92 (s, 8H, $C_{10}H_2$), 3.85 (s, 16H, CH_2); $^{13}C\{^1H\}$ NMR (125 MHz, $CDCl_3$): δ = 133.28, 131.70, 127.56, 126.27, 124.97, 41.85 ppm; pentamer: δ 7.88-7.90 (m, 10H, $C_{10}H_2$), 7.47-7.49 (m, 10H, $C_{10}H_2$), 6.86 (s, 10H, $C_{10}H_2$), 3.83 (s, 20H, CH_2); $^{13}C\{^1H\}$ NMR (125 MHz, $CDCl_3$): δ 133.20, 131.68, 127.59, 126.23, 124.93, 41.51 ppm. Single crystals of **D5$_2$** were grown by slow evaporation of a concentrated of **D5$_2$** solution in chloroform.

Synthesis of thioether T5$_3$

An oven-dried NMR tube was charged with 1,4-naphthalene trimer disulfide **D5$_3$** (5.0 mg, 0.008 mmol) in dried chloroform-*d* (1 mL). Under a cone of nitrogen, HMPT (9 μL, 0.049 mmol) was added to the NMR tube and the tube was inverted gently several times to mix. The reaction was allowed to sit at ambient temperature for 2 hours. The solution was then concentrated, and the crude solid was sonicated with 30 mL of deionized water giving a cloudy white solution. The solid was separated from its aqueous counterpart by centrifugation and washed a second time with fresh deionized water. ^{1}H NMR (500 MHz,

$CDCl_3$): δ 7.73-7.74 (m, 6H, $C_{10}H_2$), 7.23-7.25 (m, 6H, $C_{10}H_2$), 6.55 (s, 6H, $C_{10}H_2$), 3.99 (s, 12H, CH_2); $^{13}C\{^1H\}$ NMR (125 MHz, $CDCl_3$): δ 33.50, 131.73, 126.06, 125.63, 124.62, 34.36 ppm.

Synthesis of 2,6-naphthalene disulfide structures ($D6_2$ – $D6_5$)

In a 50 mL round bottom flask, 2,6-naphthalene dithiol (**6**) (10 mg, 0.045 mmol) and I_2 (34.6 mg, 0.136 mmol) were added in 15 mL acetonitrile. $CuCl_2{\cdot}2H_2O$ (6.2 mg, 0.036 mmol) was added to the flask. The solution was stirred for 30 minutes. The reaction was quenched with saturated sodium sulfite and diluted with toluene. The organic layer was washed with deionized water (2X). The solution was dried with $MgSO_4$, filtered, and concentrated. The powder was then redissolved in 3 mL of chloroform and purified by GPC (90% combined yield: 30% dimer; 45% trimer, 10% tetramer, 5% pentamer). ^1H NMR: dimer: δ 7.27 (d, 4H, $C_{10}H_2$), 7.16 (d, 4H, $C_{10}H_2$, J = 8.5 Hz), 6.92 (s, 4H, $C_{10}H_2$), 3.86 (d, 4H, CH_2, J = 15.0 Hz), 3.57 (d, 4H, CH_2, J = 15.0 Hz); $^{13}C\{^1H\}$ NMR (125 MHz, $CDCl_3$): δ 136.29, 131.33, 127.68, 127.18, 126.55, 45.45 ppm; trimer: δ 7.58 (d, 6H, $C_{10}H_2$, J = 8.0 Hz), 7.38 (s, 6H, $C_{10}H_2$), 7.18 (d, 6H, $C_{10}H_2$, J = 8.5 Hz), 3.69 (s, 12H, CH_2); $^{13}C\{^1H\}$ NMR (125 MHz, $CDCl_3$): δ 134.45, 132.51, 128.41, 128.24, 127.94, 43.52 ppm; tetramer: δ 7.51 (d, 8H, $C_{10}H_2$, J = 8.5 Hz), 7.47 (s, 8H, $C_{10}H_2$), 7.18 (d, 8H, $C_{10}H_2$, J = 8.0 Hz), 3.54 (s, 16H, CH_2). Single crystals of **$D6_2$** were grown by slow evaporation of a concentrated of **$D6_2$** solution in chloroform.

Synthesis of thioether T6$_3$

An oven-dried NMR tube was charged with 2,6-naphthalene trimer disulfide **D6$_3$** (4.5 mg, 0.007 mmol) in dried chloroform-*d* (1 mL). Under a cone of nitrogen, HMPT (8 µL, 0.044 mmol) was added to the NMR tube and the tube was inverted gently several times to mix. The reaction was allowed to sit at ambient temperature for 2 hours. The solution was then concentrated, and the crude solid was sonicated with 30 mL of deionized water giving a cloudy white solution. The solid was separated from its aqueous counterpart by centrifugation and washed a second time with fresh deionized water, giving a white solid in 70% yield. ^{1}H NMR (500 MHz, $CDCl_3$): δ 7.31 (d, 6H, $C_{10}H_2$, J = 7.0 Hz), 7.14 (s, 6H, $C_{10}H_2$), 6.98 (d, 6H, $C_{10}H_2$, J = 7.0 Hz), 3.84 (s, 12H, CH_2); $^{13}C\{^1H\}$ NMR (125 MHz, $CDCl_3$): δ 136.23, 132.05, 128.29, 127.47, 127.44, 36.99 ppm.

CHAPTER III

SYNTHESIS AND PRODUCT DISTRIBUTION OF A LIBRARY OF BIPHENYL-BASED MACROCYCLIC CYCLOPHANES: A CLOSER LOOK AT HOW DYNAMIC COVALENT CHEMISTRY IS A GREAT ASSET FOR CYCLOPHANE SYNTHESIS

Introduction

The search for bioactive compounds can be understood as searching for a molecular key for a biological lock.[1] Traditionally, there are two approaches to identify the right compound: (a) rational design, which looks for a single correct key or (b) combinatorial chemistry, which generates a vast collection of keys that are assayed by high throughput screening to determine which one is the right fit. A third approach, dynamic covalent chemistry (DCC), generates interconverting keys resulting from all the possible combinations of fragments. Contrasting to approach (b), which is based on extensive libraries of pre-synthesized keys, DCC implements the reversible connection of components to give "virtual" libraries, which comprise all possible keys that may be generated. The overall process thus bypasses the need to actually synthesize all possible compounds by letting the target act as a template and perform the assembly of the optimal compound from a virtual set of components. This approach reveals the key composition that has the strongest interaction with the lock (thermodynamic control) or the key that forms fastest within the lock (kinetic control) (Figure 3.1).

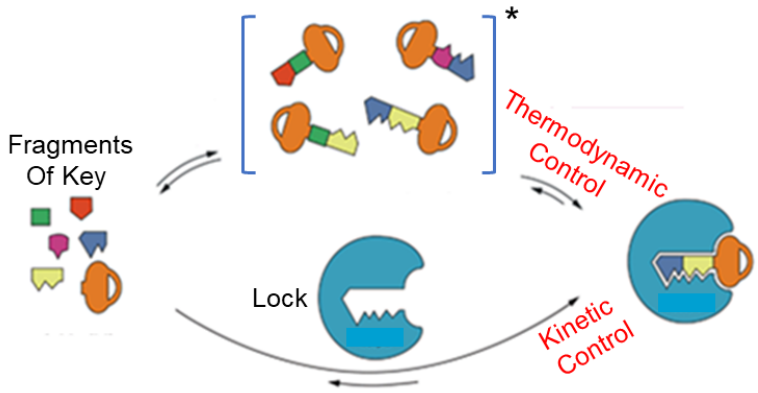

Figure 3.1. Representation of the principle of DCC as applied to the discovery of bioactive compounds. A dynamic library of keys is generated from reversibly connecting fragments. * Denotes a virtual dynamic library. Reproduced with permission from *Chem. Soc. Rev*. **2007**, *36* , 151–160 - Published by The Royal Society of Chemistry.

DCC has been utilized not only in the search for bioactive substances but also in the field of supramolecular synthetic chemistry. While traditional syntheses have provided many elegant examples of 2D and 3D cyclophanes,[2] stepwise syntheses have been a bottleneck to new synthetic discoveries. Particularly, many classical macrocycles were not accessible without the use of the high dilution principle,[3] which is necessary to minimize the formation of competing polymerization reactions from cross-couping of reactive precursors. DCC, on the other hand, has provided a powerful new route for synthesis of macrocycles by generating multiple equilibrating products and semi-stable intermediates. Reactions can proceed along kinetic or thermodynamic pathways, depending on chosen reaction conditions. This feature of DCC is an improvement over the high dilution principle, which among many disadvantages, limits the possibility of using concentration as a factor to control product distribution. A recently published 3D adaptive cage, for instance, was synthesized through the combination of multiple reversible chemistries.[4] Incorporating three different functional groups (thiols, aldehydes

and hydrazides) into two building blocks led to strongly fluorescent hydrazone- and disulfide-based tripodal and tetrapodal aromatic cage-type architectures (Figure 3.2). While various polymeric, macrocyclic and cage constituents could be expressed in the system, the cage was the only constituent formed predominantly due to favorable π-π stacking and hydrogen bonds. The cage could also deliberately disassemble through controlled component exchange, highlighting the desirable repeated bond breaking/forming property of DCC.

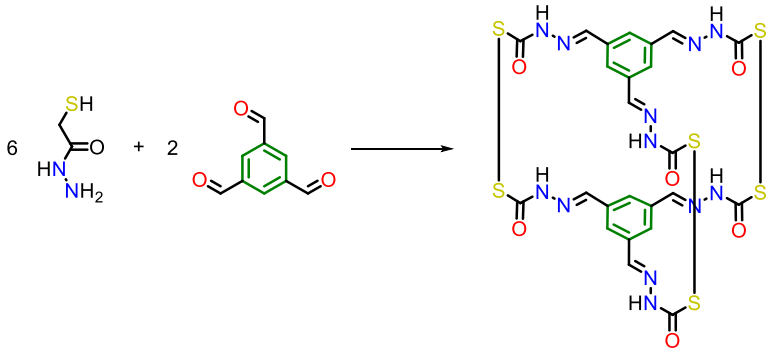

Figure 3.2. Generation of dynamic combinatorial libraries from aromatic aldehyde, thiol and hydrazide using hydrazone and disulfide reversible covalent reactions. The highly fluorescent cage arises as a thermodynamically stable product.

Besides understanding the reversible behavior of DCC bonds to prepare new architectures with unusual topologies, controlling product distribution is another main interest of the DCC field. A system in which self-assembly can direct DCC bond formation towards two different types of products was recently reported (Figure 3.3).[5] The authors designed an amphiphilic building block functionalized with two thiol groups. Under basic conditions, thiol-disulfide exchange occurred, enabling the formation of cyclic oligomers. Without stirring, self-assembly of cyclic trimers and tetramers into a

mixture of large macrocycles (up to 51mers) was observed (Figure 3.3, left). With stirring, the autocatalytic emergence of a single species of hexamers occurred (Figure 3.3, right). Such behavior is reminiscent of theories on the origin of life and the role of autocatalysis in the emergence of specific molecules.[6]

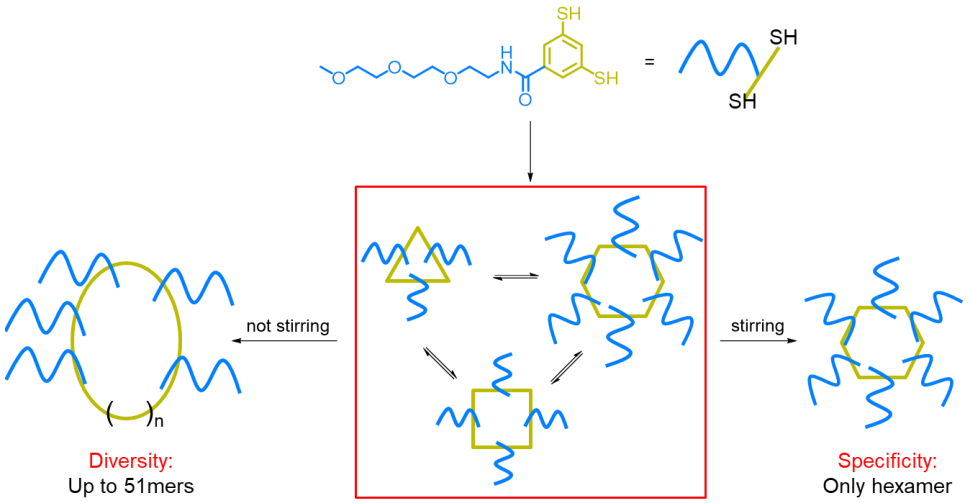

Figure 3.3. Dynamic combinatorial chemistry of one building block leading to two different pathways: specificity or diversity.

As discussed in chapter II, the promising behavior of our pnictogen ions within thiol disulfide exchange environments led our laboratory to apply dynamic covalent reactivity toward synthesizing cyclophanes.[7] The disulfide products are formed under thermodynamic control, where dithiols yield 2D macrocycles and trithiols yield more complex 3D cages. These disulfide derivatives can be covalently captured as their more stable thioether analogs, and the overall two-step process proceeds in very high yields in less than two days.[8] We wanted to see these approaches applied to the preparation of

other unknown cyclophane structures for both fundamental study and applications in organic and/or fluorescent materials. We will show in this chapter that our tandem approach of dynamic covalent self-assembly and sulfur extrusion can synthesize new symmetrical biphenyl-linked disulfide and thioether macrocycles, which are variants of the venerable phenyl-bridged paracyclophane "nanohoops" (Scheme 3.1).

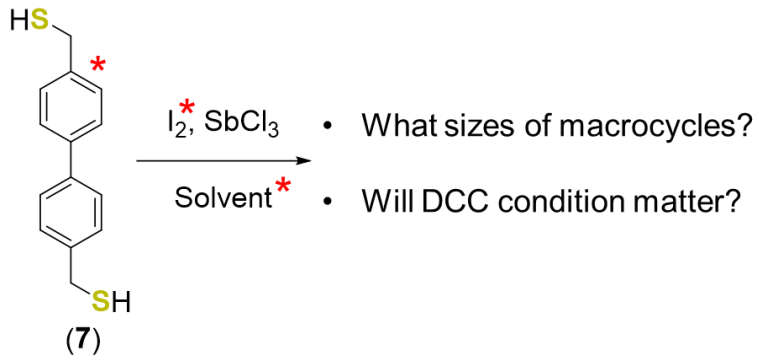

Scheme 3.1. Proposed metal-directed self-assembly of ligand (**7**) into different-sized macrocycles and manipulation of disulfide product distribution based on small changes in DCC reaction conditions. Red asterisks denote conditions that are varied in the study.

In both DCC and metal-directed self-assembly, the various interactions between ligands, metal ions – solvent, ligands – metal ions, and ligands – solvent are under dynamic exchange, leading us to hypothesize that the nature of our equilibrating disulfides is sensitive to reaction conditions; therefore, we expect that by tuning the reaction conditions, we can favor targeted members of the associated libraries in high yield. This chapter will also highlight multiple studies on different thermodynamic conditions (such as solvent, reagent equivalents, and concentration – denoted as asterisks in Scheme 3.1) that can affect the yield of each species in the library.

Results and Discussion

Synthesis of a new library of disulfide and thioether macrocyclic cyclophanes from thiol building block (7)

We decided to investigate a new thiol ligand to form a library of 2D macrocycles. Self-assembly of ligand (**7**) gave a collection of different-sized disulfide macrocycles (Scheme 3.2).[9] Gel permeation chromatography (GPC) separated the mixture of disulfides into four different species, which we categorized as dimeric to pentameric disulfide macrocycles **D7**$_2$ – **D7**$_5$. ^{1}H NMR spectra of disulfide compounds **D7**$_2$ – **D7**$_5$ showed identical signals: each features a set of doublets in the aromatic region and one single methylene signal, confirming the repetitive biphenyl units.

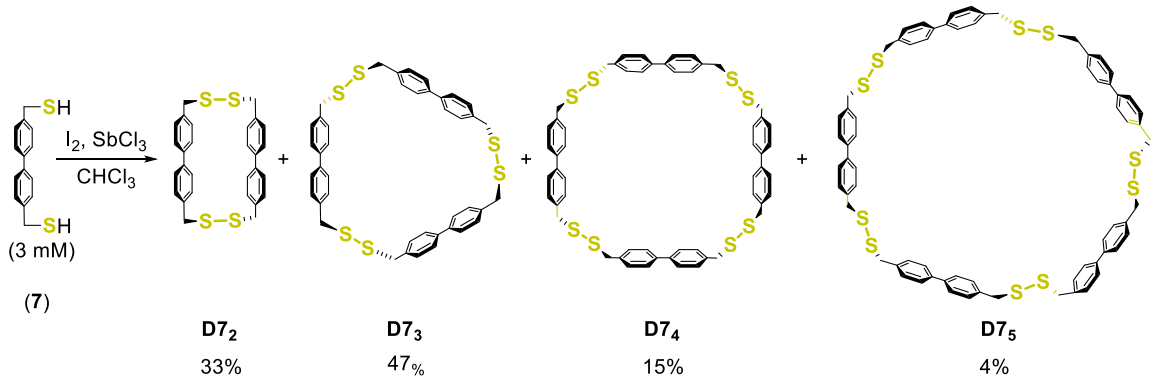

Scheme 3.2. Self-assembly of thiol (**7**) to give a library of new disulfide macrocycles **D2**$_7$ – **D7**$_5$.

Macrocycles larger than the pentamer **D7**$_5$ were not observed in any reaction conditions, in contrast to the presence of the hexamer in the oxidation reaction of thiol (**6**) and heptamer in the oxidation reaction of thiol (**1**) (Figure 3.4). Self-assembly reaction of thiol (**8**), on the other hand, only gives dimeric and trimeric disulfide macrocycles, regardless of reaction conditions. Experimental data from these four self-assembly

reactions suggests that the more rigid thiols tend to give a more diverse library of disulfide macrocycles, such as in the case of (**1**) and (**6**). Moderately flexible thiols like (**7**) give higher-ordered species, though the reaction tends to favor smaller-sized rings due to entropic effects. Flexible thiols like (**8**) seems to only give lower-ordered species like dimers and trimers. Previous studies in our laboratory on As_2L_3 and Sb_2L_3 cryptands (where L is a dithiolate ligand) revealed that small differences in ligand geometries can result in significant differences in the helicity of the metal–ligand cryptands and the stereochemistry of the metal coordination within the assembled complexes.[10] We are thus not surprised that small differences in ligand flexibility can now also have a significant effect on the type of self-assembled macrocycles that can form in solution. Future studies will incorporate other thiols of different degrees of flexibility to verify this hypothesis.

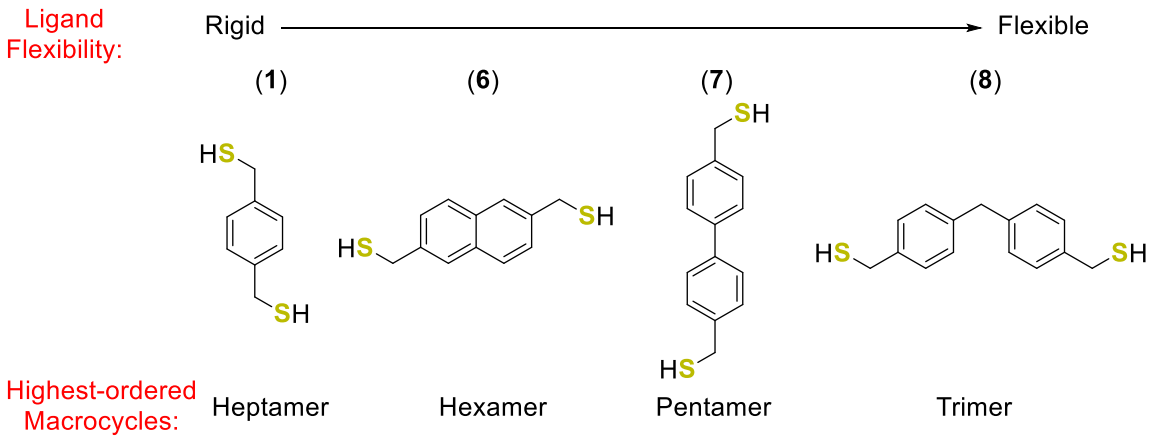

Figure 3.4. Some dithiols that have been oxidized using our metal-directed self-assembly approach. More flexible thiols tend to give lower-ordered species such as dimeric or trimeric disulfide macrocycles.

The disulfide species **D7**$_2$ – **D7**$_5$ are under dynamic equilibrium, but they can be covalently trapped *via* sulfur extrusion to generate the more stable thioethers **T7**$_2$ – **T7**$_5$. Similar types of signals are observed in the spectra for the thioethers (two doublets and

one singlet) with the methylene signals shifting downfield going from disulfide to thioether macrocycles. We were able to grow single crystals of thioethers **T7$_2$**, **T7$_3$** and **T7$_4$** (Figure 3.5). While both compound **T7$_2$** and **T7$_3$** crystallize in space group P21/c, **T7$_4$** crystallizes in space group P-1. A closer study of the crystal structures suggests that **T7$_2$** is structurally more similar to **T7$_4$** than **T7$_3$**, which is reasonable since **T7$_4$** can be viewed as two molecules of **T7$_2$**. For example, the dihedral angles in the biphenyl units of **T7$_2$** and **T7$_4$** are similar to each other and both show deviation from the typical 32° dihedral angle[11] found in unstrained biphenyls (36.68° and 49.94° for **T7$_2$** and 36.30^o and 48.66^o for **T7$_4$**). **T7$_3$**, on the other hand, possesses very different dihedral angles of 3.40°, 6.52° and 46.90°. While the thioether motifs of **T7$_4$** twist outward to allow the biphenyl units to fold-in to minimize the cavity volume, **T7$_3$** crystalizes with a molecule of chloroform solvent to occupy the empty pore. The C–S–C angles within the cyclophanes are all in the expected range 100 – 105^o for cyclic thioethers.[12]

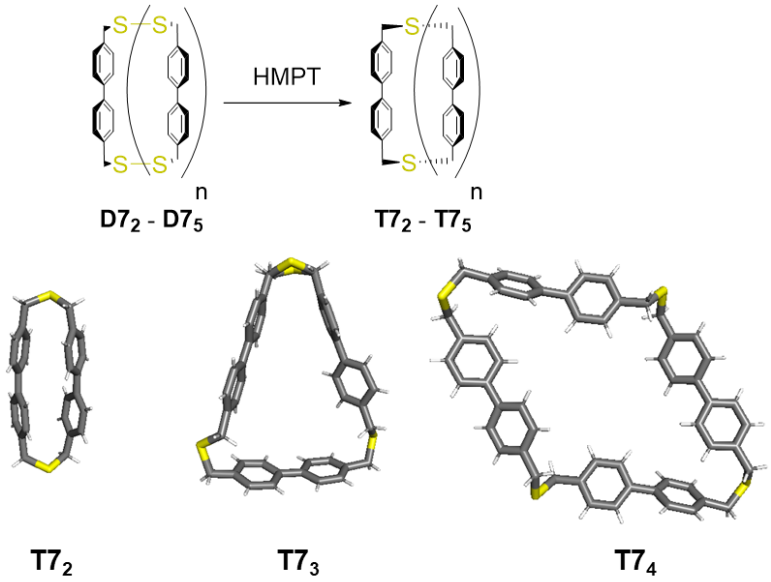

Figure 3.5. Sulfur extrusion of disulfides **D7$_2$** – **D7$_5$** gives rise to thioethers **T7$_2$** – **T7$_5$**. Crystal structures of **T7$_2$**, **T7$_3$** and **T7$_4$** are shown at the bottom.

Controlling product distribution ***D7₂ – D7₅***

Although reaction time, solvent, and concentration effects are all well-known to affect distributions in dynamic covalent mixtures[13], they are not well-studied in the context of pnictogen additives to disulfide libraries. We sought to investigate these effects on our self-assembling systems of thiol (**7**). The first condition that we chose to modify is solvent since we have observed that the ability of the solvent to solubilize any oligomeric reaction intermediates is an important property in limiting the precipitation of insoluble oligomers.[14] Self-assembly of thiol (**7**) produces four disulfide species of different sizes (**D7₂** – **D7₅**). We found that at 3 mM of (**7**), 2 equiv. I_2 and 2 equiv. $SbCl_3$, **D7₃** is the dominant species across all solvents (Table 3.1). The yield of **D7₃** is ~50% in reaction with chloroform or benzene while the yield of this compound can be optimized to 75% with tetrachloroethane (TCE) as the solvent, suggesting that TCE may interact with **D7₃** and increase the relative stability of this compound over **D7₂**, **D7₄**, and **D7₅**. In general, at 3 mM solution, **D7₂** and **D7₄** form in ~15 – 30% while **D7₅** is the least dominant species across all systems, which is reasonable due to entropic effects.

Solvent	D7₂	D7₃	D7₄	D7₅
Chloroform	33	47	15	4
Dichloromethane	11	64	17	6
Benzene	21	56	17	5
Toluene	30	66	3	-
Tetrachloroethane	12	75	13	-

Table 3.1. Solvent effect observed in the oxidation reaction of thiol (**7**). **D7₃** is the dominant species across all solvents. Reactions ran at 3 mM solution.

We next investigated the effect of concentration on the product distribution of **D7$_2$** – **D7$_5$**. We ran NMR scale reactions on 1 equiv. (**7**), 2 equiv. I_2 and 2 equiv. $SbCl_3$ in the solvent systems listed in Table 3.1. For each solvent, we ran the reaction in a range of 0.125 mM to 6 mM thiol concentration (Figure 3.6). We hypothesized that at lower concentrations, the formation of higher-ordered macrocycles will be prevented, as it is harder for one building block to have access to multiple others due to the presence of many interfering solvent molecules. In this case, we expect ligand–solvent interactions to dominate over ligand–ligand interactions, favoring the formation of lower-ordered species such as dimers and trimers. Our experimental data aligns with our hypothesis, as seen in Figure 3.6. As concentration decreases, the yields of **D7$_4$** and **D7$_5$** decrease and these two compounds stop forming at ~ 1 mM solution. **D7$_3$** is the dominant species in the range of 2 – 6 mM solution, but totally disappear at 0.125 mM. This concentration is where **D7$_2$** becomes the only species in solution (Figure 3.6, top spectrum). We conclude that the reaction's concentration has a profound effect on the amount of each disulfide species.

We were curious if the dominance of **D7$_2$** at low concentration can be replicated using a different amount of I_2. We repeated the reactions with 1 equiv. (**7**), 2 equiv. $SbCl_3$ and increased the amount of I_2 to 4 equiv. To our surprise, the yield of each disulfide species hardly changes, even at highly diluted conditions (Table 3.2). **D7$_2$**, which is

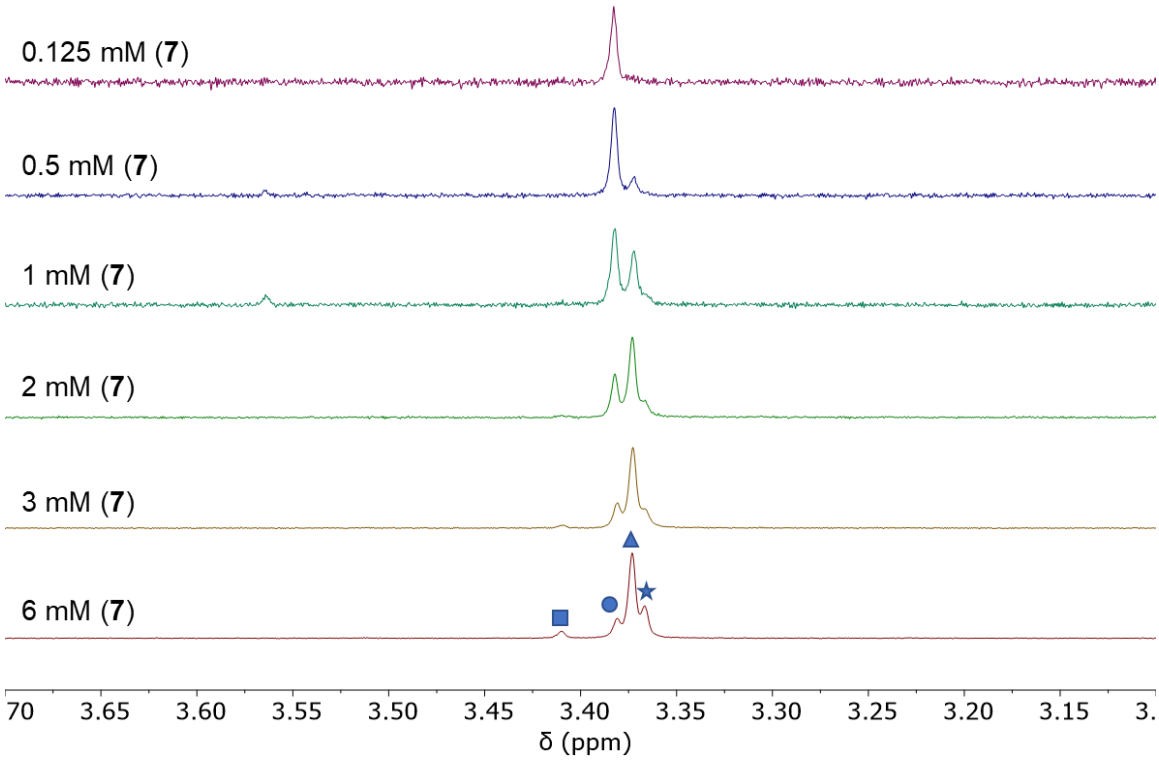

Figure 3.6. Product distribution of **D7$_2$** to **D7$_6$** as the concentration of (**7**) is changed from 6 mM to 0.125 mM in C_6D_6. Reaction condition: 1 equiv. (**7**), 2 equiv. I_2, 2 equiv. $SbCl_3$. Circle denotes **D7$_2$**, triangle denotes **D7$_3$**, star denotes **D7$_4$**, and square denotes **D7$_5$**.

expected to be the dominant species at low concentration, only has its yield increase by 1.2 times with a 24-fold dilution. **D7$_3$** continues to form in high yield across all concentrations, similar to the behavior observed in Table 3.1. It appears that at high equivalents of I_2, the reaction is not very dependent on ligand–solvent interactions and instead, favors other interactions such as ligand–I_2 interactions. This behavior is replicated across other solvent systems, suggesting that concentration effects do not play a significant role on the distribution of disulfide products at high equivalents of I_2. These studies show that our equilibrating disulfide species are very sensitive to changes in reaction conditions and can be interesting targets for future adaptive chemistry studies.

Concentration	**D7$_2$**	**D7$_3$**	**D7$_4$**	**D7$_5$**
3	38	47	12	3
1	41	43	12	4
0.5	43	41	11	4
0.25	49	40	11	-
0.125	48	44	8	-

Table 3.2. Product distribution of **D7$_2$** to **D7$_6$** as the concentration of (**7**) is changed from 6 mM to 0.125 mM in $CDCl_3$. Reaction condition: 1 equiv. (**7**), 4 equiv. I_2, 2 equiv. $SbCl_3$.

Conclusions

We have shown the synthesis of a new family of 8 biphenyl-based disulfide and thioether macrocycles. Solution and solid-state characterization tools confirmed the identity of these new macrocycles, which are promising targets for fundamental studies and materials chemistry application. By changing the internal handles (reagent equivalents, concentration, and solvent), we were able to regulate the disulfide distribution. These studies suggest that our equilibrating disulfides are very sensitive to reaction conditions. Further work will explore the external handles such as guests that might also affect the product distribution and utilize "Design of Experiments" (DOE) to optimize individual members of our equilibrating disulfides.[15]

Experimental procedure

^{1}H NMR spectra were measured using Varian INOVA and Bruker 500 and 600 MHz spectrometers and ^{13}C Bruker-600 spectrometer in $CDCl_3$ and C_6D_6. Spectra were referenced using the residual solvent resonances as internal standards and reported in ppm. Single crystal X-ray diffraction studies were performed on a Bruker SMART APEX

diffractometer. Commercially available reagents were used as received. The reported yields are for isolated samples.

Synthesis of biphenyl-based disulfides structures $D7_2$ – $D7_5$

In a 250 mL round bottom flask, (**7**) (148 mg, 0.60 mmol) and I_2 (427 mg, 1.68 mmol) were added in 100 mL chloroform. $SbCl_3$ (109 mg, 0.48 mmol) was added to the flask and the dark purple solution was stirred for 16 hours at room temperature. Reaction was quenched with saturated sodium sulfite and the organic layer was washed with deionized water (2X). The solution was dried with $MgSO_4$, filtered and concentrated. The powder was then redissolved in 3 mL of chloroform and purified by GPC (65% combined yield: 20% dimer; 32% trimer, 11% tetramer; 2% pentamer). ^{1}H NMR (500 MHz, $CDCl_3$): **D7$_2$**: δ = 7.13 (s, 8H, C_6H_2), 7.06 (d, 4H, C_6H_2), 6.96 (d, 4H, C_6H_2) 3.68 (s, CH_2), 3.61(s, CH_2); ^{13}C{^{1}H}NMR (125 MHz, $CDCl_3$): δ = 138.60, 137.46, 129.00, 126.27, 43.49 ppm; **D7$_3$**: δ = 7.50 (d, 12H, C_6H_2), 7.22 (d, 12H, C_6H_2), 3.60 (s, 12H, CH_2); ^{13}C{^{1}H}NMR (125 MHz, $CDCl_3$): δ = 139.42, 136.06, 130.03, 126.83, 42.85 ppm; **D7$_4$**: δ = 7.50 (d, 16H, C_6H_2), 7.28 (d, 16H, C_6H_2), 3.59 (s, 16H, CH_2); ^{13}C{^{1}H}NMR (125 MHz, $CDCl_3$): δ = 139.47, 136.41, 129.83, 126.94, 42.70 ppm; **D7$_5$**: δ = 7.49 (d, 20H, C_6H_2), 7.27 (d, 20H, C_6H_2), 3.63 (s, 12H, CH_2); ^{13}C{^{1}H}NMR (125 MHz, $CDCl_3$): δ = 139.41, 136.38, 129.79, 126.91, 42.82 ppm.

Synthesis of biphenyl-based thioethers structures $T7_2$ – $T7_5$

An oven-dried 250 mL round bottom flask was charged with the mixture of compound **D7$_2$ – D7$_5$** in dried chloroform (100 mL). The solution was sparged with N_2 for 25

minutes. HMPT (240 µL, 1.30 mmol) was added to the flask and the reaction was allowed to go for 2 days at 60°C with gentle stirring. The solution was then washed with deionized water and concentrated to give a slightly yellow solid. The solid was sonicated in methanol and filtered through a filter paper. The solid was dissolved in 3 mL of chloroform and purified by GPC (50% combined yield: 10% dimer; 28% trimer, 10% tetramer; 2% pentamer). ^{1}H NMR (500 MHz, $CDCl_3$): **T7$_2$**: δ = 6.97 (d, 8H, C_6H_2), 6.95 (d, 8H, C_6H_2), 3.86 (s, 8H, CH_2), $^{13}C\{^{1}H\}$NMR (500 MHz, $CDCl_3$): δ = 138.92, 137.08, 129.17, 126.48, 38.71 ppm; **T7$_3$**: δ = 7.38 (d, 12H, C_6H_2), 7.06 (d, 12H, C_6H_2), 3.75 (s, 12H, CH_2); $^{13}C\{^{1}H\}$NMR (500 MHz, $CDCl_3$): δ = 139.56, 138.25, 129.61, 127.05, 36.20 ppm; **T7$_4$**: δ = 7.39 (d, 16H, C_6H_2), 7.22 (d, 16H, C_6H_2), 3.70 (s, 16H, CH_2); **T7$_5$**: δ = 7.55 (d, 20H, C_6H_2), 7.35 (d, 20H, C_6H_2), 3.65 (s, 12H, CH_2); $^{13}C\{^{1}H\}$NMR (500 MHz, $CDCl_3$): δ = 139.53, 137.20, 129.71, 127.14, 35.08 ppm. Crystal of **T7$_2$**, **T7$_3$** and **T7$_4$** were grown by slow evaporation from a saturated solution of each compound in chloroform.

Product distribution of $D7_2 – D7_5$ in different solvents and concentrations

In a 20 mL scintillation vial, 6.6 mg of (**7**) (0.027 mmol) was added to 13.63 mg of I_2 (0.054 mmol) and 12.18 mg of $SbCl_3$ (0.054 mmol) in 4.47 mL $CDCl_3$ (6 mM solution). Serial dilutions were conducted until a concentration of 0.125 mM was reached. The reactions were allowed to proceed overnight and the solutions in each vial were analyzed through ^{1}H NMR spectroscopy to determine the product distribution. This procedure was repeated using C_6D_6, CD_2Cl_2, $C_2D_2Cl_4$, and $C_6D_6CD_3$.

* The same experiments were repeated using 27.26 mg of I_2 as the starting amount before serial dilutions. This amount represented 4 equiv. I_2. Experiment conducted in all deuterated solvents listed above.

CHAPTER IV

SYNTHESIS OF UNSYMMETRICAL 2D MACROCYCLES AND 3D "BASKET" CAGES: SELF-SORTING AS AN IMPORTANT ASSET FOR CYCLOPHANE SYNTHESIS

Introduction

Nature uses selective methods to construct complex biomolecular structures, often exploiting multiple weak interactions to direct the outcome.[1] This high selectivity depends on the information encoded in the species responsible for every recognition event.[2] For instance, the self-assembly of the DNA double helix requires the highly precise base-pairing of only complementary nitrogenous bases (adenine – thymine and cytosine – guanine).[3] Other small molecules of life such as carbohydrates, amino acids and fatty acids, are able to not only self-assemble to form macromolecules, but also to self-sort into a cell, where multiple levels of compartmentalization allow the coexistence of several different functional architectures.[4]

A popular method of mimicking complex biomolecular machines exploits the self-sorting[5] of different sets of molecules into a small number of well-defined molecular aggregates. By letting multiple individual components assemble into the final product, many challenging multi-component complexes have been reported.[6] In many cases, the mixture of different components leads to formation of homo-supramolecular assemblies, which is known as the process of narcissistic self-sorting.[7] Social self-sorting[8] is comparatively rare in supramolecular assemblies due to the difficulty of incorporating different components into a single unsymmetrical complex. In recent years, there has

been much research focusing on social self-sorted complexes through favorable secondary interactions. One example of such system is the first hetero-alternating supramolecular oligomer from two isomers of cinnamoyl α-cyclodextrin (red and yellow components in Figure 4.1).[9] In this case, hydrophobic interactions, π···π stacking and hydrogen bonding interactions function cooperatively to create an alternating oligomer, reminiscent of biological materials such as hemoglobin[10] that are composed of two kinds of building blocks. Self-sorting has also been efficiently utilized for the construction of other architectures such as 3D cages[11] and "meso-helicates".[12]

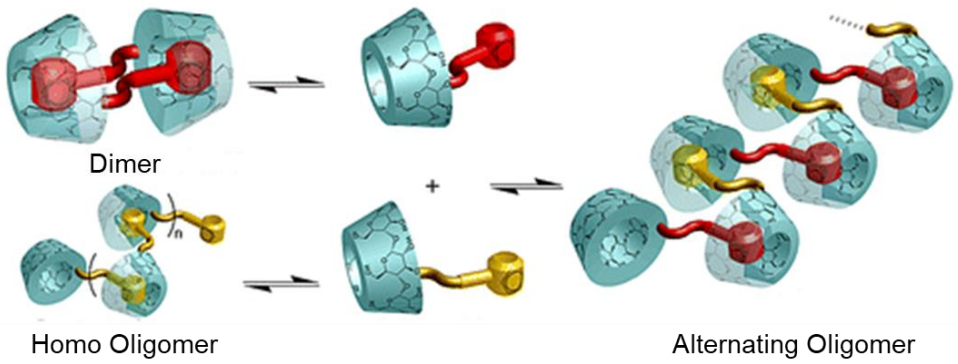

Figure 4.1. Social self-sorting of two isomers of cinnamoyl α-cyclodextrin to give alternating oligomer. Reprinted (adapted) with permission from *J. Am. Chem. Soc*. **2009**, *131*, 12339–12343. Copyright 2009 American Chemical Society

Self-sorting behavior has been introduced to materials science to increase the performance of organic materials.[13] For instance, the transcription of 2D information encoded in a monolayer on the surface of 3D supramolecular architectures has been described. The reactive monolayers are immersed in solutions containing propagators and a base catalyst to activate the thiol nucleophiles. Thiol-disulfide exchange then covalently captures the propagator and reproduces new thiolates on the surface for continuing

polymerization, giving self-sorted structures on the surfaces. This template-directed synthesis is shown to increase the activity of multicomponent photosystems by more than a factor of 12.

Besides utilizing self-sorting behavior to prepare new architectures with unusual topologies and properties, understanding the factors that can direct the formation of one type of self-sorted product is another main interest of the field. For instance, self-assembled imine-based macrobicyclic cryptand-type organic cages can display remarkable self-sorting behavior with high selectivity (Scheme 4.1).[14] In a mixture containing an amine and two different aldehydes differing by only one atom (a benzene core versus a pyridine core), only the pyridine-core aldehyde reacts with the amine to give an imine-based cage, leaving 100% of the benzene-core aldehyde unreacted by the end of the reaction. The exclusive formation of the pyridine cage is supported by attractive interactions between the pyridine N atom in one cage arm and two imine C–H bonds of the adjacent cage arm. This experiment explains the effect of the presence of a heteroatom on the self-sorting process. Other amines and aldehydes in this study help elucidate the effect of electrostatic interaction, delocalization, and the flexibility of the building blocks to form a macrobicyclic cage.

As highlighted in the previous three chapters, self-assembly has been a powerful process for synthetic chemists to assemble large, complex organic molecules.[15] Our

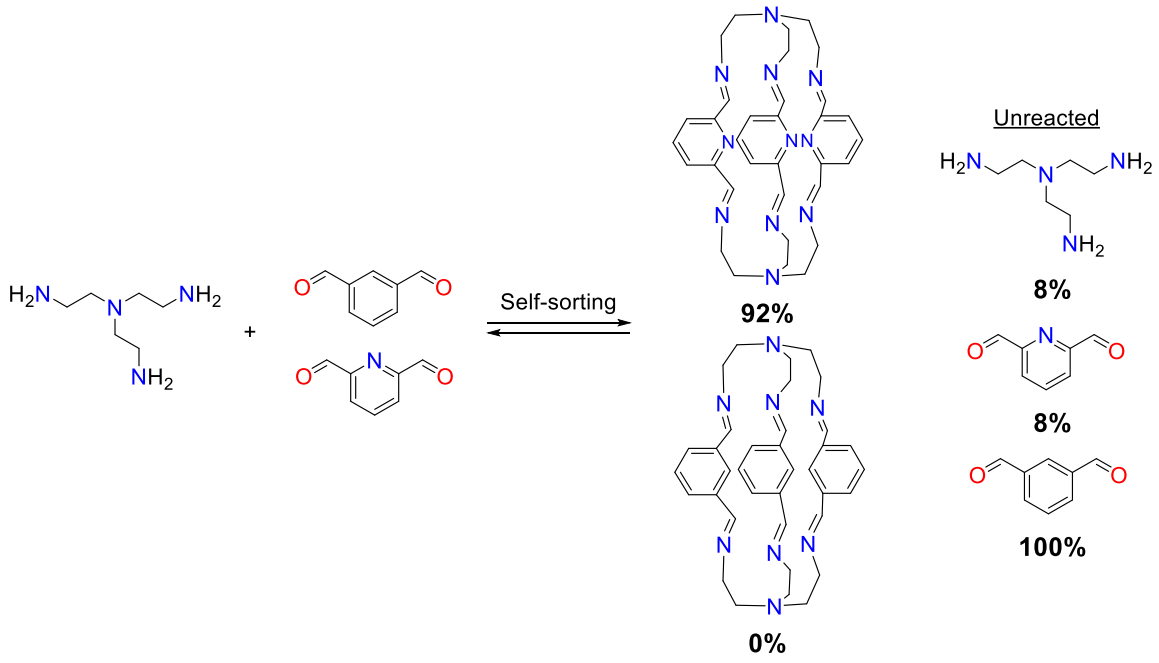

Scheme 4.1. Self-sorting experiment between one amine and two different aldehydes. Only one imine-based cage arises as the dominant product.

laboratory has utilized self-assembly to develop highly efficient routes to complex 2D and 3D organic cyclophanes by a simple treatment of thiol ligands and a pnictogen source with iodine (Scheme 4.2, left).[16] The equilibrating thermodynamic mixtures of discrete disulfides can be "kinetically trapped" *via* sulfur-extrusion chemistry to yield complex thioether cyclophanes.[17] This efficient two-step process of self-assembly and kinetic capture provides cyclophanes in scalable, high-yielding reactions. Despite being a useful tool, self-assembly typically only uses one type of building block and is thus not widely employed for constructing a multi-component assembly. This chapter will highlight our efforts at incorporating self-sorting behavior to gain access to lower-symmetry cyclophanes by mixing different types of oligothiol ligands.[18] We attempted self-sorting in two different systems: (a) combination of two dithiol building blocks leading to 2D

unsymmetrical macrocycles of different sizes and (b) combination of a dithiol and a trithiol building blocks leading to 3D “basket” cages.

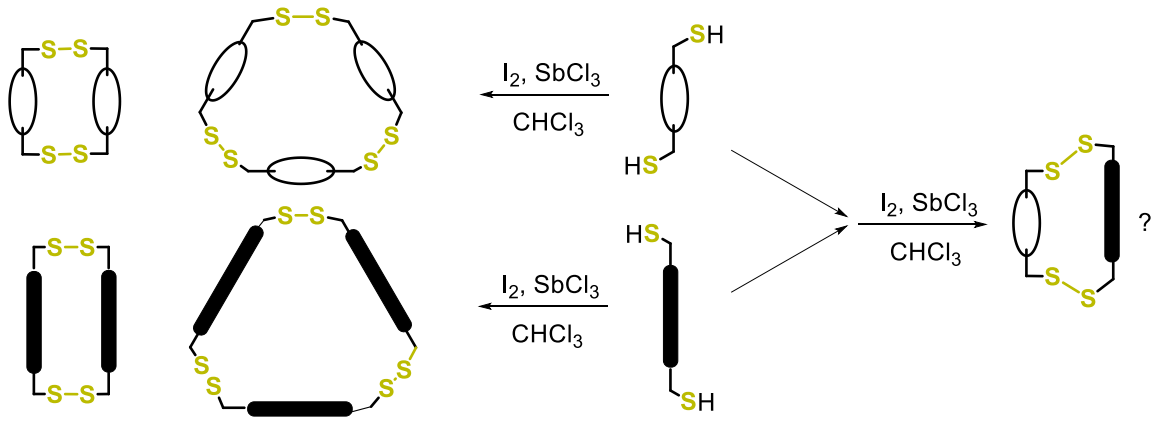

Scheme 4.2. (Left): Self-assembly of thiol building blocks leads to multiple disulfide-based cyclophanes of different sizes. (Right): Mixing two different thiol building blocks can lead to different unsymmetrical disulfide-based products.

The dynamic nature of the disulfide linkages in our cyclophanes allow the macrocycles/cages to break and reform rapidly until the most stable product arises within a chosen reaction condition.[16] In the same way, we expect to adjust the yield of each member of the library in our “mixed” system by tuning different experimental conditions, such as solvent, initial ratios of substrates, and concentrations. With the right condition, we hypothesize that it is possible to bias the reaction towards preferentially forming the elusive unsymmetrical macrocycles. These compounds have been desirable targets of traditional stepwise synthetic methods for decades and would serve as great samples to study host-guest chemistry, optoelectronic properties, and use as monomers for new polymeric materials.

Results and Discussion

*Synthesis of a new library of disulfide and thioether 2D unsymmetrical cyclophanes from thiol building blocks (**1**) and (**7**)*

As discussed in the previous chapters, our metal-directed self-assembly method is able to synthesize known, hard-to-make cyclophanes in improved yields and in far shorter times than in using traditional synthetic methods (Scheme 4.2, left).[16] We have also proven the efficiency of our approach by synthesizing multiple libraries of previously unknown cyclophanes.[19] We imagined that self-sorting can be introduced to our approach as a tool to prepare unsymmetrical macrocycles and cages featuring a combination of different di- and tri-thiols. Different thiol building blocks can lead to symmetrical assemblies in which one ligand finds another copy of itself (narcissistic self-sorting), or unsymmetrical species featuring different ligands (social self-sorting), or a combination of both. This study would showcase how dynamic covalent chemistry, self-assembly, self-sorting, and covalent capture are efficiently combined to assist us in the formation of new, complex organic structures.

We started by allowing the phenyl-based ligand (**1**) to assemble with the biphenyl-based ligand (**7**). Upon mixing 1 equiv. of each ligand, 2 equiv. I_2 and 2 equiv. $SbCl_3$ in chloroform (3 mM solution), we observed a complex mixture of products consisting of known symmetrical macrocycles (such as **D1**$_3$, **D7**$_2$, **D7**$_3$) and unknown structures with multiple signals in the ^{1}H NMR spectra. By comparing the sizes of the macrocycles based on gel permeation chromatography, we were certain that the two new compounds must be unsymmetrical trimers **D1**$_2$**7**$_1$ and **D1**$_1$**7**$_2$ (structures in Scheme 4.3). These two compounds were synthesized in 40% yield, which is much higher than the

expected statistical yield of 19%, suggesting a moderately self-sorted system, in this case favoring the formation of social self-sorted products. We were able to grow the crystals of **D1$_2$7$_1$**, confirming the presence of this compound (Figure 4.2). The compound features C–S–S–C torsion angles near the ideal 90° with angles of 87.62°, 88.98° and 90.18°. The crystal crystalizes in the P2$_1$/c space group, and each adjacent **D1$_2$7$_1$** molecule is rotated 180^o along the a axis, perhaps to shrink the size of the unoccupied pore (Figure 4.2b).

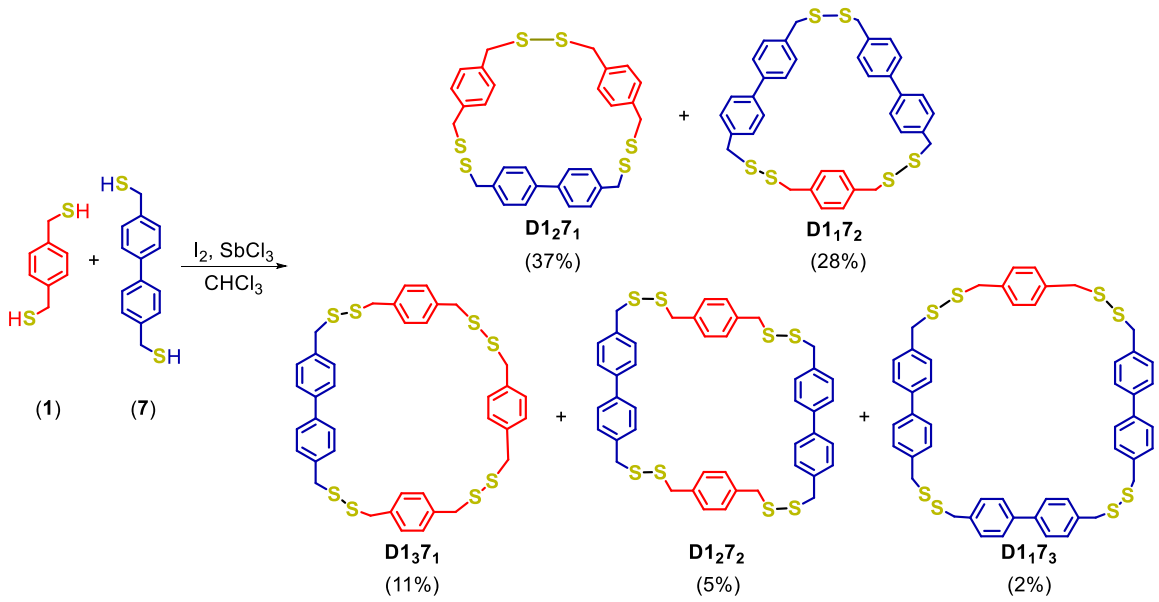

Scheme 4.3. Self-sorting of two different building blocks, bis(mercaptomethyl) phenyl (**1**) and bis(mercaptomethyl) biphenyl (**7**), leads to a variety of self-sorted products. Conditions: 4 mM (**1**), 3 mM (**7**), 8 equiv. I_2 (to thiols), 2 equiv. $SbCl_3$ (to thiols) in chloroform.

Tuning the condition to 4 mM of (**1**) and 3 mM of (**7**) with 8 equiv. I_2 and 2 equiv. $SbCl_3$ in chloroform gave us **D1$_2$7$_1$** and **D1$_1$7$_2$** in 65% yield, a >3-fold optimization over statistical yield. These conditions also provided three of the possible six tetramers **D1$_3$7$_1$**, **D1$_2$7$_2$** and **D1$_1$7$_3$**, bringing the ratio of social: narcissistic products to 85:12 (with 3% oligomers, Scheme 4.3). Since we repeatedly observed the formation of the five species shown in Scheme 4.3 (out of a statistical mixture of 21 different macrocycles), we

arrived at two conclusions. First, the self-sorting reaction of (**1**) and (**7**) favors the formation of social self-sorted products. Second, we are capable of tuning the reaction conditions to bias the formation of the social self-sorted products, as observed in the optimization of two unsymmetrical trimers. These two advantages make our approach highly desirable for the synthesis of traditionally elusive unsymmetrical structures, which are curiously absent in cyclophane literature. We did not observe the formation of the unsymmetrical dimer **D1$_1$7$_1$** in any of our conditions; we attributed this result to the significant size difference between the two building blocks (**1**) and (**7**), which made bending these rigid motifs into a single structure of dimer challenging. Our experimental design in choosing two thiols of similar shape and coordination motifs – but different sizes – simplified the formation of our desired unsymmetrical trimers and tetramers, at the expense of the unsymmetrical dimer.

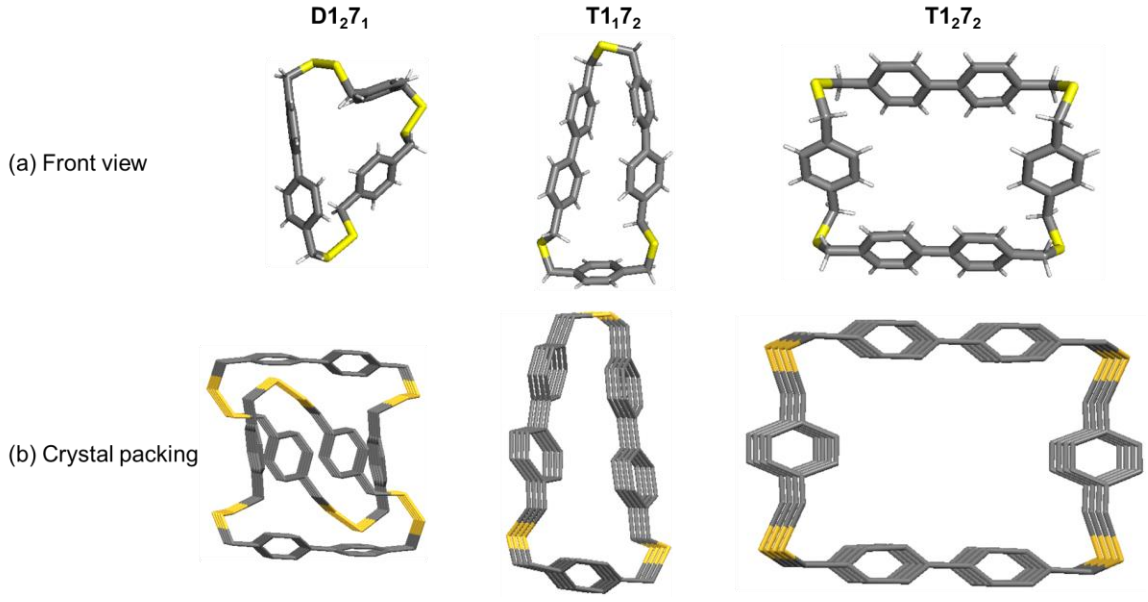

Figure 4.2. Crystal structures of disulfide **D1$_2$7$_1$** and thioethers **T1$_1$7$_2$** and **T1$_2$7$_2$**. (a) Front view of each crystal. (b) Crystal packing pattern of each structure. Hydrogen atoms omitted for clarity.

Sulfur extrusion with HMPT was conducted on all unsymmetrical disulfide species (Scheme 4.4). Each thioether features three protons (in the case of the trimers) or four protons (in the case of the tetramers) in the methylene region (~3 – 4 ppm) of the NMR spectra. **T1$_2$7$_2$** is the only tetramer that features two methylene protons, suggesting the presence of two C_2 symmetry axes in the compound, compared to the presence of only one C_2 symmetry axis in others. The aromatic region (~6.5 – 8 ppm) of each compound matches the methylene region: with the exception of the more symmetrical **T1$_2$7$_2$**, each compound features multiple pairs of doublets arising from the adjacent protons on the biphenyl units of the (**7**) fragments and the inequivalent protons from the phenyl units of the (**1**) fragments. We were able to grow single crystals of **T1$_1$7$_2$** and **T1$_2$7$_2$** (Figure 4.2), confirming the successful transformation from unsymmetrical disulfide cyclophanes into unsymmetrical thioether cyclophanes. The C–S–C angles within the cyclophanes are in the expected range for cyclic thioethers (~100 – 105^o). The dihedral angles in the biphenyl units of the (**7**) fragments are only 3.73^o for **T1$_2$7$_2$**, in contrast to 8.36^o and 32.11^o in **T1$_1$7$_2$**, indicating the need for smaller macrocycles to bend their biphenyl rings to alleviate the strain. The angle difference between the two biphenyl groups in **T1$_1$7$_2$** probably helps relieve some of the strain in the molecule as well. In the crystal packing column, each thioether molecule settles right on top of another, unlike the 180^o alternating pattern as observed in the case of **D1$_2$7$_1$** (Figure 4.2b). While **T1$_2$7$_2$** has a solvent molecule of dichloromethane in the pore, **T1$_1$7$_2$** leaves its pore empty, suggesting possibility of future host/guest studies.

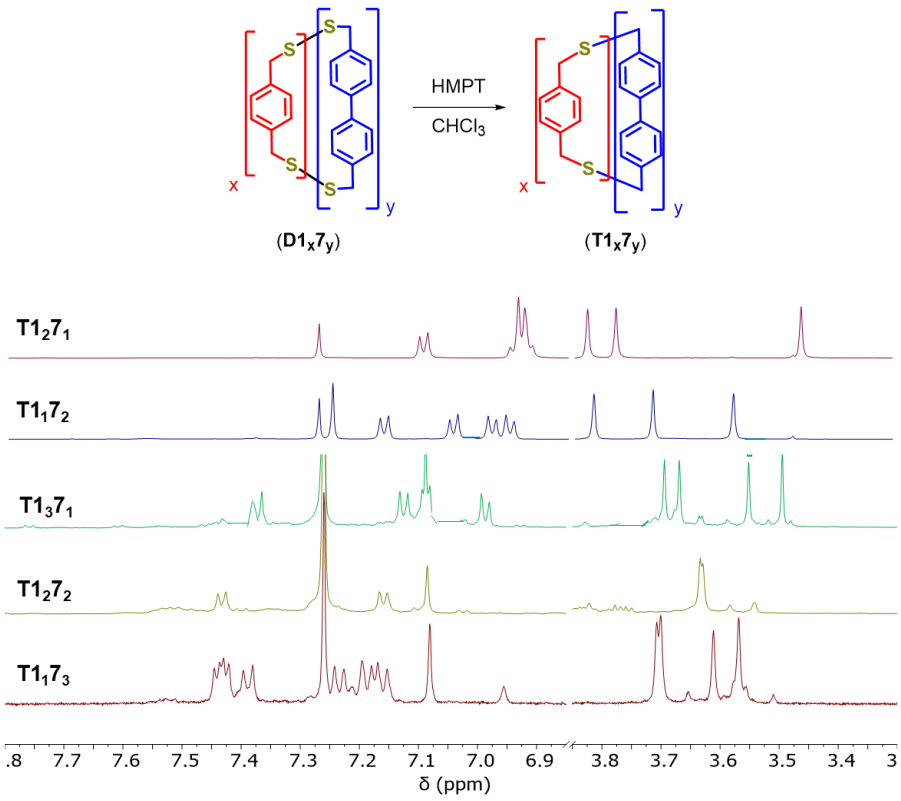

Scheme 4.4. ^{1}H NMR of unsymmetrical thioether cyclophanes, resulting from the sulfur extrusion reaction of unsymmetrical disulfide cyclophanes with HMPT ($CDCl_3$ – 7.26 ppm).

*Synthesis of a new disulfide 3D "basket" unsymmetrical cage from thiol building blocks (**7**) and (**9**)*

We wanted to apply self-sorting methods to synthesize new unsymmetrical variants of the cages and macrocycles comprising a mixture of thiols. This section focuses on an effort to extend our design strategy for self-assembling new structures, with a focus on geometrically unusual and synthetically challenging disulfides through a combination of two-fold and three-fold symmetric thiols. Due to the mismatch in the number of disulfides that can be made by each thiol, an unsymmetrical disulfide dimer between a

dithiol and a trithiol cannot be formed. The smallest unsymmetrical structure should be a trimeric "basket" with one dithiol and two trithiols, followed by a tetrameric "basket" of two dithiols and two trithiols, and so on. These structures do not possess the same high level of symmetry as earlier assemblies; therefore, the complexity of the ^{1}H NMR spectra, coupled with X-ray crystallography and mass spectrometry were used complementarily to determine the identity of each species in solution. These unsymmetrical species can also serve as precursors to unsymmetrical thioethers through covalent capture with HMPT.

Scheme 4.5 shows our attempt at self-sorting dithiol (**7**) and trithiol (**9**). Upon mixing the two thiols together, we observed the formation of narcissistic self-sorted macrocycles such as **D7**$_2$, **D7**$_3$, **D7**$_4$, a narcissistic self-sorted cage **D9**$_2$, and a new social self-sorted cage. The ^{1}H NMR spectrum in Scheme 4.5 features two doublets in the aromatic region, corresponding to the signals on the biphenyl units of fragment (**7**) of the cage. There are two singlets in the methylene region (~3 – 4 ppm) and two singlets in the methyl region (~1 – 3 ppm). We decided to heat the sample to 65^{o} so that the broad peaks could sharpen, allowing for the correct integration of each signal. It is interesting that the methylene signals associated with the (**9**) fragments are equivalent (peak d in the NMR spectrum) but the methyl signals split into two different groups (peak e and f in the NMR spectrum), suggesting that one of the methyl groups becomes chemically inequivalent to the remaining two methyl groups upon cage formation.

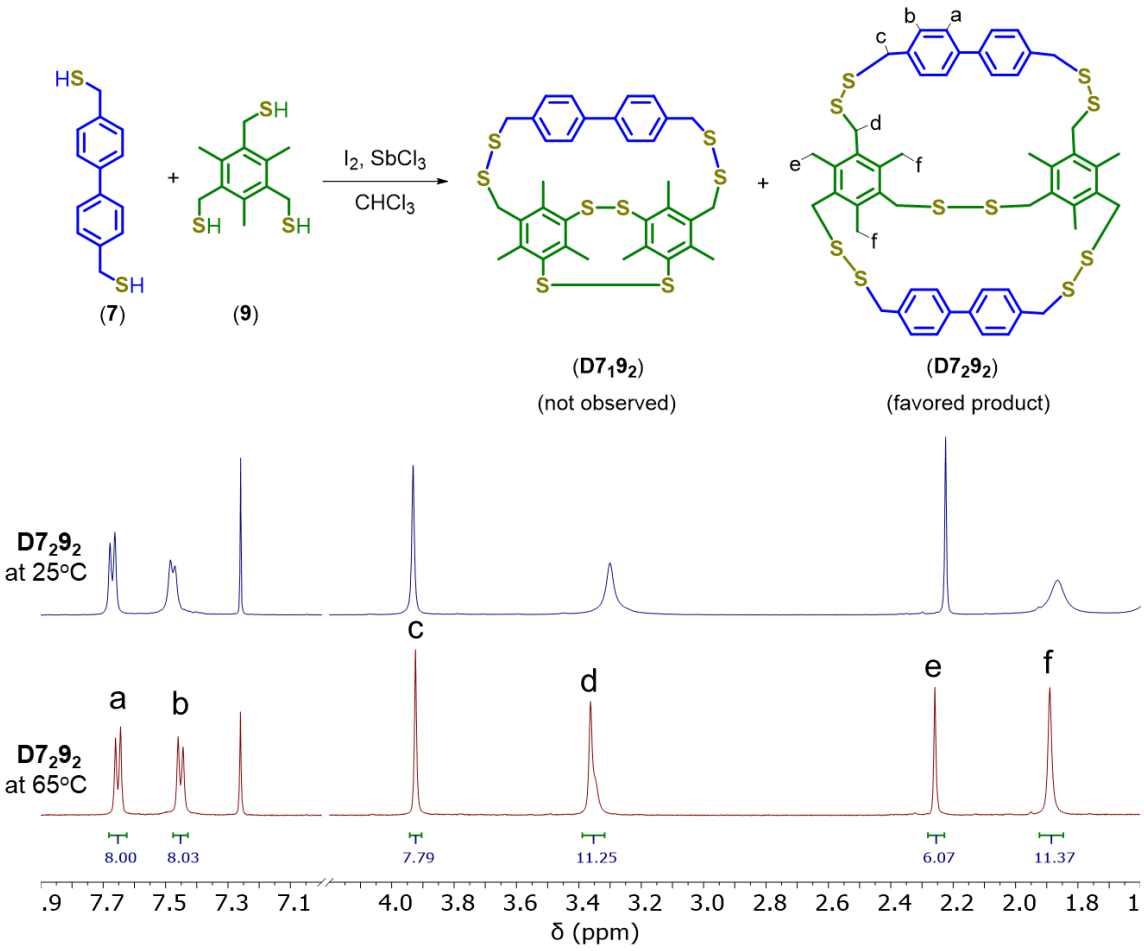

Scheme 4.5. (Top): Self-sorting of a dithiol (**7**) and a trithiol (**9**) to give "basket" – like cage **D7$_2$9$_2$**. (Bottom): ^{1}H NMR spectra of the "basket" **D7$_2$9$_2$** at 25^{o}C and at 65^{o}C ($CDCl_3$ – 7.26 ppm).

We were able to grow single crystals suitable for X-ray diffraction of **D7$_2$9$_2$** and the structure confirmed our hypothesis (Figure 4.3). The C–S–S–C torsion angles in **D7$_2$9$_2$** deviate substantially from ideality (90°), adopting highly strained conformations (88.94^o, 86.30^o, 82.32^o, 77.23^o and 76.37^o). The two (**9**) fragments of the "basket" are almost perpendicular to each other with an angle of 82.46^o, perhaps to relieve some of the strain in the "basket". Similar to what is observed with **D1$_2$7$_1$**, the crystals of **D7$_2$9$_2$** pack

in an alternating pattern, where adjacent molecules in the crystal column are 180° offset from each other, occupying the cavity to avoid unfavorably empty space. The unsymmetrical trimeric "basket" **D7$_1$9$_2$** was not favored and has not been observed yet, perhaps due to steric hindrance contributed by the methyl groups. Therefore, similar to the previous section on self-sorting of two dithiols, our choice of building blocks can dictate what products will form; in this case, the tetrameric "basket" is biased at the expense of the trimeric "basket". Future sulfur extrusion on **D7$_2$9$_2$** should give a novel thioether "basket".

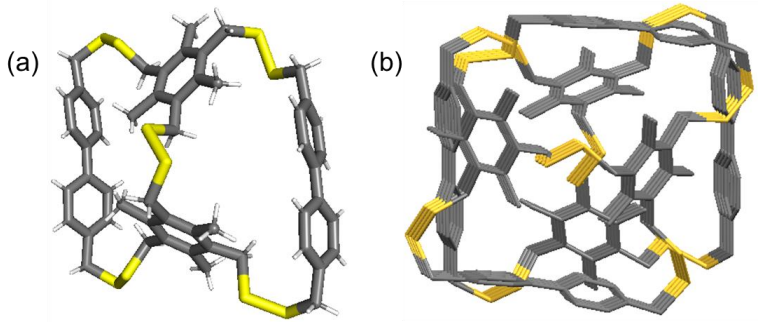

Figure 4.3. Crystal structure of **D7$_2$9$_2$**. (a) Front view. (b) Crystal packing pattern shows alternating pattern where adjacent molecules in the crystal column are 180° offset from each other to avoid an empty cavity.

Conclusions

This chapter advances the previous metal-directed self-assembly strategy by using two different thiols in tandem to provide new, elusive unsymmetrical disulfides. Two different dithiols can give multiple "mixed" macrocycles of different sizes and a dithiol – trithiol pair can give a "basket" in a single step. This approach enables substantial amplification of the unsymmetrical macrocycles/cages with small changes in reaction conditions. Covalent capture can give rise to novel unsymmetrical thioether "nanohoops"

in high yield. These collections of unsymmetrical macrocyclic cyclophanes, which aside from their pleasing aesthetics, may feature emerging properties in organic electronics, host-guest chemistry, and as monomers for new ring-opened polymerizations.

Experimental Section

^{1}H NMR spectra were measured using Varian INOVA and Bruker 500 and 600 spectrometers and ^{13}C Bruker-600 spectrometer in $CDCl_3$ and C_6D_6. Spectra were referenced using the residual solvent resonances as internal standards and reported in ppm. Single crystal X-ray diffraction studies were performed on a Bruker SMART APEX diffractometer. Commercially available reagents were used as received. The reported yields are for isolated samples.

Synthesis of a library of disulfides from thiols (1) and (7)

In a 250 mL round bottom flask, thiol (**1**) (68 mg, 0.40 mmol), thiol (**7**) (73.8 mg, 0.30 mmol) and I_2 (1.42 g, 5.60 mmol) were added in 100 mL chloroform. $SbCl_3$ (319 mg, 1.40 mmol) was added to the flask and the black solution was stirred for 4 hours at room temperature. The reaction was quenched with saturated sodium sulfite and the organic layer was washed with deionized water (2X). The solution was dried with $MgSO_4$, filtered and concentrated. The powder was then redissolved in 3 mL of chloroform (some insoluble solids that were probably polymers), filtered through a 0.45 µm PTFE membrane and purified by GPC (quantitative yield: 2% **D1$_1$7$_3$**, 5% **D1$_2$7$_2$**, 11% **D1$_3$7$_1$**, 28% **D1$_1$7$_2$**, 37% **D1$_2$7$_1$**, 14% **D1$_3$**). ^{1}H NMR (500 MHz, $CDCl_3$):

- Compound **D1$_2$7$_1$**: δ 7.71 (d, 4H, C_6H_2, J = 8.0 Hz), 7.51 (d, 4H, C_6H_2, J = 8.0 Hz), 6.90 (d, 4H, C_6H_2, J = 8.0 Hz), 6.79 (d, 4H, C_6H_2, J = 8.0 Hz), 3.92 (s, 4H, CH_2),

3.42 (s, 4H, CH_2), 3.19 (s, 4H, CH_2); $^{13}C\{^1H\}$ NMR (150 MHz, $CDCl_3$): δ = 139.93, 137.34, 136.32, 135.54, 130.83, 129.84, 129.57, 127.08, 43.36, 42.90, 42.81 ppm. Single crystals were grown by diffusion of pentane into a concentrated chloroform solution of **D1$_2$7$_1$**.

- Compound **D1$_1$7$_2$**: δ 7.49 (d, 4H, C_6H_2, *J* = 8.0 Hz), 7.46 (d, 4H, C_6H_2, *J* = 8.0 Hz), 7.28 (d, 4H, C_6H_2, *J* = 8.0 Hz), 7.14 (d, 4H, C_6H_2, *J* = 8.0 Hz), 7.09 (s, 4H, CH_2), 3.68 (s, 4H, CH_2), 3.63 (s, 4H, CH_2), 3.45 (s, 4H, CH_2); $^{13}C\{^1H\}$ NMR (150 MHz, $CDCl_3$): δ = 140.14, 139.99, 136.66, 136.52, 136.12, 130.38, 130.26, 129.72, 127.20, 127.14, 43.53, 43.12, 42.77 ppm.
- Compound **D1$_3$7$_1$**: δ 7.53 (d, 4H, C_6H_2, *J* = 8.2 Hz), 7.30 (d, 4H, C_6H_2, *J* = 8.2 Hz), 7.13 (d, 4H, C_6H_2, *J* = 8.1 Hz), 7.10 (s, 4H, CH_2), 7.08 (d, 4H, C_6H_2, *J* = 8.1 Hz), 3.66 (s, 4H, CH_2), 3.56 (s, 4H, CH_2), 3.52 (s, 4H, CH_2), 3.45 (s, 4H, CH_2); $^{13}C\{^1H\}$ NMR (125 MHz, $CDCl_3$): δ = 140.05, 139.97, 136.91, 136.55, 136.41, 130.27, 130.24, 129.67, 127.20, 127.15, 43.22, 43.19, 43.17, 42.96 ppm.
- Compound **D1$_2$7$_2$**: δ 7.51 (dd, 8H, C_6H_2, *J* = 8.1 Hz), 7.41 (d, 4H, C_6H_2, *J* = 8.1 Hz), 7.29 (d, 4H, C_6H_2, *J* = 8.0 Hz), 7.23 (d, 4H, C_6H_2, *J* = 8.0 Hz), 7.19 (s, 4H, C_6H_4), 7.15 (d, 4H, C_6H_4, *J* = 8.5 Hz), 3.67 (s, 2H, CH_2), 3.65 (s, 4H, CH_2), 3.61 (s, 4H, CH_2), 3.60 (s, 2H, CH_2), 3.56 (s, 2H, CH_2), 3.51 (s, 2H, CH_2); $^{13}C\{^1H\}$ NMR (125 MHz, TCE-d_2): δ = 139.45, 139.40, 139.30, 136.77, 136.52, 136.48, 136.41, 136.24, 136.14, 129.99, 129.90, 129.66, 129.49, 129.41, 129.32, 126.86, 126.80, 42.85, 42.78, 42.74, 42.69 ppm.
- Compound **D1$_1$7$_3$**: δ 7.52 (d, 4H, C_6H_2, *J* = 8.2 Hz), 7.48 (dd, 4H, C_6H_2, *J* = 8.2 Hz), 7.29 (d, 4H, C_6H_2, *J* = 8.3 Hz), 7.25 (d, 4H, C_6H_2, *J* = 8.2 Hz), 7.22 (d, 4H, C_6H_2, *J* = 8.2 Hz), 7.18 (s, 4H, C_6H_2), 7.14 (d, 4H, C_6H_2, *J* = 8.3 Hz), 3.63 (s, 4H, CH_2), 3.61 (s,

4H, CH_2), 3.57 (s, 4H, CH_2), 3.52 (s, 4H, CH_2); $^{13}C\{^1H\}$ NMR (125 MHz, TCE-d_2): δ = 139.51, 139.45, 139.37, 136.54, 136.48, 136.40, 136.21, 129.94, 129.85, 129.74, 129.41, 129.38, 126.93, 126.89, 42.82, 42.74, 42.70, 42.68 ppm.

Synthesis of thioether T1$_2$7$_1$

An oven-dried NMR tube was charged with **D1$_2$7$_1$** (28.7 mg, 0.049 mmol) in dried $CDCl_3$ (1 mL). Under a cone of nitrogen, HMPT (120 µL, 0.652 mmol) was added to the NMR tube and the tube was inverted gently several times to mix. The reaction was allowed to sit at ambient temperature for 2 hours. The solution was then washed with deionized water and concentrated to give a white solid. The solid was sonicated in methanol and filtered through a filter paper. The undissolved solid was retrieved from the paper by chloroform giving 10 mg of the product **T1$_2$7$_1$** (42% yield). ^1H NMR (600 MHz, $CDCl_3$): δ 7.08 (d, 4H, C_6H_2, J = 8.4 Hz), 6.91-6.95 (m, 12H, C_6H_2), 3.83 (s, 4H, CH_2), 3.78 (s, 4H, CH_2), 3.48 (s, 4H, CH_2); $^{13}C\{^1H\}$ NMR (150 MHz, $CDCl_3$): δ 138.85, 138.52, 138.38, 135.96, 128.95, 128.86, 128.63, 126.45, 38.44, 38.24, 35.94 ppm.

Synthesis of thioether T1$_1$7$_2$

An oven-dried NMR tube was charged with **D1$_1$7$_2$** (14.6 mg, 0.022 mmol) in dried $CDCl_3$ (800 µL). Under a cone of nitrogen, HMPT (54 µL, 0.294 mmol) was added to the NMR tube and the tube was inverted gently several times to mix. The reaction was allowed to sit at ambient temperature for 2 hours. The solution was then washed with deionized water and concentrated to give a white solid. The solid was sonicated in methanol and filtered through a filter paper. The undissolved solid was retrieved from the paper by

chloroform, giving 5.7 mg of the product **T1$_1$7$_2$** (46% yield). ^{1}H NMR (600 MHz, $CDCl_3$): δ 7.24 (s, 4H, C_6H_4), 7.15 (d, 4H, C_6H_2, J = 8.4 Hz), 7.04 (d, 4H, C_6H_2, J = 8.4 Hz), 6.97 (d, 4H, C_6H_2, J = 7.8 Hz), 6.95 (d, 4H, C_6H_2, J = 7.8 Hz), 3.82 (s, 4H, CH_2), 3.72 (s, 4H, CH_2), 3.59 (s, 4H, CH_2); $^{13}C\{^1H\}$ NMR (150 MHz, $CDCl_3$): δ 139.66, 138.75, 138.33, 137.37, 136.92, 129.45, 129.25, 129.00, 127.20, 126.37, 38.15, 36.23, 34.61 ppm. Single crystals were grown by slow evaporation of a concentrated of **T1$_1$7$_2$** solution in chloroform.

Synthesis of thioether T1$_3$7$_1$

An oven-dried NMR tube was charged with **D1$_3$7$_1$** (4 mg, 0.006 mmol) in dried $CDCl_3$ (500 µL). Under a cone of nitrogen, HMPT (9 µL, 0.048 mmol) was added to the NMR tube and the tube was inverted gently several times to mix. The reaction was allowed to sit at ambient temperature for 2 hours. The solution was then washed with deionized water and concentrated to give a white solid. The solid was sonicated in methanol and filtered through a filter paper. The undissolved solid was retrieved from the paper by chloroform, giving 3.0 mg of the product **T1$_3$7$_1$** (80% yield). ^{1}H NMR (500 MHz, CDCl3): δ 7.36 (d, 4H, C_6H_2, J = 6.6 Hz), 7.13 (d, 4H, C_6H_2, J = 6.6 Hz), 7.09 (s, 4H, CH_2), 7.08 (d, 4H, C_6H_2, J = 6.6 Hz), 6.99 (d, 4H, C_6H_2, J = 6.6 Hz), 3.69 (s, 4H, CH_2), 3.67 (s, 4H, CH_2), 3.55 (s, 4H, CH_2), 3.49 (s, 4H, CH_2). $^{13}C\{_1H\}$ NMR (125 MHz, $CDCl_3$): δ 139.52, 137.54, 137.46, 136.90, 136.63, 129.27, 129.22, 129.17, 129.13, 127.02, 35.99, 35.87, 35.55, 35.06 ppm.

Synthesis of thioether $T1_2 7_2$

An oven-dried NMR tube was charged with **$D1_2 7_2$** (7.1 mg, 0.009 mmol) in dried $CDCl_3$. Under a cone of nitrogen, HMPT (13 µL, 0.070 mmol) was added to the NMR tube and the tube was inverted gently several times to mix. The reaction was allowed to sit at ambient temperature for 2 hours. The solution was then washed with deionized water and concentrated to give a white solid. The solid was sonicated in methanol and filtered through a filter paper. The undissolved solid was retrieved from the paper by chloroform, giving 5.2 mg of the product **$T1_2 7_2$** (83% yield). ^{1}H NMR (500 MHz, $CDCl_3$): δ 7.43 (d, 8H, C_6H_2, *J* = 6.6 Hz), 7.17 (d, 8H, C_6H_2, *J* = 6.6 Hz), 7.09 (s, 8H, C_6H_2), 3.63 (s, 8H, CH_2), 3.62 (s, 8H, CH_2). $^{13}C\{^1H\}$ NMR (125 MHz, $CDCl_3$): δ 137.47, 137.00, 129.59, 129.57, 129.26, 126.99, 35.72, 35.41 ppm. A solution of **$T1_2 7_2$** in dichloromethane was layered under benzene and allowed to slowly diffuse to obtain single crystals suitable for XRD.

Synthesis of thioether $T1_1 7_3$

An oven-dried NMR tube was charged with **$D1_1 7_3$** (7.5 mg, 0.008 mmol) in dried $CDCl_3$ (500 µL). Under a cone of nitrogen, HMPT (6 µL, 0.033 mmol) was added to the NMR tube and the tube was inverted gently several times to mix. The reaction was allowed to sit at ambient temperature for 2 hours. The solution was then washed with deionized water and concentrated to give a white solid. The solid was sonicated in methanol and filtered through a filter paper. The undissolved solid was retrieved from the paper by chloroform, giving 5.3 mg of the product **$T1_1 7_3$** (85% yield). ^{1}H NMR (500 MHz, $CDCl_3$): δ 7.44 (d, 4H, C_6H_2, *J* = 4.2 Hz), 7.43 (d, 4H, C_6H_2, *J* = 4.2 Hz), 7.38 (d, 4H,

C_6H_2, *J* = 8.0 Hz), 7.24 (d, 4H, C_6H_2, *J* = 8.0 Hz), 7.18 (d, 4H, C_6H_2, *J* = 8.0 Hz), 7.17 (d, 4H, CH_2, *J* = 8.0 Hz), 7.08 (s, 4H, C_6H_2), 3.71 (s, 4H, CH_2), 3.70 (s, 4H, CH_2), 3.61 (s, 4H, CH_2), 3.57 (s, 4H, CH_2). $^{13}C\{^1H\}$ NMR (125 MHz, $CDCl_3$): δ 139.53, 139.44, 139.34, 137.64, 137.44, 136.82, 129.63, 129.57, 129.55, 129.13, 128.98, 127.04, 126.98, 126.95, 35.85, 35.62, 35.42, 34.72 ppm.

Synthesis of D7$_2$9$_2$ from thiols (7) and (9)

In a 250 mL round bottom flask, thiol (**7**) (24.6 mg, 0.40 mmol), thiol (**9**) (51.5 mg, 0.30 mmol) and I_2 (152 mg, 5.60 mmol) were added in 70 mL chloroform. $SbCl_3$ (136 mg, 1.40 mmol) was added to the flask and the solution was stirred overnight at room temperature. Reaction was quenched with saturated sodium sulfite and the organic layer was washed with deionized water (2X). The solution was dried with $MgSO_4$, filtered and concentrated. The powder was then redissolved in 3 mL of chloroform (some insoluble solids that were probably polymers), filtered through a 0.45 µm PTFE membrane and purified by GPC, giving **D7$_2$9$_2$** in 15% yield. ^1H NMR (500 MHz, $CDCl_3$): δ 7.66 (d, 8H, C_6H_2, *J* = 7.9 Hz), 7.48 (d, 8H, C_6H_2, *J* = 7.9 Hz), 3.93 (s, 8H, CH_2), 3.30 (s, 12, CH_2), 2.23 (s, 6H, CH_3), 1.87 (s, 12H, CH_3). Single crystals were grown by slow evaporation of a concentrated of **D7$_2$9$_2$** solution in chloroform.

CHAPTER V

SYNTHESIS OF SYMMETRICAL AND UNSYMMETRICAL HYDROCARBON MACROCYCLES: A 3-STEP APPROACH TOWARDS NEW CYCLOPHANES

Introduction

The intrinsic interest in cyclophanes first began in 1899 with the synthesis of metacyclophane by Pellegrin,[1] and that excitement blossomed among synthetic chemists with the discovery of paracyclophane in 1951 by Cram.[2] In 1969, Vögtle revolutionized the field by introducing the concept of preparing dithiacyclophanes (or thioether cyclophanes), followed by oxidation and extrusion of sulfur dioxide (SO_2) (Route 1 or R1 in Scheme 5.1) as a method of preparing [2.2]-metacyclophanes (**10**).[3] The extrusion of SO_2 has involved both pyrolyses[4] and photolyses.[5] UO's own Virgil Boekelheide subjected dithiacyclophanes to the Stevens rearrangement (later extended to include the Wittig rearrangement), followed by a Hofmann elimination as a method of preparing [2.2]-metacyclophane-l,9-dienes (**11**) (R2, Scheme 5.1).[6] Subsequently, the method of ring contraction of dithiacyclophanes has also made use of the benzyne Stevens rearrangement (R3, Scheme 5.1)[7] and the elimination step has involved sulfoxide (S=O) pyrolyses and the use of Raney nickel.[7] Finally, the sulfur extrusion step has been extended to include photolyses of dithiacyclophanes (R4, Scheme 5.1).[8]

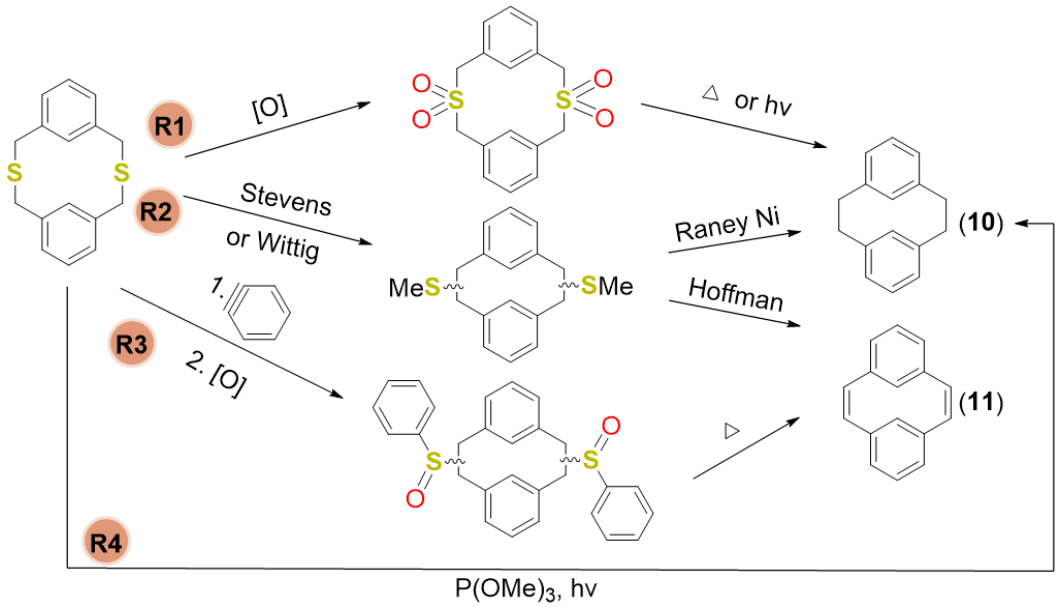

Scheme 5.1. Four main routes to synthesize [2.2]-metacyclophane (**10**) and [2.2]-metacyclophane-l,9-diene (**11**) from a thioether cyclophane precursor.

In a review on cyclophanes in 1972, Vögtle stated, "the ultimate achievement of work in the cyclophane field would be the synthesis of the fully bridged [2.2.2.2.2.2]-(1,2,3,4,5,6) cyclophane and its hexaene."[9] In 1979, Boekelheide was able to synthesize the former compound in 2.8% total yield, for which he proposed the trivial name "superphane" (Scheme 5.2).[10] The multi-step synthetic scheme required many high-temperature reactions for sequential addition of each bridging unit: pyrolysis of 2,4,5-trimethylbenzyl chloride and dimerization of the product gave intermediate (**12**). Formylation, reduction, and chlorination were used to install benzyl chloride functional groups, to which pyrolysis gave the desired tetrabridged cyclophane (**13**). A second round of formylation, reduction, and chlorination installed two more benzyl chloride functional groups. Finally, pyrolysis gave "superphane" (**14**). Since all positions in "superphane" are in bridged conformations, distortion of the benzene rings does not

relieve strain to any appreciable extent. Therefore, studies of the physical and chemical properties of this "holy grail" has given interesting insights on the effects of severe strain with planar benzene rings.[11]

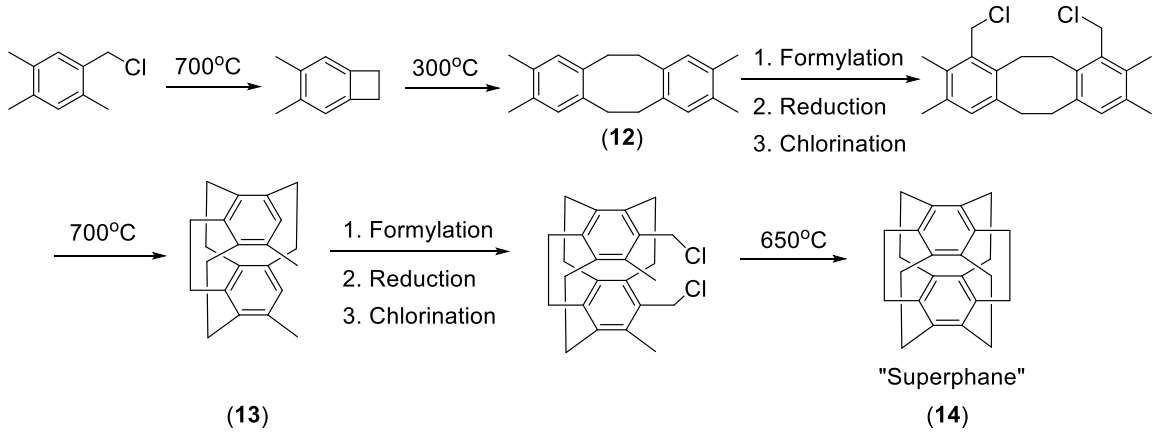

Scheme 5.2. Stepwise synthesis of "superphane" (**14**) requires sequential addition of each bridging unit.

Another "holy grail" of the cyclophane field is Vögtle's tetrahedral hydrocarbon cage $C_{36}H_{36}$, in which four benzene rings are connected by ethylene units (Figure 5.1a). This cage was synthesized after 7 steps in about 3% yield .[12] The limiting step was the final macrocyclization, which was achieved in only 11% yield despite using high-dilution conditions. Fifty years after the synthesis of this cage, chemists are still actively trying to find better synthetic approaches, since Vögtle pointed out that the scaffold of this hydrocarbon cage is a cut-out structure of C_{60} and therefore attractive as a synthetic target.[12] In 2019 the Mastalerz's laboratory successfully simplified the synthetic method to access $C_{36}H_{36}$ by utilizing the high yielding dynamic covalent imine bond formation in the first step.[13] After only 4 steps, they were able to synthesize $C_{36}H_{36}$ and other larger, previously unknown cages such as derivatives of $C_{72}H_{72}$ and $C_{84}H_{84}$ (Figure 5.1b). The

overall yield for the 4-step synthesis of the $C_{72}H_{72}$ derivative is already 1.4 % higher than that reported for a smaller $C_{60}H_{60}$ (which Vögtle reported in 0.8 % after 20 steps).[13] Mastalerz' work showcases the importance of incorporating DCC in the synthetic scheme to replace some traditional methods in making complex cyclophanes.

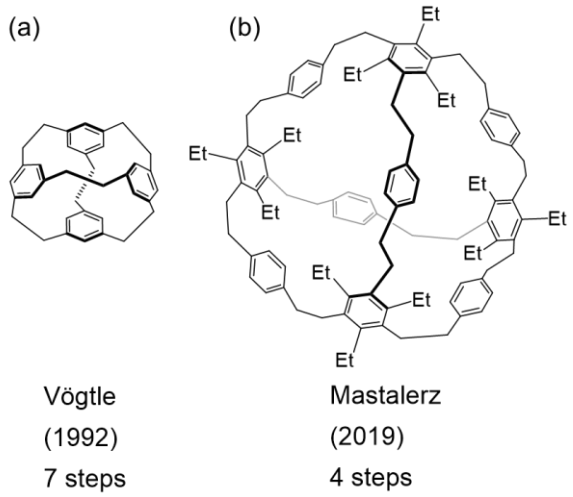

Figure 5.1. (a) Vögtle's stepwise approach requires 7 steps to synthesize the $C_{36}H_{36}$ cage. (b) Mastalerz's approach using DCC requires only 4 steps to synthesize the larger, previous unknown derivative of $C_{72}H_{72}$ cage.

As seen in the previous chapters, our approach in the DWJ laboratory eliminates the need for caustic, high-temperature methods and avoids low yields that result from the rapid formation of unfavorable insoluble oligomers (Scheme 5.3).[14] The key Sb^{III} additive during the self-assembly step avoids the formation of disulfide polymers that plagued early efforts aimed at synthesizing discrete disulfides.[15] We observe multiple thermodynamically stable macrocycles ranging from dimers through pentamers (and sometimes up to heptamers) and 3D cages such as tetrahedra. Our method also complements modern research on DCC disulfide chemistry by providing a method to

isolate and kinetically capture individual members of such equilibrating systems *via* sulfur extrusion with HMPT (Scheme 5.3).[16]

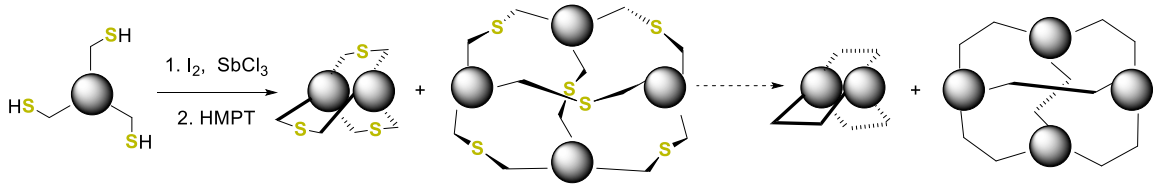

Scheme 5.3. Two-step approach to synthesize thioether cyclophanes through disulfide cyclophane intermediates. The overarching goal of this project is to extend our method into a three-step approach to access hydrocarbon cyclophanes.

Because the synthesis of disulfide cyclophanes and the kinetically trapped thioether cyclophanes is simple and quick, we are mindful of exploring the potential of these cyclophanes in applications as well. Our overarching goal has been to successfully synthesize strained hydrocarbon cyclophanes which are known products from thioether precursors *via* multiple routes as shown in Scheme 5.1. We are mindful of the fact that many challenging geometries, such as large pentameric and hexameric macrocycles, unsymmetrical macrocycles, and tetrahedra can be set up and "locked' in position by the formation of stable thioether bonds. Therefore, hydrocarbon cyclophanes possessing these unique topologies are approachable if we can standardize a method to remove the final sulfur atoms in the thioethers. Due to the confined geometries of the often-distorted aromatic rings in these systems, we expect to observe fundamentally interesting physical and chemical properties of this new class of compounds. Some of the studies can investigate the degrees of strain, degrees of aromaticity, metal capture capabilities, fluorescent properties, and optoelectronic properties. In particular, our research can also have broader impacts in the polymer community if the proposed cyclophanes can serve as

new precursors in the "parylene process" and related polymer market sub-segments (Scheme 5.4).[17] The parylene process, which uses substituted [2.2]-paracyclophanes as single source precursors, has been a rapidly growing $200M/year industry within the $2B conformal/insulating coating market, with its growth attributed mainly to its use in medical devices (a $40B market). Therefore, new classes of strained hydrocarbon cyclophanes can be promising monomers for the parylene process.

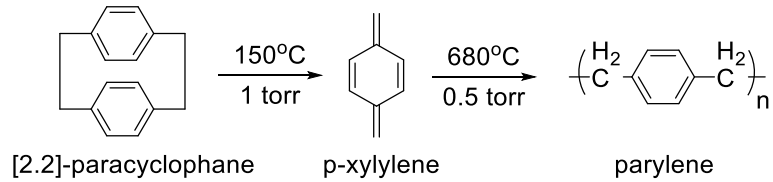

Scheme 5.4. The steps in the parylene process: [2.2]-paracyclophane is heated under vacuum and vaporized into a dimeric gas. The gas is then pyrolyzed to cleave the dimer to its monomeric form p-xylylene. In the deposition chamber, the monomer gas deposits on the surfaces as thin, transparent parylene film.

This chapter will discuss our first four hydrocarbon cyclophanes using a tandem approach of self-assembly/self-sorting, covalent capture, and sulfur photoextrusion with triethylphosphite [$P(OEt)_3$]. We were able to form new hydrocarbon cyclophanes, which are congeners of [2.2] and [2.2.2]-paracyclophane. With the new approach, we have successfully addressed a bottleneck in classical cyclophane syntheses, which, as previously discussed in this chapter, are low-yielding, stepwise, and lengthy syntheses.

Results and Discussion

Synthesis of Biphenyl-based Symmetrical Hydrocarbon Macrocyclic Cyclophanes from Biphenyl-based Disulfide Macrocyclic Cyclophanes

Our supramolecular approach has served as a powerful strategy in which new disulfide and thioether cyclophanes can be made in cases where strain and complex design are difficult to conceive or do not possess selectivity to be formed *via* classical coupling techniques (Chapter II).[18] We have commented on a few factors influencing the self-assembly method and provide a more in-depth investigation of the assembly of the larger-sized macrocycles and cages (Chapter III).[19] We are thus encouraged to come up with a more general method to synthesize hydrocarbon cyclophanes, taking advantage of the well-studied four main routes for extruding the final sulfur atoms (Scheme 5.1). This work would be a great addition to the field of cyclophane chemistry, which despite numerous exotic and spectacular 3D cyclophanes, has been impeded by lengthy and tedious syntheses requiring stepwise modification and lack of functional group tolerances.

Route 1 (R1) in Scheme 5.1 was first attempted on **T7$_3$** since this thioether formed in highest yield after the 2-step self-assembly/covalent capture from thiol (**7**) building block. Oxidation of **T7$_3$** with mCPBA yielded a new sulfone cyclophane **S7$_3$** in 60% yield (Scheme 5.5a). ^{1}H NMR shows two doublets in the aromatic region and one singlet in the methylene region, confirming the symmetry equivalence of the repeating biphenyl units in the macrocycles (Scheme 5.5c). The methylene signal shows up at 4.4 ppm, which is shifted further downfield compared to δ observed for **T7$_3$** at 3.5 ppm, consistent with the withdrawing nature of the SO_2 groups. We were able to grow a single crystal of **S7$_3$**,

which confirmed the identity of this compound. Analysis shows that **S7$_3$** possesses very strained dihedral angles in the biphenyl unit: 22.76^o, 27.75^o and 50.00^o compared to the typical 32^o found in unstrained biphenyls. Nonetheless, this strain was not sufficient to facilitate complete sulfur extrusion from this structure. While such sulfones may hold interest as hosts and novel macrocycles (which are interesting studies in their own right), we sought a more reliable method to synthesize hydrocarbon cyclophanes in these systems. R2 in Scheme 5.1 was also attempted with no success. Methylation on **T7$_3$** at the sulfur atom position proved to be very challenging since the putative methylated cyclophane was not soluble in either organic or aqueous solvent. Furthermore, the synthesis of the methylating reagent is highly hazardous, making this an undesirable approach for both research and industry.

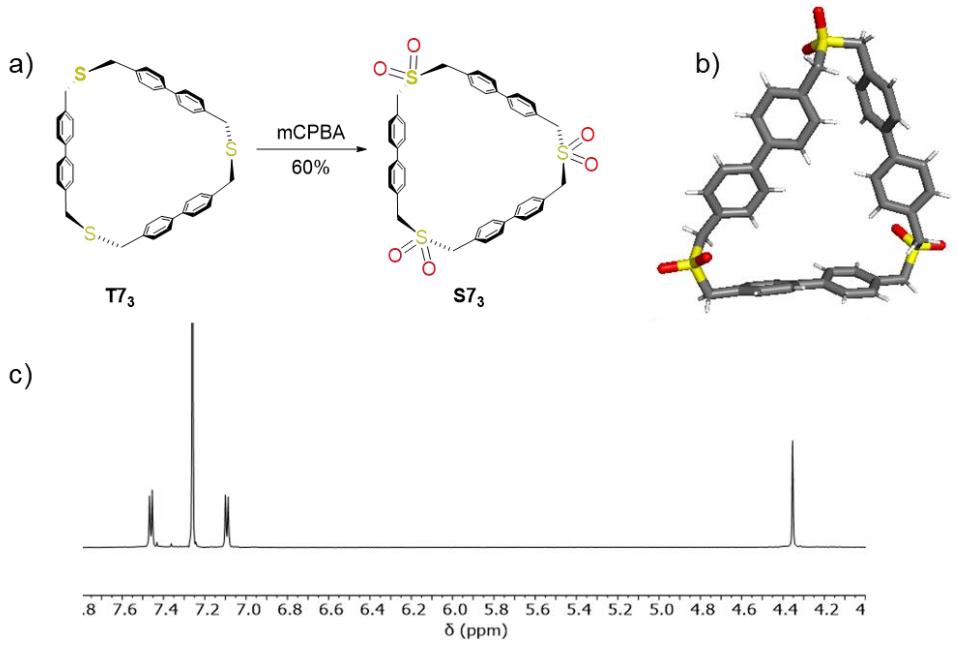

Scheme 5.5. (a) Synthesis of sulfone macrocyclic cyclophane **S7$_3$** from thioether macrocyclic cyclophane **T7$_3$**. (b) Crystal structure of **S7$_3$**. Solvent molecules are omitted for clarity. Carbon atoms shown in grey, hydrogen atoms shown in white, sulfur atoms shown in yellow and oxygen atoms shown in red. (c) ^{1}H NMR spectrum of compound **S7$_3$** ($CDCl_3$ – 7.26 ppm).

We were finally able to form hydrocarbon cyclophanes by photochemical sulfur extrusion as seen in R4, Scheme 5.1.[8] Subjecting the mixture of thioether cyclophanes **T7$_2$** – **T7$_5$** (which has been obtained from HMPT reaction with disulfide mixture **D7$_2$** – **D7$_5$**) to $P(OEt)_3$ under UV light irradiation gave us predominantly hydrocarbons **H7$_2$** and **H7$_3$** in combined 70% yield (Scheme 5.6). These two hydrocarbon cyclophanes have not been previously observed in literature and would have been very challenging to obtain using traditional methods. GPC easily separated the two species, giving a 30% and 40% yield after 3 steps, respectively. Both compounds feature the typical two aromatic doublets and one methylene singlet at ~3 ppm (Scheme 5.6). With our 3-step approach, we have successfully solved the low-yielding aspect of classical methods by incorporating DCC disulfide bond formation in the first step, which guarantees quantitative yield of the key disulfide intermediates. UV light irradiation is also mild compared to the use of reagents such as the Borch reagent to methylate the thioethers (R2, Scheme 5.1) or *in-situ* benzyne formation (R3, Scheme 5.1). Our 3-step approach (self-assembly, covalent capture, photochemistry) takes several days to a week, compared to much lengthier traditional approaches using cross-coupling reactions.

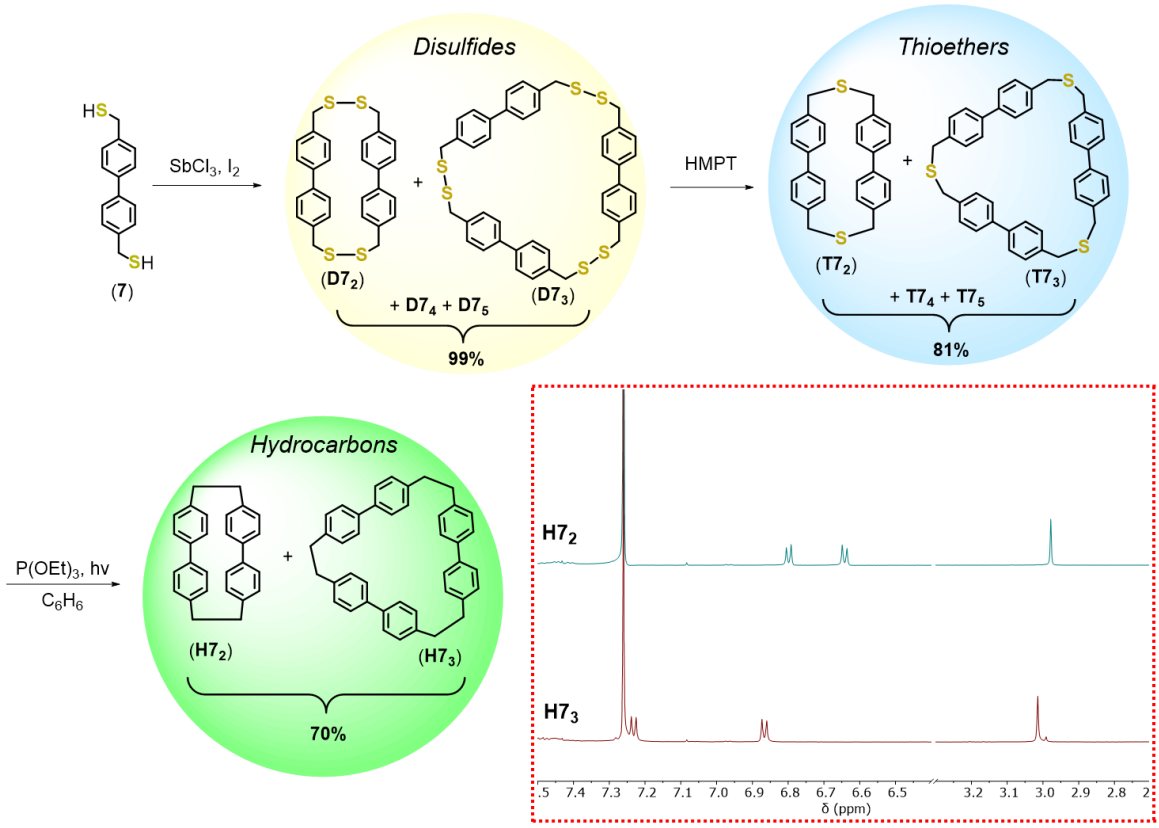

Scheme 5.6. A 3-step approach from thiol (**7**) to disulfide **D7**$_2$ – **D7**$_5$, thioether **T7**$_2$ – **T7**$_5$ and hydrocarbon **H7**$_2$ – **H7**$_3$ cyclophanes. ^{1}H NMR spectra of two new symmetrical hydrocarbon cyclophanes **H7**$_2$ and **H7**$_3$ ($CDCl_3$ – 7.26 ppm).

Synthesis of Phenyl- and Biphenyl-"Mixed" Unsymmetrical Hydrocarbon Macrocyclic Cyclophanes from A Mixture of Two Thiols

Alternative methods to synthesize hydrocarbon cyclophanes exist. For instance, alkyne metathesis[20] can be utilized to synthesize hydrocarbon cages in higher yields, but it does not allow the synthesis of less symmetrical compounds from more than one building block. Mastalerz's protocol, therefore, is a very attractive approach as it provides large unsymmetrical 3D cages in yields as much as 10x higher than those obtained from original stepwise approach. For instance, the reaction of a diamine and a trialdehyde (or a

triamine and a dialdehyde) can give the necessary unsymmetrical imine building blocks to generate the cage scaffold. Mastalerz's approach (reduction and nitrosylation of the imine bonds, followed by the Overberger reaction) has yielded unsymmetrical derivatives of large cages like the "cubic" $C_{72}H_{72}$, the synthesis of which has not been previously reported.[13]

In a similar fashion, self-sorting of two different thiols has provided us with a library of different-sized unsymmetrical disulfide macrocyclic cyclophanes in good yields (Chapter IV).[19] These unsymmetrical disulfide macrocycles have also been efficiently converted into their corresponding unsymmetrical thioether macrocycles *via* reaction with HMPT. We were curious to see if our photochemical sulfur extrusion approach would give rise to unsymmetrical hydrocarbon cyclophanes. We thus subjected two unsymmetrical trimer thioethers **T1$_2$7$_1$** and **T1$_1$7$_2$** to react with $P(OEt)_3$ under UV light irradiation (Scheme 5.7), giving two unsymmetrical trimer hydrocarbons **H1$_2$7$_1$** and **H1$_1$7$_2$** in around 60 – 70% yield for each compound.

Scheme 5.7, bottom shows the ^{1}H NMR spectra of two unsymmetrical species post-synthetic reaction workup. Each compound features one singlet (a, a') and two triplets (b, b', c, c') in the methylene region, which is the most convincing evidence that complete sulfur extrusion has occurred (the presence of the thioether bridge prevents coupling between the inequivalent methylene protons otherwise). The aromatic region of

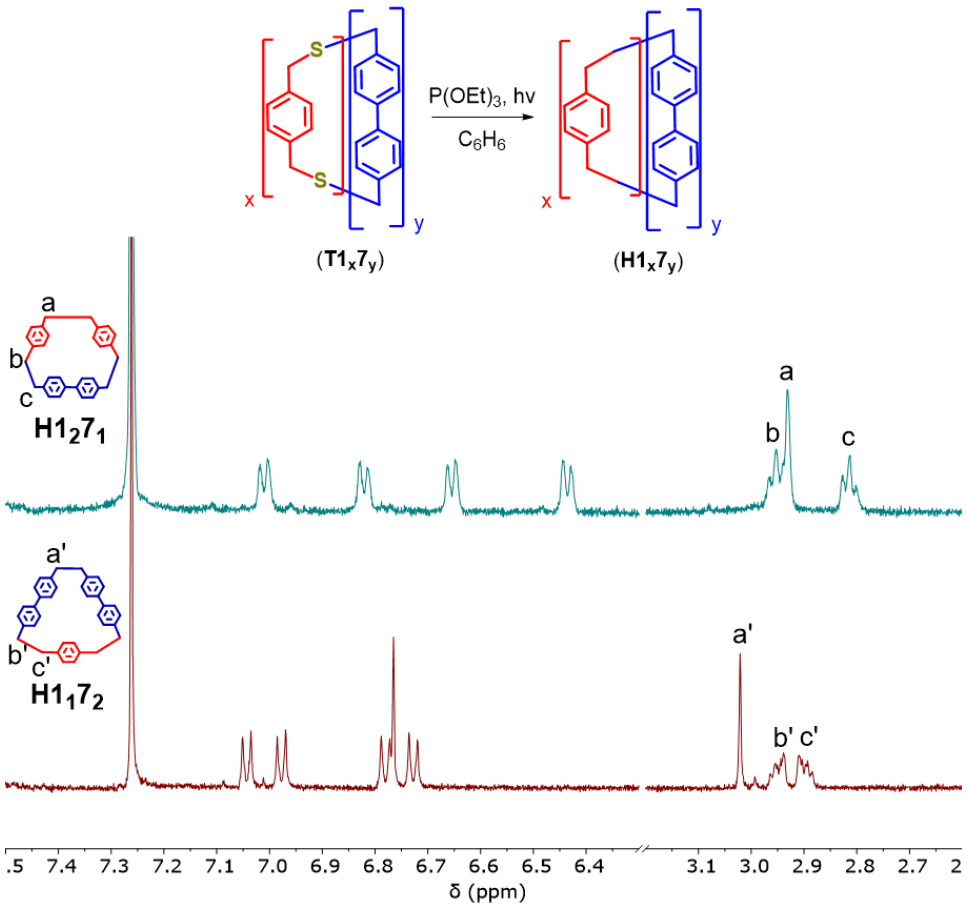

Scheme 5.7. (Top): Photochemical sulfur extrusion of unsymmetrical thioether cyclophanes to give unsymmetrical hydrocarbon cyclophanes. (Bottom): ^{1}H NMR spectra of two new unsymmetrical hydrocarbon cyclophanes **H1$_2$7$_1$** and **H1$_1$7$_2$** ($CDCl_3$ – 7.26 ppm).

the top spectrum featuring 4 doublets confirms the structure **H1$_2$7$_1$**, whereas **H1$_1$7$_2$** features 4 doublets for the inequivalent rings of the (**7**) fragment and 1 singlet for the equivalent protons on the (**1**) fragment. To the best of our knowledge, these are the first examples of unsymmetrical hydrocarbon cyclophanes synthesized with self-sorting in the first step to ensure the high-yielding formation of the right macrocyclic backbone.

Our ability to form unsymmetrical hydrocarbon cyclophanes from unsymmetrical thioether cyclophanes is quite remarkable since photochemical sulfur extrusion

undergoes a multistep radical mechanism, beginning with the formation of a R–CH_2· radical, followed by self-dimerization to form the hydrocarbon (Scheme 5.8).[21] Since our thioethers are unsymmetrical, we would expect two different types of radical species R–CH_2· and R'–CH_2·. Nonetheless, we observed no formation of symmetrical hydrocarbons, such as **H1**$_x$ or **H7**$_y$ (where x and y are integers) that would result when similar radicals recombine. Therefore, the complete sulfur extrusion with no side reaction may render our approach an excellent general strategy to form new classes of unsymmetrical hydrocarbon cyclophanes.

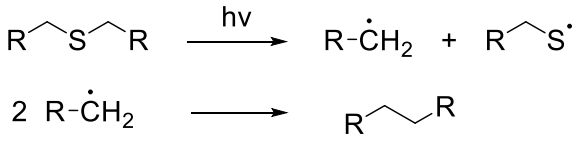

Scheme 5.8. Simplified mechanism of photochemical sulfur extrusion. We observed no formation of symmetrical hydrocarbons $(RCH_2)_2$ or $(R'CH_2)_2$ despite starting with 2 different thioethers $(RCH_2)S$ and $(R'CH_2)S$.

Conclusions

The hydrocarbon cyclophanes reported in this chapter have proven inaccessible by traditional cyclophane syntheses. Using self-assembly or self-sorting in the first step has allowed us to access different disulfide macrocycles/cages that have unique geometry in high yield. Stepwise sulfur extrusion, first with HMPT, then with $P(OEt)_3$ under UV light irradiation, can efficiently remove the sulfur atoms with no side reaction. The merit of our new approach lies in its promise to deliver previously unattainable cyclophanes and to study the emergent properties of these compounds, as targets to enrich the cyclophane field and as potential feedstock for the parylene process.

Experimental Section

^{1}H NMR spectra were measured using Varian INOVA and Bruker 500 and 600 MHz spectrometers and ^{13}C Bruker-600 spectrometer in $CDCl_3$ and C_6D_6. Spectra were referenced using the residual solvent resonances as internal standards and reported in ppm. Single crystal X-ray diffraction studies were performed on a Bruker SMART APEX diffractometer. Commercially available reagents were used as received. The reported yields are for isolated samples.

Synthesis of sulfone $S7_3$ from thioether $T7_3$

In a 20 mL scintillation vial, thioether **T7₃** (40 mg, 0.063 mmol) and mCPBA 75% by wt. (30.4 mg, 0.132 mmol) were added in 2 mL of dried dichloromethane. Solution was stirred at 0°C and slowly warmed to room temperature overnight. Reaction was diluted with CH_2Cl_2 and washed twice with saturated sodium bicarbonate and the organic layer was washed with deionized water (2X). The solution was dried with $MgSO_4$, filtered and concentrated, giving 20 mg of the sulfone product **S7₃** (60 % yield). ^{1}H NMR (500 MHz, $CDCl_3$): δ 7.45 (d, 12H, C_6H_2, J = 6.8 Hz), 7.10 (d, 12H, C_6H_2, J = 6.8 Hz), 4.35 (s, 12H, CH_2)); $^{13}C\{^{1}H\}$ NMR (125 MHz, $CDCl_3$): δ 140.95, 131.23, 127.94, 127.49, 60.42. A solution of the **S7₃** in chloroform was layered under benzene and allowed to slowly diffuse to obtain single crystals suitable for XRD.

General procedure for the 3-step approach to disulfide, thioether and hydrocarbon cyclophanes

In an NMR tube, thiol (**7**) (15 mg, 0.06 mmol) and I_2 (31 mg, 0.12 mmol) were added in 1 mL $CDCl_3$. $SbCl_3$ (28 mg, 0.12 mmol) was added to the tube and the reaction was shown

to complete rapidly through ^{1}H NMR spectroscopy. The reaction was allowed to run for 8 hours to ensure the most stable disulfides would form. After 8 hours, the solution was diluted with chloroform and quenched with saturated sodium sulfite and the organic layer was washed with deionized water (2X). The solution was dried with $MgSO_4$, filtered and concentrated to yield a white powder. The powder was redissolved in 1 mL $CDCl_3$. Under a cone of nitrogen, HMPT (90 µL, 0.48 mmol) was added to the NMR tube and the tube was inverted gently several times to mix. The reaction was left to sit at ambient temperature for 2 hours, at which point NMR spectroscopy indicated complete conversion to the thioethers. The solution was washed with deionized water and concentrated to give a white solid. The solid was sonicated in methanol and filtered through a filter paper. The undissolved solid was retrieved from the paper by chloroform, giving a mixture of thioether dimer – pentamer **T7$_2$ – T7$_5$**. The powder was redissolved in 1 mL C_6D_6. $P(OEt)_3$ (90 µL, 0.48 mmol) was added to the NMR tube and the tube was inverted gently several times to mix. The sample was irradiated with a medium-pressure Hg lamp for 14 hours. The reaction was quenched with water and washed multiple times with deionized water. GPC was utilized to separate the samples, giving 30% and 40% yield (overall yield after 3 steps) of **H7$_2$** and **H7$_3$**. ^{1}H NMR (500 MHz, $CDCl_3$): **H7$_2$**: δ 6.79 (d, 4H, C_6H_2, J = 6.7 Hz), 6.65 (d, 4H, C_6H_2, J = 6.7 Hz), 2.98 (s, CH_2); MS (m/z), calculated for $C_{28}H_{25}$ $(M+H)^+$ 361.1956, found 361.2054; **H7$_3$**: δ 7.22 (d, 12H, C_6H_2, J = 6.8 Hz), 6.87 (d, 12H, C_6H_2, J = 6.8 Hz), 3.01 (s, 12H, CH_2); $^{13}C\{^{1}H\}$NMR (125 MHz): δ 138.97, 138.17, 129.52, 126.25, 35.97 ppm. MS (m/z), calculated for $C_{42}H_{37}$ $(M+H)^+$ 541.2895, found 541.2990.

Synthesis of compound H1$_2$7$_1$

An oven-dried NMR tube was charged with **T1$_2$7$_1$** (10 mg, 0.017 mmol) in dried C_6D_6 (1 mL). Under a cone of nitrogen, $P(OEt)_3$ (200 µL, 1.17 mmol) was added to the NMR tube and the tube was inverted gently several times to mix. The reaction was irradiated with a medium-pressure Hg lamp at ambient temperature for 6 hours. The solution was then concentrated to give a light-yellow liquid. A silica plug (20% EtOAc: 80% hexane) was run to give 4.6 mg of product **H1$_2$7$_1$** (70% yield). ^{1}H NMR (600 MHz, $CDCl_3$): δ 7.00 (d, 4H, C$_6$*H*$_2$, *J* = 8.0 Hz), 6.83 (d, 4H, C$_6$*H*$_2$, *J* = 7.8 Hz), 6.65 (d, 4H, C$_6$*H*$_2$, *J* = 7.8 Hz), 6.44 (d, 4H, C$_6$*H*$_2$, *J* = 8.0 Hz), 2.95 (t, 4H, C*H*$_2$), 2.93 (s, 4H, C*H*$_2$), 2.81 (t, 4H, C*H*$_2$). ^{13}C{^{1}H} NMR (150 MHz, $CDCl_3$): δ 140.04, 139.04, 137.95, 137.16, 129.56, 128.92, 127.12, 126.90, 37.72, 36.43, 31.18 ppm. MS (m/z), calculated for $C_{30}H_{39}$ $(M+H)^+$ 389.2269, found 389.2249.

Synthesis of compound H1$_1$7$_2$

An oven-dried NMR tube was charged with **T1$_1$7$_2$** (8.4 mg, 0.015 mmol) in dried C_6D_6 (1 mL). Under a cone of nitrogen, $P(OEt)_3$ (190 µL, 1.15 mmol) was added to the NMR tube and the tube was inverted gently several times to mix. The reaction was irradiated with a medium-pressure Hg lamp at ambient temperature for 8 hours. The solution was then concentrated to give a light-yellow liquid. A silica plug (20% EtOAc: 80% hexane) was run to give 4.1 mg of product **H1$_1$7$_2$** (60% yield). ^{1}H NMR (500 MHz, 4$CDCl_3$): δ 7.04 (d, 4H, C$_6$*H*$_2$, *J* = 8.2 Hz), 6.98 (d, 4H, C$_6$*H*$_2$, *J* = 8.2 Hz), 6.77 (d, 4H, C$_6$*H*$_2$, *J* = 8.0 Hz), 6.76 (s, 4H, C*H*$_2$), 6.73 (d, 4H, C$_6$*H*$_2$, *J* = 8.0 Hz), 3.02 (s, 4H, C*H*$_2$), 2.96 – 2.94 (m, 4H, C*H*$_2$), 2.91 – 2.89 (m, 4H, C*H*$_2$). ^{13}C{^{1}H} NMR (150 MHz, $CDCl_3$): δ 139.21,

139.19, 138.75, 138.18, 129.94, 129.27, 129.23, 129.08, 126.69, 126.44, 36.86, 36.64, 35.40 ppm. MS (m/z), calculated for $C_{36}H_{33}$ $(M+H)^+$ 465.2582, found 465.2680.

APPENDIX:

CRYSTALLOGRAPHY

X-ray Crystallography. Diffraction intensities were collected at 173 K on a Bruker Apex2 DUO CCD diffractometer using CuKα radiation, λ= 1.54178 Å. Absorption corrections were applied by SADABS.[1] Structures were solved by direct methods and Fourier techniques and refined on F^2 using full matrix least-squares procedures. All non-H atoms were refined with anisotropic thermal parameters. H atoms in all structures were refined in calculated positions in a rigid group model. Space groups were determined based on systematic absences. These disordered solvent molecules were treated by SQUEEZE.[2] All calculations were performed by the Bruker SHELXL-2014 package.[3]

Chapter II

- Crystallographic Data for **D5$_2$** (CCDC **1859804**): $C_{24}H_{20}S_4$, M = 436.64, 0.13 x 0.10 x 0.03 mm, T = 173(2) K, Monoclinic, space group $P2_1/n$, a = 7.1311(2) Å, b = 8.3942(3) Å, c = 17.2693(6) Å, β = 95.931(2)°, V = 1028.20(6) Å^3, Z = 2, D_c = 1.410 Mg/m^3, μ(Cu) = 4.289 mm^{-1}, F(000) = 456, $2\theta_{max}$ = 133.14°, 6792 reflections, 1808 independent reflections [R_{int} = 0.0438], R1 = 0.0323, wR2 = 0.0859 and GOF = 1.040 for 1808 reflections (127 parameters) with I>2σ(I), R1 = 0.0345, wR2 = 0.0881 and GOF = 1.040 for all reflections, max/min residual electron density +0.311/-0.217 eÅ^{-3}.

- Crystallographic Data for **D6$_2$** (CCDC **1859805**): $C_{24}H_{20}S_4$, M = 436.64, 0.09 x 0.08 x 0.02 mm, T = 173(2) K, Orthorhombic, space group $Aba2$, a = 10.8663(5) Å, b =

8.5571(3) Å, c = 22.5617(10) Å, V = 2097.88(15) Å^3, Z = 4, D_c = 1.382 Mg/m^3, μ(Cu) = 4.204 mm^{-1}, F(000) = 912, $2\theta_{max}$ = 133.09°, 7433 reflections, 1802 independent reflections [R_{int} = 0.0521], R1 = 0.0705, wR2 = 0.1777 and GOF = 1.020 for 1802 reflections (127 parameters) with I>2σ(I), R1 = 0.0799, wR2 = 0.1885 and GOF = 1.021 for all reflections, max/min residual electron density +0.582/-0.257 eÅ^{-3}. The structure of **D6$_2$** was determined in orthorombic (*Cmca* and *Aba*2) and monoclinic ($P2_1/c$ and *Pc*) space groups. In centro-symmetrical space groups the ligand is disordered over two positions related to two possible orientations of the molecule in the crystal structure. In non-centrosymmetrical space groups there is no such the disorder. The Flack parameter is 0.43(2) in *Aba*2 and 0.46(2) in *Pc*. The structure of **D6$_2$** refined in space group *Aba*2 is given as the final in the paper as having the highest symmetry but without the mentioned disorder. The C-C bond distances in **D6$_2$** have been determined with limited precision due to the disorder. All calculations were performed by the Bruker SHELXL-2014/7 package.[3]

Chapter III

- Crystallographic Data for **T7$_2$** (CCDC **1884077**): $C_{28}H_{24}S_2$, M = 424.59, 0.07 x 0.04 x 0.04 mm, T = 173(2) K, Monoclinic, space group $P2_1/c$, a = 20.9413(14) Å, b = 13.7902(11) Å, c = 14.7593(12) Å, β = 90.050(6)°, V = 4262.3(6) Å^3, Z = 8, Z'=2, D_c = 1.323 Mg/m^3, μ(Cu) = 2.341 mm^{-1}, F(000) = 1792, $2\theta_{max}$ = 133.14°, 35340 reflections, 7416 independent reflections [R_{int} = 0.0761], R1 = 0.0646, wR2 = 0.1558 and GOF = 1.026 for 7416 reflections (542 parameters) with I>2σ(I), R1 = 0.0804, wR2 = 0.1681 and GOF = 1.026 for all reflections, max/min residual electron density +0.853/-0.299

eÅ^{-3}. It was found that the needle crystal of **1884077** used for data collection is a twin consisting of two domains with ratio 0.31/0.69.

- Crystallographic Data for **T7$_3$** (CCDC **1884075**): $C_{44}H_{38}Cl_6S_3$, M = 875.62, 0.12 x 0.02 x 0.015 mm, T = 120(2) K, Monoclinic, space group $P2_1/c$, a = 20.8036(11) Å, b = 5.6365(4) Å, c = 35.382(2) Å, β = 93.946(4)°, V = 4139.0(4) Å^3, Z = 4, D_c = 1.405 Mg/m^3, μ(Cu) = 5.444 mm^{-1}, F(000) = 1808, $2\theta_{max}$ = 89.06°, 11110 reflections, 3149 independent reflections [R_{int} = 0.0651], R1 = 0.1221, wR2 = 0.3368 and GOF = 1.043 for 3149 reflections (450 parameters) with I>2σ(I), R1 = 0.1637, wR2 = 0.3632 and GOF = 1.075 for all reflections, max/min residual electron density +0.416/-0.382 eÅ^{-3}. Crystals of the investigated compounds are formed as small thin needles and give weak X-ray diffraction at high angles. Even using a strong *Incoatec* IμS Cu source for **1884075,** it was possible to collected data only up to $2\theta_{max}$ = 89.06° and 99.56°, respectively. Thus resolution for these structures is low, but the found structures clear shown the structure and composition of the compound. One of two solvent molecules $CHCl_3$ in **1884075** is highly disordered in a general position and around an inversion center, respectively. The corrections of the X-ray data by SQUEEZE are 228 electron/cell; the required values are 232 electron/cell for four $CHCl_3$ molecules in **1884075**.

- Crystallographic Data for **T7$_4$**: (CCDC **1979193**): $C_{56}H_{48}S_4$, M = 849.18, 0.08 x 0.04 x 0.01 mm, T = 173(2) K, Triclinic, space group P-1, a = 5.6965(3) Å, b = 14.1754(7) Å, c = 14.6313(6) Å, α = 99.998(4)°, β = 100.933(4)°, γ = 99.669(4)°, V =

1117.49(10) Å^3, Z = 1, Z'=0.5, D_c = 1.262 Mg/m^3, μ(Cu) = 2.232 mm^{-1}, F(000) = 448, $2\theta_{max}$ = 148.43°, 10071 reflections, 4272 independent reflections [R_{int} = 0.0322], R1 = 0.0473, wR2 = 0.1222 and GOF = 0.955 for 4272 reflections (367 parameters) with I>2σ(I), R1 = 0.0522, wR2 = 0.1290 and GOF = 0.955 for all reflections, max/min residual electron density +0.517/-0.266 eÅ^{-3}. H atoms in **1979193** were found on the residual density map and refined with isotropic thermal parameters.

Chapter IV

- Crystallographic Data for **D1$_2$7$_1$** (CCDC **1884078**): $C_{30}H_{28}S_6$, M = 580.88, 0.06 x 0.04 x 0.02 mm, T = 173(2) K, Triclinic, space group *P*-1, a = 10.1303(4) Å, b = 12.8333(5) Å, c = 22.9283(11) Å, α = 77.847(3)°, β = 83.562(4)°, γ = 78.309(2)°, V = 2846.0(2) Å^3, Z = 4, Z'=2, D_c = 1.356 Mg/m^3, μ(Cu) = 4.573 mm^{-1}, F(000) = 1216, $2\theta_{max}$ = 133.70°, 41027 reflections, 9869 independent reflections [R_{int} = 0.0623], R1 = 0.0561, wR2 = 0.1562 and GOF = 1.033 for 9869 reflections (674 parameters) with I>2σ(I), R1 = 0.0755, wR2 = 0.1698 and GOF = 1.044 for all reflections, max/min residual electron density +0.987/-0.651 eÅ^{-3}. Space groups were determined based on systematic absences and intensity statistics.

- Crystallographic Data for **T1$_1$7$_2$** (CCDC **1884076**): $C_{36}H_{32}S_3$, M = 560.79, 0.18 x 0.02 x 0.02 mm, T = 173(2) K, Monoclinic, space group $P2_12_12_1$, a = 5.9598(3) Å, b = 12.9349(7) Å, c = 37.287(2) Å, V = 2874.4(3) Å^3, Z = 4, D_c = 1.296 Mg/m^3, μ(Cu) = 2.528 mm^{-1}, F(000) = 1184, $2\theta_{max}$ = 133.14°, 12589 reflections, 4927 independent reflections [R_{int} = 0.0652], R1 = 0.0504, wR2 = 0.1190 and GOF = 0.924 for 4927

reflections (352 parameters) with I>2σ(I), R1 = 0.0722, wR2 = 0.1335 and GOF = 0.924 for all reflections, the Flack = 0.04(2), max/min residual electron density +0.205/-0.212 eÅ^{-3}. The structure of **1884076** was determined in chiral space group symmetry $P2_12_12_1$ with the Flack parameter is 0.04(2)

- Crystallographic Data for **T1$_2$7$_2$** (CCDC **1884074**): $C_{45}H_{42}Cl_2S_4$, M = 781.92, 0.08 x 0.01 x 0.01 mm, T = 173(2) K, Monoclinic, space group $P2_1/n$, a = 16.152(4) Å, b = 5.5339(12) Å, c = 22.599(5) Å, β = 107.429(15)°, V = 1927.2(7) Å^3, Z = 2, Z' = 0.5, D_c = 1.347 Mg/m^3, μ(Cu) = 3.781 mm^{-1}, F(000) = 820, $2\theta_{max}$ = 99.56°, 10516 reflections, 1960 independent reflections [R_{int} = 0.1651], R1 = 0.0864, wR2 = 0.1787 and GOF = 0.972 for 1960 reflections (217 parameters) with I>2σ(I), R1 = 0.1667, wR2 = 0.2086 and GOF = 1.004 for all reflections, max/min residual electron density +0.262/-0.251 eÅ^{-3}. Crystals of the investigated compounds are formed as small thin needles and give weak X-ray diffraction at high angles. Even using a strong *Incoatec* IμS Cu source for **1884074** it was possible to collected data only up to $2\theta_{max}$ = 99.56°. Thus resolution for these structures is low, but the found structures clear shown the structure and composition of the compound. A solvent molecule CH_2Cl_2 in **1884074** are highly disordered in a general position and around an inversion center, respectively. The corrections of the X-ray data by SQUEEZE are 88 electron/cell; the required values are 84 electron/cell for two CH_2Cl_2 molecules respectively in **1884074**.

Chapter V

- Crystallographic Data for **S7$_3$** (CCDC **1979192**): $C_{47}H_{41}Cl_6O_6S_3$, M = 1010.68, 0.17 x 0.04 x 0.04 mm, T = 173(2) K, Triclinic, space group *P*-1, *a* = 10.0586(4) Å, *b* = 15.3902(6) Å, *c* = 15.5730(5) Å, α = 84.844(2)°, β = 83.235(2)°, γ = 78.415(3)°, *V* = 2339.77(15) Å^3, *Z* = 2, Z'=1, D_c = 1.435 Mg/m^3, μ(Cu) = 4.994 mm^{-1}, *F*(000) = 1042, $2\theta_{max}$ = 133.19°, 29750 reflections, 8193 independent reflections [R_{int} = 0.0663], R1 = 0.0527, wR2 = 0.1371 and GOF = 1.029 for 8193 reflections (523 parameters) with I>2σ(I), R1 = 0.0701, wR2 = 0.1469 and GOF = 1.029 for all reflections, max/min residual electron density +0.682/-0.453 eÅ^{-3}. One of two solvent molecules $CHCl_3$ in **1979192** is highly disordered in a general position around an inversion center and was treated by SQUEEZE.[2] The correction of the X-ray data by SQUEEZE is 105 electron/cell; the required value is 116 electron/cell for two solvent molecules $CHCl_3$ in the full unit cell.

- Crystallographic Data for **D12$_9$2**: $C_{52}H_{54}S_{10}$. 0.75 ($CHCl_3$) M = 4356.31, T = 173(2) K, Monoclinic, space group $P2_1/c$, *a* = 11.3540(6) Å, *b* = 29.3205(18) Å, *c* = 31.4598(18) Å, α = 90°, β = 91.709(4)°, γ = 90°, *V* = 10468.5(10) Å^3, *Z* = 8, Z'=0, D_c = 1.382 Mg/m^3, μ(Cu) = 5.236 mm^{-1}, *F*(000) = 4556.0, $2\theta_{max}$ = 99.642°, 10071 reflections, 4272 independent reflections [R_{int} = 0.0322], R1 = 0.0732, and GOF = 0.979 for 10621 reflections (1186 parameters) with I>2σ(I), wR2 = 0.2000 and GOF = 0.979 for all reflections. In the structure there are two symmetrically independent molecules. One of solvent molecules is disordered over two positions. Diffraction at high angles is weak. Data have been collected only to 100 degrees (vs. 133 degrees needed).

REFERENCES CITED

CHAPTER I

(1) Gilbert, H. F. "Molecular and Cellular Aspects of Thiol–Disulfide Exchange". *Advances in Enzymology and Related Areas of Molecular Biology*. **1990**, *63*, pp. 69–172.

(2) a) Jocelyn, P. C. The Standard Redox Potential of Cysteine-Cystine from the Thiol-Disulphide Exchange Reaction with Glutathione and Lipoic Acid. *Eur. J. Biochem.* **1967**, *2*, 327–331; b) Sakai, H. A Ribonucleoprotein Which Catalyzes Thiol-Disulfide Exchange in the Sea Urchin Egg. *J. Biol. Chem*. **1967**, *242*, 1458–1461; c) Ukuwela, A. A.; Bush, A. I.; Wedd, A. G.; Xiao, Z. Glutaredoxins employ parallel monothiol-dithiol mechanisms to catalyze thiol-disulfide exchanges with protein disulfides. *Chem. Sci.*, **2018**, *9*, 1173–1183; d) Stöcker, S.; Maurer, M.; Ruppert, T.; Dick, T. P. A role for 2-Cys peroxiredoxins in facilitating cytosolic protein thiol oxidation. *Nat. Chem. Biol*. **2018**, *14*, 148–155.

(3) Panzella, L.; Ebato, A.; Napolitano, A.; Koike, K. The Late Stages of Melanogenesis: Exploring the Chemical Facets and the Application Opportunities. *Int. J. Mol. Sciences* **2018**, *19*, 1753−1768.

(4) Rowan, S. J.; Cantrill, S. J.; Cousins, G. R. L.; Sanders, J. K. M.; Stoddart, F. Dynamic Covalent Chemistry. *Angew. Chem. Int. Ed*. **2002**, *41*, 898–952.

(5) Otto, S.; Furlan, R. L. E.; Sanders, J. K. M. Selection and Amplification of Hosts From Dynamic Combinatorial Libraries of Macrocyclic Disulfides. *Science* **2002**, *297*, 590–593.

(6) a) Corbett, P. T.; Tong, L. H.; Sanders, J. K. M.; Otto, S. Diastereoselective Amplification of an Induced-Fit Receptor from a Dynamic Combinatorial Library *J. Am. Chem. Soc*. **2005**, *127*, 8902–8903 b) Otto, S; Kubik, S. Dynamic Combinatorial Optimization of a Neutral Receptor That Binds Inorganic Anions in Aqueous Solution**.** *J. Am. Chem. Soc*. **2003**, *125*, 7804–7805.

(7) a) Jäger, R.; Vögtle. F. A New Synthetic Strategy towards Molecules with Mechanical Bonds: Nonionic Template Synthesis of Amide-Linked Catenanes and Rotaxanes. *Angew. Chem. Int. Ed*. **1997**, *36*, 930–944; b) Breault, G. A.; Hunter, C. A.; Meyers, P. C. Supramolecular Topology. Tetrahedron **1999**, *55*, 5265–5293

(8) Furusho, Y.; Oku, T.; Hasegawa, T.; Tsuboi, A.; Kihara, N.; Takata, T. Dynamic Covalent Approach to [2]- and [3]Rotaxanes by Utilizing a Reversible Thiol–Disulfide Interchange Reaction. *Chem. Eur. J*. **2003**, *9*, 2895–2903.

(9) Cougnon, F. B. L.; Ponnuswamy, N.; Jenkins, N. A.; Pantoş, G. D.; Sanders, J. K. M. Structural Parameters Governing the Dynamic Combinatorial Synthesis of Catenanes in Water. *J. Am. Chem. Soc*. **2012**, *134*, 19129–19135.

(10) Caprice, K.; Pupier, M.; Kruve, A.; Schalley, C. A.; Cougnon, F. B. L. Imine-Based [2]Catenanes in Water. *Chem. Sci*. **2018**, *9*, 1317–1322.

(11) Cacciapaglia, R.; Di Stefano, S.; Mandolini, L. Metathesis Reaction of Formaldehyde Acetals: An Easy Entry into the Dynamic Covalent Chemistry of Cyclophane Formation. *J. Am. Chem. Soc.* **2005**, *127*, 13666–13671.

(12) Wang, D.; Capel Ferrón, C.; Li, J.; Gámez-Valenzuela, S.; Ponce Ortiz, R.; López Navarrete, J. T.; Hernández Jolín, V.; Yang, X.; Peña Álvarez, M.; García Baonza, V.; Hartl, F.; Ruiz Delgado, M. C.; Li, H. New Multiresponsive Chromic Soft Materials: Dynamic Interconversion of Short 2,7-Dic yanomethylenecarbazole-Based Biradicaloid and the Corresponding Cyclophane Tetramer. *Chem. Eur. J*. **2017**, *23*, 13776–13783.

(13) Ji, Q.; Le, H. T. M.; Wang, X.; Chen, Y.-S.; Makarenko, T.; Jacobson, A. J.; Miljanić, O. Š. Cyclotetrabenzoin: Facile Synthesis of a Shape-Persistent Molecular Square and Its Assembly into Hydrogen-Bonded Nanotubes. *Chem. Eur. J*. **2015**, *21*, 17205–17209.

(14) Wang, Q.; Yu, C.; Zhang, C.; Long, H.; Azarnoush, S.; Jin, Y.; Zhang, W. Dynamic Covalent Synthesis of Aryleneethynylene Cages through Alkyne Metathesis: Dimer, Tetramer, or Interlocked Complex? *Chem. Sci*. **2016**, *7*, 3370–3376.

(15) Brachvogel, R.-C.; Hampel, F.; Delius, M. von. Self-Assembly of Dynamic Orthoester Cryptates. *Nat Commun.* **2015**, *6*, 1–7.

(16) a) Chen, P.; Zhoua, P.; Yang, J. In situ supramolecular polymerization promoted by the marriage of dynamic covalent bonding and pillar[5]arene-based host–guest interaction. *Chem. Commun*. **2017**, *53*, 1144–1147; b) Qu, H.; Wang, Y.; Li, Z.; Wang, X.; Fang, H.; Tian, Z.; Cao, X. Molecular Face-Rotating Cube with Emergent Chiral and Fluorescence Properties. *J. Am. Chem. Soc*. **2017**, *139*, 18142–18145; c) Chavez, A. D.; Evans, A. M.; Flanders, N. C.; Bisbey, R. P.; Vitaku, E.; Chen, L. X.; Dichtel, W. R. Equilibration of Imine-Linked Polymers to Hexagonal Macrocycles Driven by Self-Assembly. *Chem. Eur. J*. **2018**, *24*, 3989–3993.

(17) a) Lehn, J.-M. Toward Complex Matter: Supramolecular Chemistry and Self-Organization. *Proc. Nat. Ac. Sci*. **2002**, *99*, 4763–4768; b) Altmann, P. J.; Pothig, A. A pH-Dependent, Mechanically Interlocked Switch: Organometallic [2]Rotaxane vs. Organic [3]Rotaxane *Angew. Chem. Int. Ed*. **2017**, *56*, 15733 – 15736; c) Allen, C. D.; Link, A. J. Self-Assembly of Catenanes from Lasso Peptides. *J. Am. Chem. Soc*. **2016**, 138, 14214−14217; d) W. M. Bloch, J. J. Holstein, B. Dittrich, W. Hiller, G. H. Clever. Hierarchical Assembly of an Interlocked M_8L_{16} Container. *Angew. Chem. Int. Ed*. **2018**, *57*, 5534–5538.

(18) a) Caspar, D. L.; Klug, A. Physical principles in the construction of regular viruses. *Cold Spring Harb. Symp. Quant. Biol*. **1962**, *27*, 1−24; b) Bancroft, J. B.; Hills, G. J.; Markham, R. A study of the self-assembly process in a small spherical virus formation of organized structures from protein subunits *in vitro*. *Virology*, **1967**, *31*, 354−379; c) Alniss, H. Y.; Anthony, N. G.; Khalaf, A. I.; Mackay, S. P.; Suckling, C. J.; Waigh, R. D.; Wheate, N. J.; Parkinson, J. A. Rationalising Sequence Selection by Ligand Assemblies in the DNA Minor Groove: The Case for Thiazotropsin A. *Chem. Sci*. **2012**, *3*, 711–722.; d) Seeman, N. C.; Sleiman, H. F. DNA nanotechnology. *Nat. Rev. Mat.*, **2017**, *3*, 17068−

(19) a) Green, D. E.; Hechter, O. Assembly of Membrane Subunits. *Proc. Nat. Ac. Sci.* **1965**, *53*, 318–325; b) Israelachvili, J. N.; Mitchell, D. J.; Ninham, B. W. Theory of self-assembly of hydrocarbon amphiphiles into micelles and bilayers. *J. Chem. Soc., Faraday Trans. 2*, **1976**, *72*, 1525−1568; c) Zhang, Z.; Shen, W.; Ling, J.; Yan, Y.; Hu, J.; Cheng, Y. The fluorination effect of fluoroamphiphiles in cytosolic protein delivery. *Nat. Commun*. **2018**, *9*, 1377−1384.

(20) Tseng, Y.-T.; Wang, S.-M.; Huang, K.-J.; Lee, A. I.-R.; Chiang, C.-C.; Wang, C.-T. Self-Assembly of Severe Acute Respiratory Syndrome Coronavirus Membrane Protein. *J. Biol. Chem*. **2010**, *285*, 12862–12872.

(21) Walls, A. C.; Park, Y.-J.; Tortorici, M. A.; Wall, A.; McGuire, A. T.; Veesler, D. Structure, Function, and Antigenicity of the SARS-CoV-2 Spike Glycoprotein. *Cell* **2020**, *180*, 281−292.

(22) http://universe-review.ca/R10-38-life.htm. Accessed on April 24, 2020.

(23) a) Fujita, M.; Nagao, S.; Ogura, K. Guest-Induced Organization of a Three-Dimensional Palladium(II) Cagelike Complex. A Prototype for "Induced-Fit" Molecular Recognition. *J. Am. Chem. Soc*. **1995**, *117*, 1649–1650; b) Cangelosi, V. M.; Carter, T. G.; Zakharov, L. N.; Johnson, D. W. Observation of reaction intermediates and kinetic mistakes in a remarkably slow self-assembly reaction. *Chem. Commun.* **2009**, 5606–5608.

(24) a) Fujita, M. Molecular Self-Assembly Organic Versus Inorganic Approaches, Springer, Berlin, Heidelberg, **2000**, pp. 177–201; b) Lehn, J.-M. Toward Self-Organization and Complex Matter. *Science* **2002**, *295*, 2400–2403; c) Yoneya, M.; Tsuzuki, S.; Yamaguchi, T.; Sato, S.; Fujita, M. Coordination-Directed Self-Assembly of $M_{12}L_{24}$ Nanocage: Effects of Kinetic Trapping on the Assembly Process**.** *ACS Nano*, **2014**, *8*, 1290–1296.

(25) Salgado, E. N.; Radford, R. J.; Tezcan, F. A. Metal-Directed Protein Self-Assembly. *Acc. Chem. Res.* **2010**, *43*, 661–672.

(26) Grommet, A. B.; Nitschke, J. R. Directed Phase Transfer of an $Fe^{II}{}_4L_4$ Cage and Encapsulated Cargo. *J. Am. Chem. Soc*. **2017**, *139*, 2176–2179.

(27) Zhou, X. -P.; Liu, J.; Zhan, S.-Z.; Yang, J.-R.; Li, D.; Ng, K.-M.; Sun, R. W.; Che, C.-M. A high-symmetry coordination cage from 38- or 62-component self-assembly. *J. Am. Chem. Soc*. **2012**, *134*, 8042–8045.

(28) Zhang, K.; Zhang, L.; Feng, G.-F.; Hu, H.; Chang, F.-F.; Huang, W. Two Types of Anion-Induced Reconstruction of Schiff-Base Macrocyclic Zinc Complexes: Ring-Contraction and Self-Assembly of a Molecular Box. *Inorg. Chem*. **2016**, *55*, 16–21.

(29) Chakrabarty, R.; Mukherjee, P. S.; Stang, P. J. Supramolecular Coordination: Self-Assembly of Finite Two- and Three-Dimensional Ensembles. *Chem. Rev*. **2011**, *111*, 6810–6918.

(30) Frisbie, S. H.; Ortega, R.; Maynard, D. M.; Sarkar, B. The Concentrations of Arsenic and Other Toxic Elements in Bangladesh's Drinking Water. *Env. Health Pers.* **2002**, *110*, 1147–1153.

(31) Vickaryous, W. J.; Herges, R.; Johnson, D. W. Arsenic–π Interactions Stabilize a Self-Assembled As_2L_3 Supramolecular Complex. *Angew. Chem. Int. Ed*. **2004**, *43*, 5831–5833.

(32) a) Vickaryous, W. J.; Healey, E. R.; Berryman, O. B.; Johnson, D. W. Synthesis and Characterization of Two Isomeric, Self-Assembled Arsenic−Thiolate Macrocycles. *Inorg. Chem*. **2005**, *44*, 9247–9252; (b) Carter, T. G.; Healey, E. R.; Pitt, M. A.; Johnson, D. W. Secondary Arsenic-Oxygen Interactions in Arsenic-Thiolate Coordination Complexes. *Inorg. Chem*. **2005**, *44*, 9634–9636; c) Cangelosi, V. M.; Sather, A. C.; Zakharov, Z. N.; Berryman, O. B.; Johnson, D. W. Diastereoselectivity in the Self-Assembly of $As_2L_2Cl_2$ Macrocycles is Directed by the As-π Interaction. *Inorg. Chem*. **2007**, *46*, 9278–9284; d) Cangelosi, V. M.; Zakharov, L. N.; Fontenot, S. A.; Pitt, M. A.; Johnson, D. W. Host-guest Interactions in a Series of Self-assembled $As_2L_2Cl_2$ Macrocycles. *Dalton Trans*. **2008**, *26*, 3447–3453; e) Pitt, M. A.; Zakharov, L. N.; Vanka, K.; Thompson, W. H.; Laird, B. B.; Johnson, D. W. Multiple weak supramolecular

interactions stabilize a surprisingly twisted As_2L_3 assembly. *Chem. Commun*. **2008**, *33*, 3936–3938; f) Allen, C. A.; Cangelosi, V. M.; Zakharov, L. N.; Johnson, D. W. Supramolecular Organization Using Multiple Secondary Bonding Interactions. *Cryst. Growth Des*. **2009**, *9*, 3011–3013; g) Cangelosi, V. M.; Zakharov, L. N.; Crossland, J. L.; Franklin, B. C.; Johnson, D. W. A Surprising 'Folded-in' Conformation of a Self-Assembled Arsenic-Thiolate Macrocycle. *Cryst. Growth Des*. **2010**, *10*, 1471−1473; (h) Lindquist, N. R.; Carter, T. G.; Cangelosi, V. M.; Zakharov, L. N.; Johnson, D. W. Three's Company: Co-crystallization of a Self-Assembled S_4 Metallacyclophane with Two Diastereomeric Metallacycle Intermediates. *Chem. Commun.* **2010**, *46*, 3505–3507.

(33) a) Vickaryous, W. J.; Zakharov, L. N.; Johnson, D. W. Self-Assembled Antimony-Thiolate Sb_2L_3 and $Sb_2L_2Cl_2$ Complexes. *Main Group Chem*. **2006**, *5*, 51−59; b) Cangelosi, V. M.; Zakharov, L. N.; Johnson, D. W. Supramolecular "Transmetalation" Leads to an Unusual Self-Assembled P_2L_3 Cryptand. *Angew. Chem. Int. Ed*. **2010**, *49*, 1248–1251.

(34) Collins, M. S.; Carnes, M. E.; Sather, A. C.; Berryman, O. B.; Zakharov, L. N.; Teat, S. J.; Johnson, D. W. Pnictogen-Directed Synthesis of Discrete Disulfide Macrocycles. *Chem. Commun*. **2013**, *49*, 6599–6602.

(35) Collins, M. S.; Phan, N.-M.; Zakharov, L. N.; Johnson, D. W. Coupling Metaloid-Directed Self-Assembly and Dynamic Covalent Systems as a Route to Large Organic Cages and Cyclophanes. *Inorg. Chem*. **2018**, *57*, 3486–3496.

(36) Collins, M. S.; Carnes, M. E.; Nell, B. P.; Zakharov, L. N.; Johnson, D. W. A Facile Route to Old and New Cyclophanes via Self-Assembly and Capture. *Nat. Commun.* **2016**, *7*, 11052–11059.

(37) Chatgilialoglu, C.; Asmus, K. -D. *Sulfur-Centered Reactive Intermediates in Chemistry and Biology*, Springer Science & Business Media, New York, **2013**.

(38) Ball, M.; Zhong, Y.; Fowler, B.; Zhang, B.; Li, P.; Etkin, G.; Paley, D. W.; Decatur, J.; Dalsania, A. K.; Li, H.; Xiao, S.; Ng, F.; Steigerwald, M. L.; Nuckolls, C. Macrocyclization in the Design of Organic N-Type Electronic Materials. *J. Am. Chem. Soc*. **2016**, *138*, 12861–12867.

(39) Schick, T. H. G.; Lauer, J. C.; Rominger, F.; Mastalerz, M. Transformation of Imine Cages into Hydrocarbon Cages. *Angew. Chem. Int. Ed.* **2019**, *58*, 1768−1773.

(40) Gross, J.; Harder, G.; Vögtle, F.; Stephan, H.; Gloe, K. $C_{60}H_{60}$ and $C_{54}H_{48}$: Silver Ion Extraction with New Concave Hydrocarbons. *Angew. Chem. Int. Ed*. **1995**, *34*,481–484.

(41) Schalley, C. A. Analytical Methods in Supramolecular Chemistry; John Wiley & Sons, **2012**.

(42) Shivanyuk, A.; Rebek, J. Social Isomers in Encapsulation Complexes. *J. Am. Chem. Soc*. **2002**, *124*, 12074–12075.

(43) Taylor, P. N.; Anderson, H. L. Cooperative Self-Assembly of Double-Strand Conjugated Porphyrin Ladders. *J. Am. Chem. Soc*. **1999**, *121*, 11538–11545.

(44) Rurup, W. F.; Snijder, J.; Koay, M. S. T.; Heck, A. J. R.; Cornelissen, J. J. L. Self-Sorting of Foreign Proteins in a Bacterial Nanocompartment. *J. Am. Chem. Soc*. **2014**, *136*, 3828–3832.

(45) Black, S. P.; Wood, D. M.; Schwarz, F. B.; Ronson, T. K.; Holstein, J. J.; Stefankiewicz, A. R.; Schalley, C. A.; Sanders, J. K. M.; Nitschke, J. R. Catenation and encapsulation induce distinct reconstitutions within a dynamic library of mixed-ligand Zn_4L_6 cages. *Chem. Sci*. **2016**, *7*, 2614–2620.

(46) Holloway, L. R.; Bogie, P. M.; Hooley, R. J. Controlled Self-Sorting in Self-Assembled Cage Complexes. *Dalt. Trans*. **2017**, *46*, 14719–14723.

(47) Beaudoin, D.; Rominger, F.; Mastalerz, M. Chiral Self-Sorting of [2+3] Salicylimine Cage Compounds. *Angew. Chem. Int. Ed*. **2017**, *56*, 1244–1248.

(48) a) Lirag, R. C.; Osowska, K.; Miljanić, O. Š. Precipitation-Driven Self-Sorting of Imines. *Org. Biomol. Chem*. **2012**, *10*, 4847–4850; b) Ji, Q.; Miljanić, O. Š. Distillative Self-Sorting of Dynamic Ester Libraries. *J. Org. Chem*. **2013**, *78*, 12710–12716.

(49) a) Vögtle, F.; Effler, A. H. Sterische Wechselwirkungen im Innern cyclischer Verbindungen, X. Heterocyclische [2.2]Metacyclophane. *Chem. Beri*. **1969**, *102*, 3071–3076; b) Lichtenthaler, R. G.; Vögtle, F. Vielfach überbrückte aromatische Verbindungen, 6. Dreifach verbrückte Cyclophane. *Chem. Ber.*, **1973**, *106*, 1319–1327.

(50) a) Kahouli, A.; Sylvestre, A.; Laithier, J.-F.; Pairis, S.; Garden, J.-L.; André, E.; Jomni, F.; Yangui, B. Effect of O_2 , Ar/H_2 and CF_4 Plasma Treatments on the Structural and Dielectric Properties of Parylene-C Thin Films. *J. Phys. D: App. Phys*. **2012**, *45*, 215306; b) Baumann, M. Gersdorff, J. Kreis, M. Kunat and M. Schwambera, in *CVD Polymers*, ed. K. K. Gleason, Wiley-VCH Verlag GmbH & Co. KGaA, Weinheim, Germany, **2015**, pp. 431–453.

CHAPTER II

(1) a) Dietrich-Buchecker, C.; Sauvage, J. -P. Templated Synthesis of Interlocked Macrocyclic Ligands, the Catenands. Preparation and Characterization of the Prototypical Bis-30 Membered Ring System. *Tetrahedron* **1990**, *46*, 503–512; b) Weck, M.; Mohr, B.; Sauvage, J. -P.; Grubbs, R. H. Synthesis of Catenane Structures via Ring-Closing Metathesis. *J. Org. Chem.* **1999**, *64*, 5463–5471; c) Kang, S.; Berkshire, B. M.; Xue, Z.; Gupta, M.; Layode, C.; May, P. A.; Mayer, M. F. Polypseudorotaxanes via Ring-Opening Metathesis Polymerizations of [2]Catenanes. *J. Am. Chem. Soc*. **2008**, *130*, 15246–15247.

(2) a) Sato, Y.; Yamasaki, R.; Saito, S. Synthesis of [2]Catenanes by Oxidative Intramolecular Diyne Coupling Mediated by Macrocyclic Copper(I) Complexes. *Angew. Chem. Int. Ed*. **2009**, *48*, 504–507; b) Durola, F.; Sauvage, J. -P.; Wenger, O. S. The magic effect of endocyclic but non-sterically hindering biisoquinoline chelates: From fast-moving molecular shuttles to [3]rotaxanes. *Coord. Chem. Rev*. **2010**, *254*, 1748–1759; c) Share, A. I.; Parimal, K.; Flood, A. H. Bilability is Defined when One Electron is Used to Switch between Concerted and Stepwise Pathways in Cu(I)-Based Bistable [2/3]Pseudorotaxanes. *J. Am. Chem. Soc*. **2010**, *132*, 1665–1675.

(3) Dietrich-Buchecker, C. O.; Sauvage, J. P.; Kern, J. M. Templated Synthesis of Interlocked Macrocyclic Ligands: The Catenands. *J. Am. Chem. Soc.* **1984**, *106*, 3043–3045.

(4) Megiatto, J. D.; Schuster, D. I. Alternative Demetalation Method for Cu(I)-Phenanthroline-Based Catenanes and Rotaxanes. *Org. Lett*. **2011**, *13*, 1808–1811.

(5) Down, J. L.; Lewis, J.; Moore, B.; Wilkinson, G. The Solubility of Alkali Metals in Ethers. *J. Chem. Soc*. **1959**, 3767–3773.

(6) Inthasot, A.; Tung, S. -T.; Chiu, S. -H. Using Alkali Metal Ions To Template the Synthesis of Interlocked Molecules. *Acc. Chem. Res*. **2018**, *51*, 1324–1337.

(7) Collins, M. S.; Carnes, M. E.; Sather, A. C.; Berryman, O. B.; Zakharov, L. N.; Teat, S. J.; Johnson, D. W. Pnictogen-Directed Synthesis of Discrete Disulfide Macrocycles. *Chem. Commun*. **2013**, *49*, 6599 – 6602.

(8) Collins, M. S.; Carnes, M. E.; Nell, B. P.; Zakharov, L. N.; Johnson, D. W. A Facile Route to Old and New Cyclophanes via Self-Assembly and Capture. *Nat. Commun.* **2016**, *7*, 11052–11059.

(9) Collins, M. S.; Phan, N. -M.; Zakharov, L. N.; Johnson, D. W. Coupling Metaloid-Directed Self-Assembly and Dynamic Covalent Systems as a Route to Large Organic Cages and Cyclophanes. *Inorg. Chem.* **2018**, *57*, 3486–3496.

(10) a) Zukerman-Schpector, J.; Otero-de-la-Roza, A.; Luaña, V.; Tiekink, E. R. T. Supramolecular Architectures Based on As (Lone Pair)···π(Aryl) Interactions. *Chem. Commun.* **2011**, *47*, 7608–7610; b) Moaven, S.; Yu, J.; Yasin, J.; Unruh, D. K.; Cozzolino, A. F. Precise Steric Control over 2D versus 3D Self-Assembly of Antimony(III) Alkoxide Cages through Strong Secondary Bonding Interactions. *Inorg. Chem.* **2017**, *56*, 8372–8380; c) Trubenstein, H. J.; Moaven, S.; Vega, M.; Unruh, D. K.; Cozzolino, A. F. Pnictogen bonding with alkoxide cages: which pnictogen is best? *New J. Chem.* **2019**, *43*, 14305–14312.

(11) a) Cangelosi, V. M.; Pitt, M. A.; Vickaryous, W. J.; Allen, C. A.; Zakharov, L. N.; Johnson, D. W. Design Considerations for the Group 15 Elements: The Pnictogen···π Interaction As a Complementary Component in Supramolecular Assembly Design. *Crystal Growth & Design* **2010**, *10*, 3531–3536; b) Fontenot, S. A.; Cangelosi, V. M.; Pitt, M. A. W.; Sather, A. C.; Zakharov, L. N.; Berryman, O. B.; Johnson, D. W. Design, Synthesis and Characterization of Self-Assembled As_2L_3 and Sb_2L_3 Cryptands. *Dalt. Trans*. **2011**, *40*, 12125−12131.

(12) Yang, Z.; She, M.; Yin, B.; Hao, L.; Obst, M.; Liu, P.; Li, J. Solvent-Dependent Turn-on Probe for Dual Monitoring of Ag^+ and Zn^{2+} in Living Biological Samples. *Anal. Chim. Acta* **2015**, *868*, 53–59.

(13) Park, I. -H.; Park, K. -M.; Lee, S. S. Preparation and Characterisation of Divalent Hard and Soft Metal (M = Ca, Co, Cu, Zn, Cd, Hg and Pb) Complexes of 1,10-Dithia-18-Crown-6: Structural Versatility. *Dalton Trans*. **2010**, *39*, 9696–9704.

(14) Phillips, H. A, Eelman, M. D, Burford, N. Cooperative influence of thiolate ligands on the bio-relevant coordination chemistry of bismuth. *J. Inorg. Biochem.* **2007**, *101*, 736−739.

(15) Ording-Wenker, E. C. M.; van der Plas, M.; Siegler, M. A.; Bonnet, S.; Bickelhaupt, F. M.; Fonseca Guerra, C.; Bouwman, E. Thermodynamics of the Cu^{II} μ-Thiolate and Cu^{I} Disulfide Equilibrium: A Combined Experimental and Theoretical Study. *Inorg. Chem.* **2014**, *53*, 8494–8504.

(16) Phan, N.-M.; Zakharov, L. N.; Johnson, D. W. Copper(II) Serves as an Efficient Additive for Metal-Directed Self-Assembly of over 20 Thiacyclophanes. *Chem. Commun*. **2018**, *54*, 13419–13422.

(17) a) Li, J.; Carnall, J. M. A.; Stuart, M. C. A.; Otto, S. Hydrogel Formation upon Photoinduced Covalent Capture of Macrocycle Stacks from Dynamic Combinatorial Libraries. *Angew. Chem. Int. Ed.*, **2011**, *50*, 8384–8386; b) Hsu, C. -W.; Miljanić, O. Š. Kinetically controlled simplification of a multiresponsive [10 × 10] dynamic imine library. *Chem. Commun.*, **2016**, *52* , 12357–12359.

CHAPTER III

(1) Lehn, J. -M. From supramolecular chemistry towards constitutional dynamic chemistry and adaptive chemistry. *Chem. Soc. Rev.* **2007**, *36* , 151–160.

(2) Gleiter, R.; Hopf, H. Modern Cyclophane Chemistry. Wiley-VCH: Weinheim. **2004**.

(3) Rossa L., Vögtle F. Synthesis of medio- and macrocyclic compounds by high dilution principle techniques. In: Vögtle F. (eds) Cyclophanes I. Topics in Current Chemistry. Springer, Berlin, Heidelberg. **1983**, vol 113.

(4) Drożdż, W.; Bouillon, C.; Kotras, C.; Richeter, S.; Barboiu, M.; Clément, S.; Stefankiewicz, A. R.; Ulrich, S. Generation of Multicomponent Molecular Cages using Simultaneous Dynamic Covalent Reactions. *Chem. Eur. J.* **2017**, *23*, 18010–18018.

(5) Komáromy, D.; Stuart, M. C. A.; Santiago, G. M.; Tezcan, M.; Krasnikov, V. V..; Otto, S. Self-Assembly Can Direct Dynamic Covalent Bond Formation toward Diversity or Specificity. *J. Am. Chem. Soc*. **2017**, *139*, 6234–6241.

(6) Lincoln, T. A.; Joyce, G. F. Self-Sustained Replication of an RNA Enzyme. *Science* **2009**, *323*, 1229–1232.

(7) Collins, M. S.; Carnes, M. E.; Sather, A. C.; Berryman, O. B.; Zakharov, L. N.; Teat, S. J.; Johnson, D. W. Pnictogen-Directed Synthesis of Discrete Disulfide Macrocycles. *Chem. Commun*. **2013**, *49*, 6599–6602.

(8) Collins, M. S.; Carnes, M. E.; Nell, B. P.; Zakharov, L. N.; Johnson, D. W. A Facile Route to Old and New Cyclophanes via Self-Assembly and Capture. *Nat. Commun.* **2016**, *7*, 11052 – 11059.

(9) Phan, N. -M.; Choy, E. P. K. L.; Zakharov, L. N.; Johnson, D. W. Self-sorting in dynamic disulfide assembly: new biphenyl-bridged "nanohoops" and unsymmetrical cyclophanes. *Chem. Commun*., **2019**, *55*, 11840–11843.

(10) Fontenot, S. A.; Cangelosi, V. M.; Pitt, M. A. W.; Sather, A. C.; Zakharov, L. N.; Berryman, O. B.; Johnson, D. W. Design, synthesis and characterization of self-assembled As_2L_3 and Sb_2L_3 cryptands. *Dalton Trans.* **2011**, *40*, 12125–12131.

(11) Eaton, V. J.; Steele, D. Dihedral angle of biphenyl in solution and the molecular force field. *J. Chem. Soc., Faraday Trans. 2*, **1973**, *69*, 1601–1608.

(12) Chatgilialoglu, C.; Asmus, K. -D. *Sulfur-Centered Reactive Intermediates in Chemistry and Biology*, Springer Science & Business Media, New York. **2013**.

(13) a) Brisig, B.; Sanders, J. K. M.; Otto, S. Selection and amplification of a catalyst from a dynamic combinatorial library. *Angew. Chem. Int. Ed*. **2003**, *42*, 1270–1273; b) Corbett, P. T.; Leclaire, J.; Vial, L.; West, K. R.; Wietor, J. -L.; Sanders, J. K. M.; Otto, S. Dynamic combinatorial chemistry. *Chem. Rev*. **2006**, *106*, 3652–3711.

(14) Collins, M. S.; Phan, N. -M.; Zakharov, L. N.; Johnson, D. W. Coupling Metaloid-Directed Self-Assembly and Dynamic Covalent Systems as a Route to Large Organic Cages and Cyclophanes. *Inorg. Chem*. **2018**, *57*, 3486–3496.

(15) Shear, T. A.; Lin, F.; Zakharov, L. N.; Johnson, D. W. "Design of Experiments" as a Method to Optimize Dynamic Disulfide Assemblies: Cages and Functionalizable Macrocycles. *Angew. Chem. Int. Ed*. **2020**, *59*, 1496–1500.

CHAPTER IV

(1) Wei, G.; Xi, W.; Nussinov, R.; Ma, B. Protein Ensembles: How Does Nature Harness Thermodynamic Fluctuations for Life? The Diverse Functional Roles of Conformational Ensembles in the Cell. *Chem. Rev*. **2016**, *116*, 6516–6551.

(2) Oshovsky, G. V.; Reinhoudt, D. N.; Verboom, W. Supramolecular Chemistry in Water. *Angew. Chem. Int. Ed*. **2007**, *46* , 2366–2393.

(3) Watson, J. D.; Crick, F. H. C. Molecular Structure of Nucleic Acids: A Structure for Deoxyribose Nucleic Acid. *Nature* **1953**, *171*, 737–738.

(4) Alberts, B.; Johnson, A.; Lewis, J.; Raff, M.; Roberts, K.; Walter, P. Molecular Biology of the Cell, 4th ed.; Garland Science: New York, **2002**.

(5) Wu, A.; Isaacs, L. Self-Sorting: The Exception or the Rule? *J. Am. Chem. Soc.* **2003**, *125*, 4831–4835.

(6) Safont-Sempere, M. M.; Fernández, G.; Würthner, F. Self-Sorting Phenomena in Complex Supramolecular Systems. *Chem. Rev.* **2011**, *111*, 5784–5814.

(7) Shivanyuk, A.; Rebek, J. Social Isomers in Encapsulation Complexes. *J. Am. Chem. Soc*. **2002**, *124*, 12074–12075.

(8) Taylor, P. N.; Anderson, H. L. Cooperative Self-Assembly of Double-Strand Conjugated Porphyrin Ladders. *J. Am. Chem. Soc*. **1999**, *121*, 11538–11545.

(9) Tomimasu, N.; Kanaya, A.; Takashima, Y.; Yamaguchi, H.; Harada, A. Social Self-Sorting: Alternating Supramolecular Oligomer Consisting of Isomers. *J. Am. Chem. Soc.* **2009**, *131*, 12339–12343.

(10) Bunn, H. F.; Bernard, G. *Hemoglobin--Molecular, Genetic, and Clinical Aspects*; W.B. Saunders Co., Philadelphia, PA, **1986**.

(11) Holloway, L. R.; Bogie, P. M.; Hooley, R. J. Controlled Self-Sorting in Self-Assembled Cage Complexes. *Dalton Trans.* **2017**, *46*, 14719–14723.

(12) Wiley, C. A.; Holloway, L. R.; Miller, T. F.; Lyon, Y.; Julian, R. R.; Hooley, R. J. Electronic Effects on Narcissistic Self-Sorting in Multicomponent Self-Assembly of Fe-Iminopyridine Meso-Helicates. *Inorg. Chem.* **2016**, *55*, 9805–9815.

(13) Orentas, E.; Lista, M.; Lin, N.-T.; Sakai, N.; Matile, S. A Quantitative Model for the Transcription of 2D Patterns into Functional 3D Architectures. *Nat. Chem.* **2012**, *4*, 746–750.

(14) Kołodziejski, M.; R. Stefankiewicz, A.; Lehn, J.-M. Dynamic Polyimine Macrobicyclic Cryptands – Self-Sorting with Component Selection. *Chem. Sci.* **2019**, *10*, 1836–1843.

(15) a) Altmann, P. J.; Pöthig, A. A pH-Dependent, Mechanically Interlocked Switch: Organometallic [2]Rotaxane vs. Organic [3]Rotaxane. *Angew. Chem. Int. Ed.* **2017**, *56*, 15733–15736; b) Van Raden, J.; White, B.; Zakharov, L. N.; Jasti, R. Nanohoop Rotaxanes from Active Metal Template Syntheses and Their Potential in Sensing Applications. *Angew. Chem. Int. Ed.* **2018**, *58*, 7341–7345; c) Allen, C. D.; Link, A. J. Self-Assembly of Catenanes from Lasso Peptides. *J. Am. Chem. Soc.* **2016**, *138*, 14214–14217; d) Sawada, T.; Yamagami, M.; Ohara, K.; Yamaguchi, K.; Fujita, M. Peptide [4]Catenane by Folding and Assembly. *Angew. Chem. Int. Ed.* **2016**, *55*, 4519–4522; e) Shan, W.-L.; Lin, Y.-J.; Hahn, F. E.; Jin, G.-X. Highly Selective Synthesis of Iridium(III) Metalla[2]catenanes through Component Pre-Orientation by π···π Stacking. *Angew. Chem. Int. Ed*. **2019**, *58*, 5882–5886.

(16) a) Collins, M. S.; Carnes, M. E.; Sather, A. C.; Berryman, O. B.; Zakharov, L. N.; Teat, S. J.; Johnson, D. W. Pnictogen-Directed Synthesis of Discrete Disulfide Macrocycles. *Chem. Commun*. **2013**, *49*, 6599 – 6602; b) Collins, M. S.; Phan, N.-M.; Zakharov, L. N.; Johnson, D. W. Coupling Metaloid-Directed Self-Assembly and Dynamic Covalent Systems as a Route to Large Organic Cages and Cyclophanes. *Inorg. Chem*. **2018**, *57*, 3486–3496.

(17) Collins, M. S.; Carnes, M. E.; Nell, B. P.; Zakharov, L. N.; Johnson, D. W. A Facile Route to Old and New Cyclophanes via Self-Assembly and Capture. *Nat. Commun.* **2016**, *7*, 11052 – 11059.

(18) Phan, N.-M.; L. Choy, E. P. K.; N. Zakharov, L.; W. Johnson, D. Self-Sorting in Dynamic Disulfide Assembly: New Biphenyl-Bridged "Nanohoops" and Unsymmetrical Cyclophanes. *Chem. Commun*. **2019**, *55*, 11840–11843.

(19) Phan, N.-M.; Zakharov, L. N.; Johnson, D. W. Copper(II) Serves as an Efficient Additive for Metal-Directed Self-Assembly of over 20 Thiacyclophanes. *Chem. Commun*. **2018**, *54*, 13419–13422.

CHAPTER V

(1) Pellegrin, M. Contribution à l'étude de La Réaction de Fittig. Recueil des Travaux Chimiques des Pays-Bas et de la Belgique **1899**, *18*, 457–465.

(2) Cram, D. J.; Steinberg, H. Macro Rings. I. Preparation and Spectra of the Paracyclophanes. *J. Am. Chem. Soc.* **1951**, *73*, 5691–5704.

(3) Vögtle, F.; Effler, A. H. Sterische Wechselwirkungen im Innern cyclischer Verbindungen, X. Heterocyclische [2.2]Metacyclophane. *Chem. Ber.* **1969**, *102*, 3071–3076.

(4) Sherrod, S. A.; Da Costa, R. L.; Barnes, R. A.; Boekelheide, V. Steric Effects in [2.2]Metaparacyclophanes. Steric Isotope Effect, Remote Substituent Effect on a Steric Barrier, and Other Steric Phenomena. *J. Am. Chem. Soc.* **1974**, *96*, 1565–1577.

(5) Rebafka, W.; Staab, H. A. The Pseudogeminal "Quinhydrone" of the [2.2] Paracyclophane Series. *Angew. Chem. Int. Ed.* **1974**, *13*, 203–204.

(6) Boekelheide, V. [2n]Cyclophanes: Paracyclophane to Superphane. *Acc. Chem. Res.* **1980**, *13*, 65–70.

(7) Otsubo, T.; Boekelheide, V. An Alternate Route for the Conversion of Dithia[3.3]Cyclophanes to Cyclophane-Dienes. Reaction with Benzyne Followed by Sulfoxide Pyrolysis. *Tet. Lett.* **1975**, *16*, 3881–3884.

(8) Bruhin, J.; Jenny, W. Ein neuer syntheseweg in die paracyclophanreihe photolyse der 2,11-dithia [3.3] paracyclophane. *Tet. Lett.* **1973**, *14*, 1215–1218.

(9) Vögtle, F.; Neumann, P. Stereochemistry of [2.2]Metacyclophanes. *Angew. Chem. Int. Ed.* **1972**, *11*, 73–83.

(10) Sekine, Y.; Brown, M.; Boekelheide, V. [2.2.2.2.2.2](1,2,3,4,5,6)Cyclophane: Superphane. *J. Am. Chem. Soc.* **1979**, *101*, 3126–3127.

(11) Rohrbach, W. D.; Sheley, R.; Boekelheide, V. Methylated multibridged [2n]cyclophanes. All alternate synthesis of [26](1,2,3,4,5,6) cyclophane (superphane). *Tetrahedron* **1984**, *40*, 4823–4828.

(12) Vögtle, F.; Gross, J.; Seel, C.; Nieger, M. $C_{36}H_{36}$–Tetrahedral Clamping of Four Benzene Rings in a Spherical Hydrocarbon Framework. *Angew. Chem. Int. Ed.* **1992**, *31*, 1069–1071.

(13) Schick, T. H. G.; Lauer, J. C.; Rominger, F.; Mastalerz, M. Transformation of Imine Cages into Hydrocarbon Cages. *Angew. Chem. Int. Ed*. **2019**, *58*, 1768–1773.

(14) Houk, J.; Whitesides, G. M. Characterization and Stability of Cyclic Disulfides and Cyclic Dimeric Bis(Disulfides). *Tetrahedron* **1989**, *45*, 91–102.

(15) Collins, M. S.; Carnes, M. E.; Sather, A. C.; Berryman, O. B.; Zakharov, L. N.; Teat, S. J.; Johnson, D. W. Pnictogen-Directed Synthesis of Discrete Disulfide Macrocycles. *Chem. Commun*. **2013**, *49*, 6599–6602.

(16) Collins, M. S.; Carnes, M. E.; Nell, B. P.; Zakharov, L. N.; Johnson, D. W. A Facile Route to Old and New Cyclophanes via Self-Assembly and Capture. *Nat. Commun.* **2016**, *7*, 11052–11059.

(17) Reportlinker. Global Markets for Conformal Coatings in Electronics https://www.prnewswire.com/news-releases/global-markets-for-conformal-coatings-in-electronics-273982911.html (accessed May 20, 2020).

(18) Collins, M. S.; Phan, N.-M.; Zakharov, L. N.; Johnson, D. W. Coupling Metaloid-Directed Self-Assembly and Dynamic Covalent Systems as a Route to Large Organic Cages and Cyclophanes. *Inorg. Chem.* **2018**, *57*, 3486–3496.

(19) Phan, N.-M.; L. Choy, E. P. K.; N. Zakharov, L.; W. Johnson, D. Self-Sorting in Dynamic Disulfide Assembly: New Biphenyl-Bridged "Nanohoops" and Unsymmetrical Cyclophanes. *Chem. Commun.* **2019**, *55*, 11840–11843.

(20) Lee, S.; Yang, A.; Moneypenny, T. P.; Moore, J. S. Kinetically Trapped Tetrahedral Cages *via* Alkyne Metathesis. *J. Am. Chem. Soc*. **2016**, *138*, 2182–2185.

(21) Laarhoven, W. H.; Cuppen, Th. J. H. M. The formation of stilbenes and phenanthrenes by irradiation of dibenzyl sulfides. *Tet. Lett*. **1966**, *7*, 5003–5007.

APPENDIX

(1) G. M. Sheldrick, *Bruker/Siemens Area Detector Absorption Correction Program*, Bruker AXS, Madison, WI, **1998**.

(2) Van der Sluis, P. & Spek, A. L. BYPASS: an effective method for the refinement of crystal structures containing disordered solvent regions *Acta Cryst., Sect. A.* **1990**, *A46*, 194–201.

(3) Sheldrick, G. M. SHELXT - Integrated space-group and crystal-structure determination, *Acta Cryst.* **2015**, *A71*, 3–8.